



AN ABSTRACT OF THE THESIS OF

Alphonse A. Schacher for the degree of Master of Science in  
Electrical and Computer Engineering presented on June 15, 2007.

Title: A Novel Control Design for a Wave Energy Converter

Abstract approved: \_\_\_\_\_

Ted K. Brekken

Ocean wave energy is rapidly becoming a field of great interest in the world of renewable energy. Significant advancements in design and technology are being made to make wave energy a viable alternative for our growing energy demands. The two major hurdles for ocean wave energy to make a significant contribution to our nations energy needs are the permitting of commercial wave parks and the creation of an ocean wave energy converter that is cost effective and reliable. Significant improvements in wave energy converters are now possible with the implementation of specialized generators and power electronic technologies. This allows for dynamic generator loading that gives the ability to control the buoy in order to increase power production and reliability. This thesis presents the development of a novel control design for a wave energy generator which focuses on reliability and power production.

© Copyright by Alphonse A. Schacher  
June 15, 2007  
All Rights Reserved

A Novel Control Design for a Wave Energy Converter

by

Alphonse A. Schacher

A THESIS

submitted to

Oregon State University

in partial fulfillment of  
the requirements for the  
degree of

Master of Science

Presented June 15, 2007  
Commencement June 2008

Master of Science thesis of Alphonse A. Schacher presented on  
June 15, 2007.

APPROVED:

---

Major Professor, representing Electrical and Computer Engineering

---

Director of the School of Electrical Engineering and Computer Science

---

Dean of the Graduate School

I understand that my thesis will become part of the permanent collection of Oregon State University libraries. My signature below authorizes release of my thesis to any reader upon request.

---

Alphonse A. Schacher, Author

## ACKNOWLEDGEMENTS

I would like to express my most sincere thanks to all of those who have helped me to achieve this notable accomplishment. Above all else I want to thank our Lord Jesus Christ for all the blessings he has given me, for filling my life with happiness, and for putting me in a place with so many talented and inspired individuals.

I can't say enough how much I appreciate my grandparents Helen and Alphonse Schacher for giving me all their love and teaching me to appreciate the truly important things in life. Also to my grandpa Richard Brentano for knowing how important an education would be for all of his grandchildren and for making it possible. To my parents who have helped me through it all, without them this would never be possible. They have been there with unwavering support and have always believed in me.

I want to express my deepest thanks to my big brother for always being there to shine a light on my path and help me get through it all. To my sister for being a huge supporter and for always being there to cheer me on.

I would also like to thank my colleagues for all of their hard work in helping me with this project; Aaron VanderMeulen, Peter Hogan, Dave Elwood, Ken Rhinefrank and Ean Amon.

I would like to express sincere appreciation to my professors, Annette von Jouanne, Ted Brekken, and Alan Wallace. It is their enthusiasm for what they teach that has captured my attention for a lifetime.

“Research is about traveling down 10 roads to learn that 9 of them were dead ends.”

– Alphonse A. Schacher

## TABLE OF CONTENTS

	<u>Page</u>
1. INTRODUCTION.....	1
1.1 Wave Energy Background .....	1
1.2 Motivation.....	2
1.3 Testing Facilities.....	2
2. THE OCEAN WAVE ENVIRONMENT.....	4
2.1 Wave Creation.....	4
2.2 Wave Equations.....	7
2.3 Ocean Wave Spectrum.....	8
2.4 Ocean Wave Energy.....	15
2.5 Pulsed Power.....	18
3. OPTIMUM CONTROL THEORY.....	19
3.1 Morrison Model.....	19
3.2 Energy Absorbtion.....	21
3.3 Maximum Power Capture.....	23
3.4 Phase Control by Latching.....	25
3.5 Electrical Circuit Analogy.....	26
4. NOVEL CONTROL DESIGN.....	29
4.1 Limitations.....	29
4.1.1 Velocity and Stroke Limit.....	29
4.1.2 Energy Storage Limit.....	30
4.1.3 Current Limit.....	31
4.1.4 Maximum Power Limit.....	32
4.2 Control Design.....	32
4.2.1 Conditional Damping Control.....	34
5. MODELS and SIMULATIONS.....	45
5.1 Hydrodynamics.....	46
5.2 Generator Models.....	52
5.3 Power Take-Off Models.....	60
5.4 Simulations.....	61
5.4.1 Undamped WEC.....	62
5.4.2 Optimum Reactive Control.....	63
5.4.3 Optimum Damping Control.....	67
5.4.4 Increased Damping Control.....	68
5.5.5 Conditional Damping Control.....	71

## TABLE OF CONTENTS (Continued)

	<u>Page</u>
6. HARDWARE .....	81
6.1 The WEC.....	81
6.2 Generator.....	81
6.3 PTO.....	82
6.4 Compact Rio.....	83
6.4.1 Data Acquisition.....	88
6.4.2 Controls.....	90
6.4.3 Communications.....	91
7. RESULTS and CONCLUSIONS.....	93
7.1 Results.....	93
7.2 Conclusions.....	93
8. FUTURE WORK.....	95
9. BIBLIOGRAPHY.....	97
10. APPENDIX.....	99



## LIST OF FIGURES

<u>Figure</u>	<u>Page</u>
2.1 Earth Surface Temperatures.....	5
2.2 Simple Atmospheric Circulation.....	5
2.3 Coriolis Driven Atmospheric Circulation.....	6
2.4 Pierson and Moskowitz Wave Spectra.....	10
2.5 NOAA Spectral Wave Density.....	11
2.6 NOAA Wave Profile Data.....	12
2.7 Water Particle Orbits in Shoaling Waves.....	12
2.8 Wave Dimensions.....	13
2.9 Available Power in Varied Wave Conditions.....	16
2.10 Seasonal Variation in Wave Power.....	17
2.11 Average Global Wave Power in kW/m.....	18
3.7 WEC as a Wave Maker .....	22
3.8 WEC Motion Profile .....	25
3.9 Electrical Circuit Analog to Wave Energy Converter.....	27
4.1 Generator Output Variation with Generator Damping.....	34
4.2 Conditional Damping Control.....	35
4.3 Limit Based Generator Force Controller.....	36
4.4 Plot of Hybrid Generator Damping Control.....	37
4.5 Schematic of Generator Hybrid Control.....	38
4.6 Plot of the 1kW WEC Response to Conditional Control.....	39
4.7 Plot of Exponential Control Surface.....	41
4.8 Plot of $C_{Gen}$ with Position Proportional Dependency.....	42
4.9 Plot of Multivariable Control Surface.....	43
4.10 Plot Representing Control Curve and Maximum Power Point.....	44
5.1 Schematic of WEC Controller.....	46
5.2 Schematic of Hydrodynamic Model.....	46
5.3 Schematic Developing the Wave Excitation Force.....	47
5.4 Schematic of the WEC Dynamic Response.....	48

## LIST OF FIGURES (Continued)

<u>Figure</u>	<u>Page</u>
5.5 1kW WEC Response.....	49
5.6 1kW WEC Response at Resonance.....	50
5.7 Bode Plot of the WEC Hydrodynamic Response.....	51
5.8 DQ Reference Frame.....	54
5.9 Schematic of $dq$ Transform.....	54
5.10 Flux Linkages of Permanent Magnet Motor Model.....	55
5.11 Entire Permanent Magnet Model.....	56
5.12 Fixed Three Phase Voltage Waveforms.....	57
5.13 DQ Voltage Waveforms.....	57
5.14 Variable Three Phase Voltage Waveforms.....	58
5.15 Variable DQ Voltage Waveforms.....	58
5.16 Space Vector Representation of WEC Voltages.....	59
5.17 WEC Power Take-Off.....	61
5.18 Model of Power Take-Off.....	61
5.19 1kW WEC Model.....	62
5.20 1kW WEC Response with No Load.....	63
5.21 1kW WEC Response with Reactive Control.....	64
5.22 1kW Generator Output with Reactive Control.....	65
5.23 1kW Generator Output versus Frequency and Damping.....	66
5.24 1kW WEC Response with Optimum Damping.....	67
5.25 1kW Generator Output with Optimum Damping.....	68
5.26 1kW WEC Response with Increased Damping.....	69
5.27 1kW Generator Output with Increased Damping.....	70
5.28 1kW WEC Response with Limit Control.....	71
5.29 1kW WEC Response with Conditional Damping Control.....	72
5.30 $C_{Gen}$ versus $\dot{z}_B$ from Simulation.....	73
5.31 Pierson Moskowitz Wave Spectral Density.....	74
5.32 Randomly Generated Wave Profile with $H_{1/3}=1.5$ .....	75

## LIST OF FIGURES (Continued)

<u>Figure</u>	<u>Page</u>
5.33 Randomly Generated Wave Profile with $H_{1/3}=2$ .....	76
5.34 Comparison of Two Incident Wave Profiles.....	77
5.35 1kW WEC Response to Random Wave Profile with $H_{1/3}=2$ .....	78
5.36 Close-up of WEC Response to Random Wave Profile with $H_{1/3}=2$ .....	78
5.37 Generator Force from Random Wave Profile with $H_{1/3}=2$ .....	79
5.38 Generator Output Power from Random Wave Profile with $H_{1/3}=2$ .....	79
6.1 Physical Diagram of the 1kW WEC.....	82
6.2 PowerEx PowerPack Module.....	83
6.3 Control Hardware Schematic.....	84
6.4 Interface layout of the NI compact RIO.....	85
6.5 cRIO Real-Time Controller.....	86
6.6 cRIO FPGA Chassis.....	86
6.7 cRIO I/O Modules.....	87
6.8 LabView Programming Environment.....	88
6.9 Wiring Schematic for the cRIO.....	89
6.10 Magnetostrictive Principle.....	90
6.11 MTS Linear Position Sensor.....	90
6.12 Wireless Communications for cRIO.....	91
6.13 FreeWave Ethernet Radios.....	92

## LIST OF TABLES

<u>Table</u>		<u>Page</u>
2.1	Linear Wave Properties .....	14
3.1	Mechanical and Circuit Equivalency Table.....	27

## LIST OF APPENDICIES

<u>Appendix</u>	<u>Page</u>
A. Matlab M-file Generating Stochastic Wave Profile.....	100
B. Simulation Matrix of Control Triggers and Augmentation Laws.....	102
C. Electrical Schematic of 1kW WEC.....	104

# **A NOVEL CONTROL DESIGN FOR A WAVE ENERGY CONVERTER**

## **1. INTRODUCTION**

### **1.1 Wave Energy Background**

As the world's demand for energy grows the search for viable and sustainable energy resources grows with it. It is evident that our appetite for energy will continue to grow and the need for a clean and renewable energy resource will become vital. Today wind energy is leading the march toward a more renewable energy future. Wind energy has proven to be a clean and economically viable energy source; however a more diverse energy portfolio is needed.

Ocean wave energy is poised to become the next major player in the renewable energy field, its high energy density and high availability make it an even more attractive alternative to wind energy. The predictability of ocean wave energy resources allows for hours and even days of forecasting that is only dreamed about by wind developers. The number of locations globally that lend themselves well to wave energy extraction is staggering. Fifty percent of the earth's population lives within fifty miles of an ocean. This close proximity of generation to load makes it an ideal candidate for our future energy needs.

The world's first wave energy device was patented in 1799 by Girard, in Paris. Since then, wave energy research has experienced periods of growth and periods of remission. During the 1970's oil crisis there was a strong motivation to develop alternative sources of energy. Many of the major advancements in alternative energy including ocean wave energy were seen during this period. Once the crisis abated, the interest in wave energy declined and only resurfaced whenever energy prices soared. Today, the driving factors for wave energy research include environmental concerns, the need to diversify our energy sources, loosening our dependence on foreign energy supplies, and advancements in power electronics technologies that will improve wave energy's resource potential.

## **1.2 Motivation**

Oregon State University's direct-drive wave energy buoy research focuses on a simplification of processes. In order to use conventional rotary electric generator in a wave energy converter hydraulic, pneumatic, or mechanical power conversion must be employed. There are many disadvantages to having these intermediate stages of conversion; they are often highly inefficient especially under the partial loading conditions that are characteristic of wave energy conversion. They are also generally high maintenance and require periodic service or replacement. Our goal is to replace devices employing these intermediate stages with direct-drive approaches that allow wave energy generators to respond directly to the movement of the ocean. By employing magnetic fields we can achieve contact-less mechanical energy transmission in order to harness the electrical energy. Advancements in power electronics technologies allow for the ability to efficiently extract maximum energy. In order to achieve this high efficiency a control scheme must be developed in order to dictate the behavior of the buoy. It is this controller making decisions in real-time that governs the generator loading. Once these decisions are made control signals are sent to an active IGBT power converter which gives us the ability to dynamically change the loading of the generator to affect the motion of the heaving buoy.

To date the energy systems group at Oregon State University (OSU) has produced four prototype Wave Energy Converters (WEC) that have proven the ability to effectively convert the linear motion of an ocean wave into electric power. The prototype currently under construction and that will be referred to throughout this text as the 1kW WEC, is a permanent magnet transverse flux linear generator rated for a nominal output of 1000 Watts.

## **1.3 Testing Facilities**

The practical investigations for this text were performed in the Motor Systems Resource Facility (MSRF) at OSU. In late 1993 the MSRF was initiated by a consortium of the Electric Power Research Institute (EPRI), Bonneville Power Administration (BPA), the U.S. Dept. of Energy (DOE), and Pacific Gas and Electric Company (PG&E).

The MSRF is an independent test laboratory that serves as a regional resource for conducting research and testing on electric motors, generators, and adjustable speed drives with ratings up to 300 hp. A regenerative, bi-directional vector controlled converter with an induction machine dynamometer enables both motor and generator testing. The system is designed to operate in an energy recirculation mode in which 80-90% of the demanded energy, depending on the device under test, is circulated back through the internal power system. The MSRF also features a 600A three-phase independent autotransformer with a voltage range of 0 to 600V/phase. The autotransformer phase voltage can be adjusted both manually and automatically by a gear driven system. This enables testing of single-phase machines as well as multiphase machines in balanced, unbalanced, under-voltage, or over-voltage conditions.



## **2. THE OCEAN WAVE ENVIRONMENT**

It is very important to understand the ocean wave environment in order to be able to effectively capture the wave's available energy. A clear understanding of the wave dynamics will allow for the ability to make decisions that benefit the energy capture performance of a WEC system. The following chapter introduces many of the fundamental characteristics of the ocean wave environment that will assist in this unique challenge.

### **2.1 Wave Creation**

Interestingly enough ocean energy is a condensed form of solar energy. As the sun unevenly heats the earth's surface it causes pressure differentials that drive winds. When areas exposed to the sun are warmed they radiate heat into the adjacent air above them. This causes the air's volume to expand and its pressure to drop. Areas not exposed to such solar radiation remain cooler and adjacent air retains its higher density. The areas of warmer lighter air are lifted through convection allowing the cooler denser air to move in and occupy the newly formed void. These moving air masses create the winds that sweep across the earth's surface.

With the Earth's oceans acting as giant thermal reservoirs, their ambient temperature is not significantly changed by the daily solar cycle. Areas of land on the other hand respond much more quickly to the solar radiation, resulting in large thermal and pressure gradients along the Earth's coastlines. As a result often higher than normal wind conditions occur in these regions.

Solar radiation strikes the earth more directly at the equator and tropics than in Polar Regions. Radiation also strikes the earth at a lower angle near the poles and the sun's rays must therefore penetrate a greater thickness of atmosphere. Consequently, the atmosphere above the equator receives 2.5 times more incoming solar radiation than the atmosphere above the poles. This variation in solar radiation at the poles and equator creates a heat gradient that causes warm air to move toward the poles and cold air toward the equator.

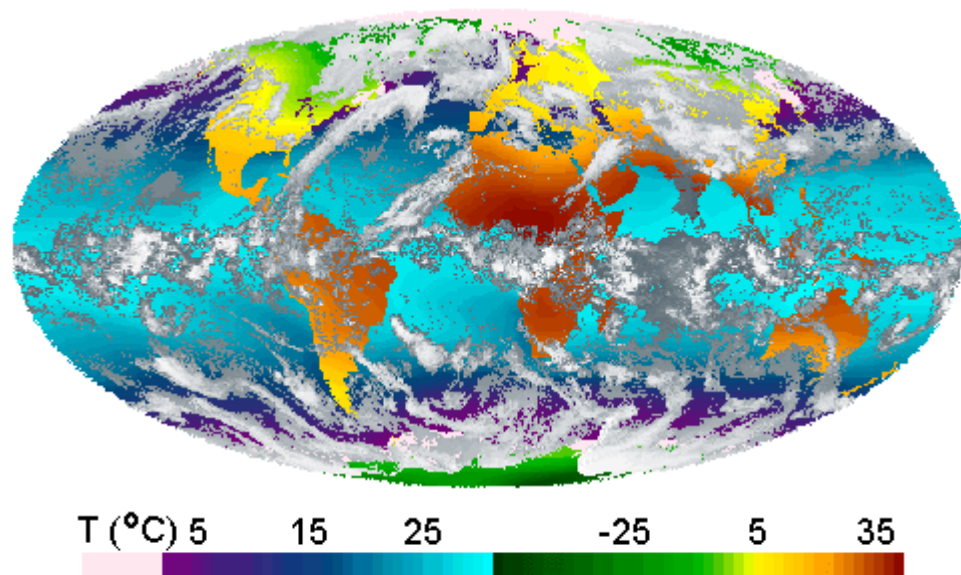


Figure 2.1 - The image shows global cloud cover, sea surface temperatures and land surface temperatures for March 24, 1998. Image courtesy of the Space Science and Engineering Center at the University of Wisconsin, Madison [25].

Global atmospheric circulation patterns would be simple if the earth did not rotate. Air flow in this idealized world would be driven by the pressure differences between the equator and poles. Warm air would rise at the equator and descend at the poles, forming a hemisphere scale convection cell illustrated in Fig 2.2.

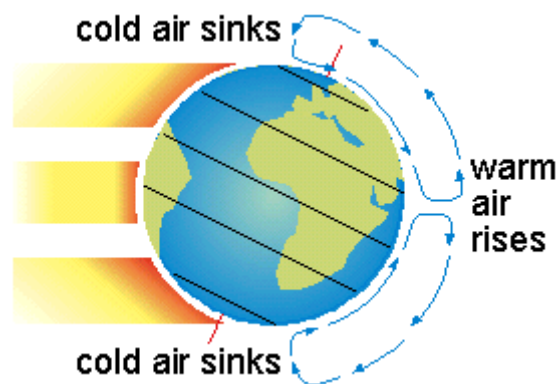


Figure 2.2 – Simple atmospheric circulation driven by thermal variations in a non rotating earth [25].

Of course the earth does rotate and the resulting Coriolis effect causes this longitudinal flow to be disrupted as winds are deflected to the right of their course in the northern hemisphere and to the left in the southern hemisphere. Atmospheric circulation is divided into three convection cells in each hemisphere. From the equator to the poles these cells are the Hadley Cell, Ferrel Cell, and Polar Cell. Figure 2.3 shows the convection cells in each hemisphere, the low and high pressure systems, and the wind patterns that result from their interaction.

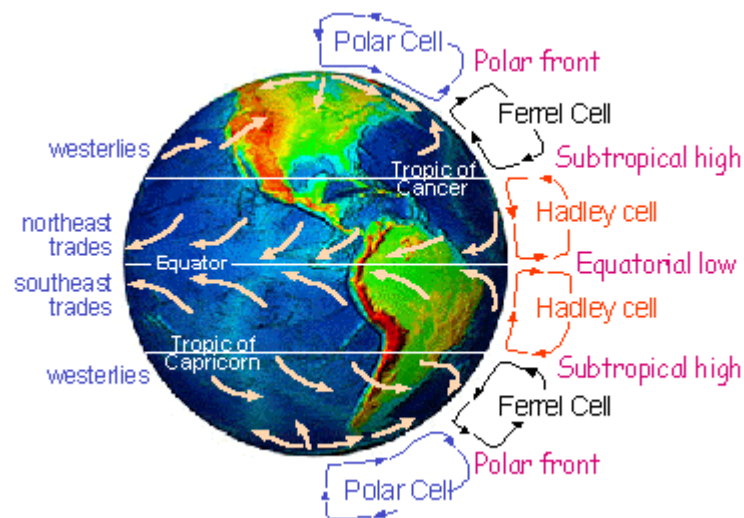


Figure 2.3 - Atmospheric Circulation and Resulting Winds [25].

These convection cells create the predominating winds across the Earth. In the Northwestern U.S. the winds are predominately out of the southwest and are referred to as the westerly winds or westerlies. These winds blow long distances across the open Pacific Ocean and create large disturbances on the oceans surface before they make landfall. As the wind blows over the ocean, it creates small ripples on the surface often called capillaries or catspaws. As these ripples grow, the wind gets better friction on the ocean surface. After a period of time, these ripples grow into chop on the water. As the wind increases and continues to blow, the chop transforms into small waves, then into larger waves and even huge swells. There are three variables that determine the size of

the wave. The winds velocity directly affects the amount of instantaneous power that can be transferred into the wave from the wind. The winds duration and fetch affect the amount of time that this power can be transferred into the wave. Together these three variables determine the total amount of energy that is stored in the wave and the result is seen as the wave's height. The term fetch refers to the horizontal distance across the waters surface which waves are able to develop. The greater the wind speed, the longer the time it blows and the larger the fetch, the bigger the waves will become. Limitation of any one of these variables will restrict the transfer of energy into the waves and limit the wave heights.

As waves grow larger, the distance between waves or the wavelength will become greater, signifying more and more energy being transferred deeper into the ocean. As this happens, waves increase their ability to sustain energy while traveling great distances across the ocean. This allows for very accurate energy forecasting hours and even days in advance. The relationship between the wavelength, water depth, and the wave period is determined by the ocean wave equation.

## 2.2 Wave Equations

The ocean wave equation is derived from the fundamental wave equation from physics that describes the evolution of harmonic waves over time. All wave behavior including radio waves, microwaves, electromagnetism, light, sound, water waves, thermal radiation, and vibration can be described by the fundamental wave equation:

$$\frac{\partial^2 u}{\partial t^2} = c^2 \nabla^2 u \quad (2.1)$$

where  $\nabla^2$  is the Laplacian,  $c$  is the velocity of propagation of the wave, and  $u$  is the displacement. Due to the fact that we are only interested in two dimensions for the case of ocean waves and we can reduce the wave equation to:

$$\frac{\partial^2 u}{\partial t^2} = c^2 \left( \frac{\partial^2 u}{\partial x^2} + \frac{\partial^2 u}{\partial y^2} \right) \quad (2.2)$$

All waves have some common features, such as the wave speed, amplitude, and period. For most waves in the physical world the speed of the wave is fairly constant and is

independent of the wave amplitude and period. For water waves however, the speed of the wave is very dependent on the water depth and the period. This makes ocean waves very unique with interesting results. After much math and manipulation and after solving for the velocity, the wave equation for water waves is shown in Equation 2.3.

$$c = \sqrt{\frac{g\lambda}{2\pi} \tanh\left(2\pi \frac{h}{\lambda}\right)} \quad (2.3)$$

Where  $c$  is the wave velocity,  $g$  is the acceleration due to gravity,  $h$  is the depth of the water, and  $\lambda$  the wavelength.

### 2.3 Ocean Wave Spectrum

This variability in wave velocities coupled with a range of wave heights and periods transforms the ocean surface into a chaotic mess. This seemingly random mixture of velocities, heights, periods, and directions is known as the wave spectrum.

Wave spectral information is available from a variety of organizations and is used widely by researchers and scientists in many different fields. Governmental organizations have many interests in the wave environment and the wave spectral data. Agencies like the Navy, National Oceanic and Atmospheric Administration (NOAA), National Science Foundation (NSF) and the Army Corp of Engineers use wave climate information in many of their research efforts.

Along the West Coast there is a large availability of wave climate information provided by NOAA, Scripps Institution of Oceanography, and even the Oregon Coastal Ocean Observing System (OrCOOS). Such sources can provide a vast array of meteorological and wave climate data. One source that has provided a wealth of information for our ocean wave energy research is NOAA's National Data Buoy Center (NDBC). The NOAA NDBC is part of the National Weather Service (NWS). NDBC designs, develops, operates, and maintains a network of several hundred data collecting buoys and coastal stations. The NDBC Station 46050 - Stonewall Banks is a moored buoy located 20 nautical miles west of Newport, OR and is a terrific resource for local wave climate information. Station 46050 is fitted with a variety of meteorological and

wave climate equipment that records wind speed and direction, wave height and period, air and water temperature, and atmospheric pressure.

The wave spectrum is often divided up into categories depending on wave period. The shortest wave periods below about 2 seconds are often ignored for the purpose of energy capture due to their high frequency and generally low energy availability. A large WEC with significant mass does not respond appreciably to this high frequency excitation. Wind waves usually considered between 2 – 10 seconds hold the largest energy in the spectrum and are the design target for most WEC systems. Generally swells are considered longer waves with periods from 10 – 25 seconds. Swells are important to consider for energy capture due to their high energy content and the ability of floating bodies to positively respond to them. The band of waves that extends beyond 25 seconds is known as infragravity waves and is the result of nonlinear shoreline interactions with long wave trains. This surge-like wave only exists in areas dictated by the local bathymetry. The infragravity wave band is shown by the broken line in Fig 2.4.

Various statistical models have been used to predict the wave spectra. Perhaps the most widely accepted is that proposed by Pierson and Moskowitz in 1964. They assumed that if the wind blew steadily for a long time over a large area, the waves would come into equilibrium with the wind, giving us the concept of a fully developed sea. Figure 2.4 shows a graph of their theoretic results which accurately predict the wave spectra for various wind conditions. The units on the vertical scale measure spectral density in units of  $[m^2/Hz]$ . This represents the square of the average wave height per unit width of frequency. The wave height squared is used to indicate the energy density at each frequency.

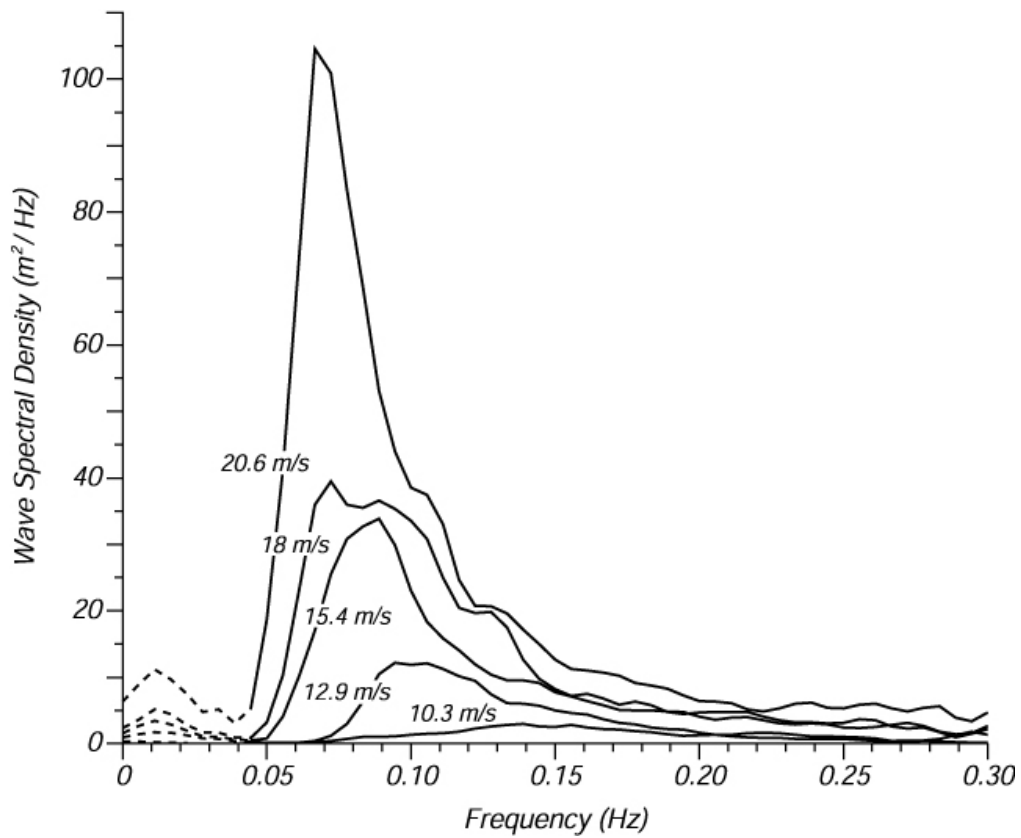


Figure 2.4. Wave spectra of a fully developed sea for different wind speeds according to Pierson and Moskowitz (1964).

All current and historical data from the NDBC buoys is easily accessed online and is presented in a variety of manners. Having access to the full database dating back to the buoys deployed allows us to develop long term trends and averages to get an idea of the areas wave climate.

Figure 2.5 is a sample frequency spectrum taken from the NDBC Station 46050.

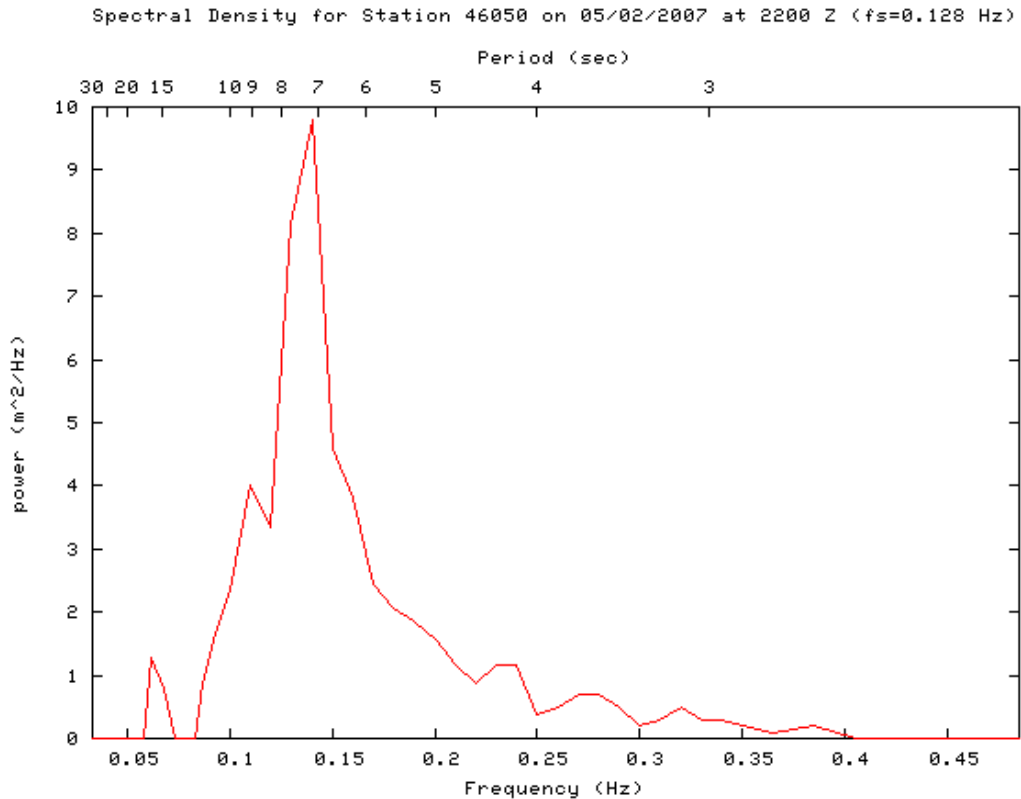


Figure 2.5 – Spectral Wave Density Data from NOAA Buoy Station 46050.

The two most significant pieces of information to consider when you are designing a WEC system are the wave height and period. Information about the dominant wave period is very important for tuning the WEC buoy to respond in resonance to the excitation force. Wave height information is also essential when designing a WEC by giving an indication of the amount of available power in the wave. These concepts will be discussed more fully in Chapter 3 on Optimum Control Theory.

Figure 2.6 shows a sample of the wave displacement recorded by the NOAA NDBC Station 46050 off the coast of Newport, OR. This data was taken during a summer wave climate.



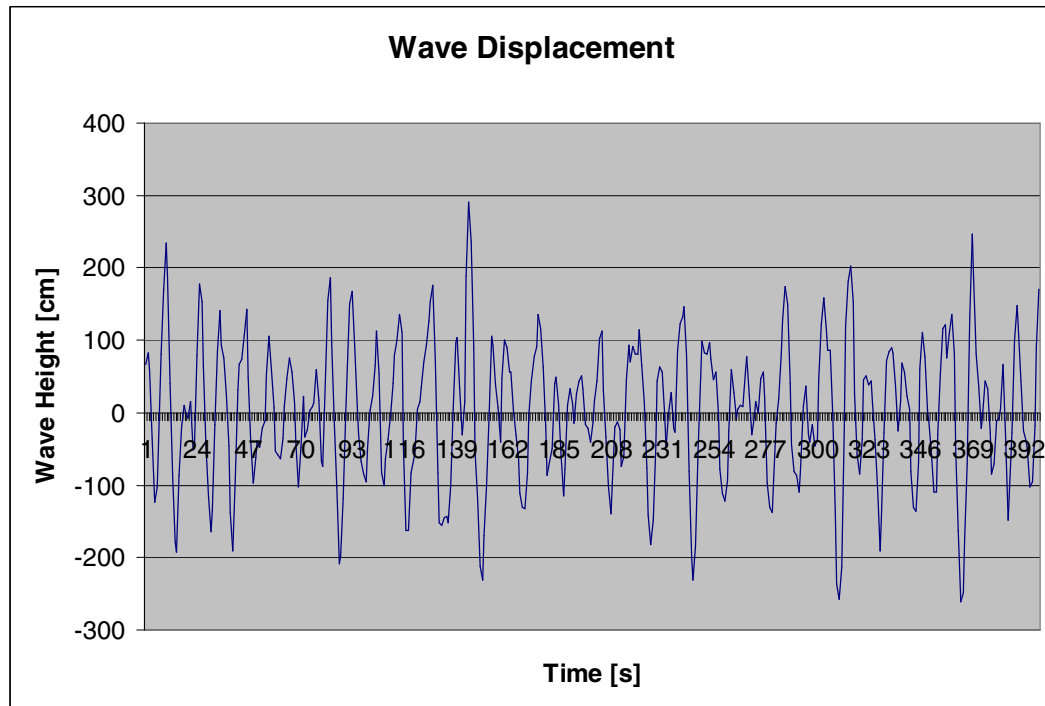


Figure 2.6 – Sample Wave Profile Data Taken from NOAA Station 46050.

An ocean wave acts to transmit energy from one region of the ocean to another. The wave does not transmit water from one area to another; however it does displace water, as a means of transmitting energy as it travels. If you were to watch the motion of a differential volume of water, often referred to as a water particle, near the water's surface you would see that it tracks in a near circular trajectory with a radius equal to the wave's amplitude. When the particle travels in this circular pattern shown by Fig 2.7, it is trading gravitational potential energy with kinetic energy in an ongoing cycle that propagates the wave's energy.

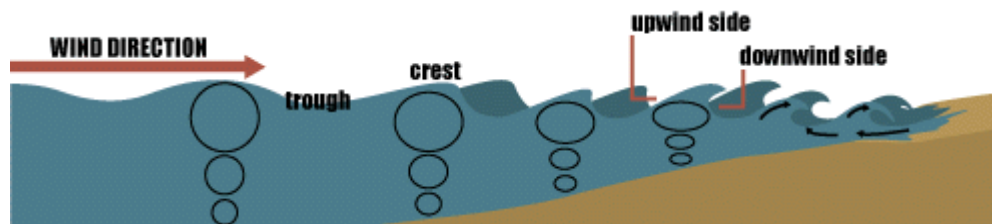


Figure 2.7 – Image Showing Water Particle Orbits in Shoaling Waves [25].

The water particles' radii decay with increased depth below the surface and can be considered negligible at a depth of  $\lambda/2$ , where  $\lambda$  is the wavelength. Equations 2.4a and 2.4b govern the particles motion with vertical position and water depth.

$$\zeta = -\frac{H \cosh k(d+z)}{2 \sinh kd} \sin(kx - \sigma * t) \quad (2.4a)$$

$$\xi = \frac{H \sinh k(d+z)}{2 \sinh kd} \cos(kx - \sigma * t) \quad (2.4b)$$

Where  $\zeta$  and  $\xi$  are the horizontal and vertical displacements,  $k$  is the wave number equal to  $\frac{2\pi}{\lambda}$ ,  $d$  is the water depth,  $z$  is the depth below the surface,  $\sigma$  is  $\frac{2\pi}{T}$  and  $T$  is the wave period. These equations can then be differentiated to get the water's velocity and acceleration which are also very important to consider when designing an effective WEC. Figure 2.8 shows the method which the wave dimensions are measured.

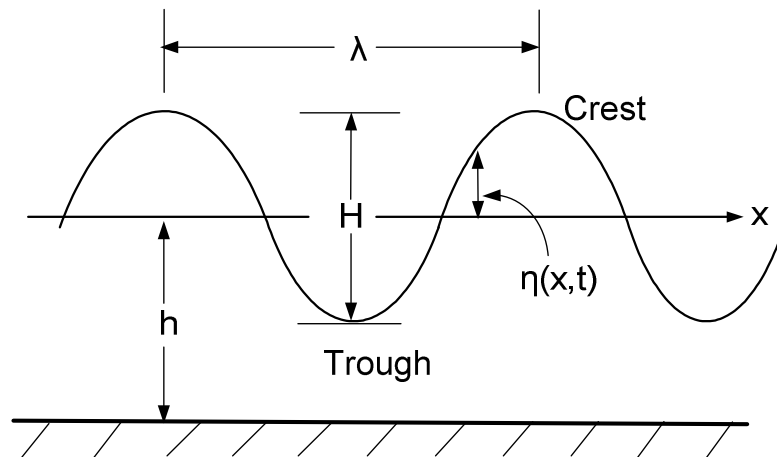


Figure 2.8 – Wave dimensions.

From the wave equation we know that waves behave differently in various water depths. For this reason the study of wave behavior has been broken into subcategories and is classified by its different depth conditions. Table 2.1 classifies some basic linear wave properties.

Table 2.1 – Linear Wave Properties.

	Condition	Wave Velocity	Wave Length
Deep Water	$\frac{d}{\lambda} > \frac{1}{2}$	$c = \sqrt{\frac{g \lambda}{2 \pi}}$	$\lambda = \frac{g T^2}{2 \pi}$
Intermediate Water	$\frac{1}{2} > \frac{d}{\lambda} > \frac{1}{20}$	$c = \sqrt{\frac{g \lambda}{2 \pi} \tanh\left(2 \pi \frac{d}{\lambda}\right)}$	$\lambda = \frac{g T^2}{2 \pi} \tanh\left(2 \pi \frac{d}{\lambda}\right)$
Shallow Water	$\frac{d}{\lambda} < \frac{1}{20}$	$c = \sqrt{g d}$	$\lambda = T \sqrt{g d}$

When the water depths are limited to either intermediate or shallow water conditions, the trajectory of the water particle flattens out into an ellipse. This is because the sea floor is an impermeable barrier which eliminates particle motion in the vertical direction. A particle at the sea floor is then restricted to only horizontal motion.

We can see from Equations 2.3 and from Table 2.1 that wave velocities decay as they reach shallower water. In order to satisfy the conservation of energy the waves must maintain the same energy. To do this the waves' height actually increases as they enter shallow water. When waves approach shallower water near shore they begin to drag across the ocean floor. It is this friction that makes the waves slow down which causes the wavelength to reduce. The ocean floor also drives the energy below the surface upward, giving rise to the increased wave height. The longer the swell period, the more energy is under the water. This means that long-period waves will grow much more than short-period waves. As the waves pass into shallower water, they become steeper and more unstable. As more energy is pushed upward it will finally reach a point where the waves break. Waves generally break at the point when the wave height reaches about 80% of the water depth.

It is important that the deployment of a WEC is well enough offshore that it is outside of the potential breaking wave region. Wave forces as a result of breaking waves can reach magnitudes 8-10 times that of the same non-breaking wave. The cost of power transmission should also be considered when determining the offshore distance of a WEC.

## 2.4 Ocean Wave Energy

There are several methods of quantifying the available energy in a wave. Because waves are a continuous progression of energy it is often customary to present this in the form of power incident on a plane that is perpendicular to the wave direction per unit crest length. To do this we must first look at the available energy per unit surface area. The energy is composed of both kinetic and potential energy so it is important to consider both forms. The available potential energy is determined by the amount of mass that is displaced from the mean water level and is simply an extension of the potential energy equation:

$$E_p = mgh \quad [\text{J}] \quad (2.5)$$

Wave potential energy takes the form of Equation 2.6:

$$E_p = \frac{1}{16} \rho g H^2 \quad [\text{J/m}^2] \quad (2.6)$$

where energy is measured in Joules per unit surface area. The kinetic energy is due to the water particles motion and is governed by the kinetic energy equation:

$$E_k = \frac{1}{2} m v^2 \quad [\text{J/m}^2] \quad (2.7)$$

where the particles velocity can be determined by differentiating the displacements  $\zeta$  and  $\xi$ . The wave kinetic energy is also found to be:

$$E_k = \frac{1}{16} \rho g H^2 \quad [\text{J/m}^2] \quad (2.8)$$

Summing these two terms together leads to the total energy per unit surface area.

$$E = \frac{1}{8} \rho g H^2 \quad [\text{J/m}^2] \quad (2.9)$$

Multiplying by wavelength gives the amount of energy in one wavelength  $\lambda$ , which now gives us the energy per unit crest length.

$$E_L = \frac{1}{8} \rho g H^2 \lambda \quad [\text{J/m}] \quad (2.10)$$

We know that all of the energy is transmitted completely with each successive wave. Then all we need to do is simply divide the energy by the wave period  $T$  to get the power per unit crest length:

$$P = \frac{1}{8} \frac{\rho g H^2 \lambda}{T} \quad [\text{W/m}] \quad (2.11)$$

It's worth noting that performing this conversion from energy per unit surface area to power per unit crest length is equivalent to multiplying the energy by the waves' group velocity  $c_g$ , where  $c_g = \frac{1}{2} \sqrt{\frac{g\lambda}{2\pi}}$ .

In deep water the wavelength is equal to  $\lambda = \frac{gT^2}{2\pi}$  and the power can be expressed as:

$$P = \frac{1}{16\pi} \rho g^2 H^2 T \quad [\text{W/m}] \quad (2.12)$$

Figure 2.9 illustrates the relationship between wave height and period to the power per meter crest length.

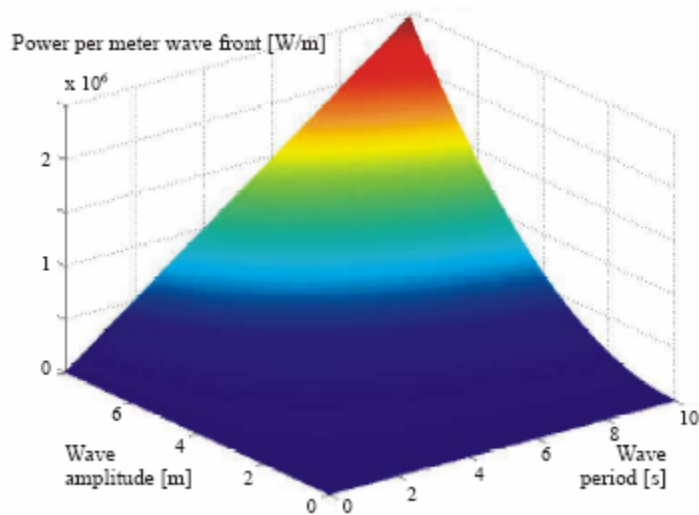


Figure 2.9 – Available Power in Varied Wave Conditions [27].

Winter storms that contain high winds can drive waves to have significantly greater wave heights than in summer conditions. Research done by the National Data Buoy Center reveals this seasonal variation in available energy. A ten year study shows power averages of 50kW/m in winter and 10kW/m averages in summer for Oregon

beaches. Interestingly this trend compares closely to the local energy demands of the Northwest, because winter months require an additional energy demand for heating homes. Figure 2.10 shows this seasonal variation in wave energy.

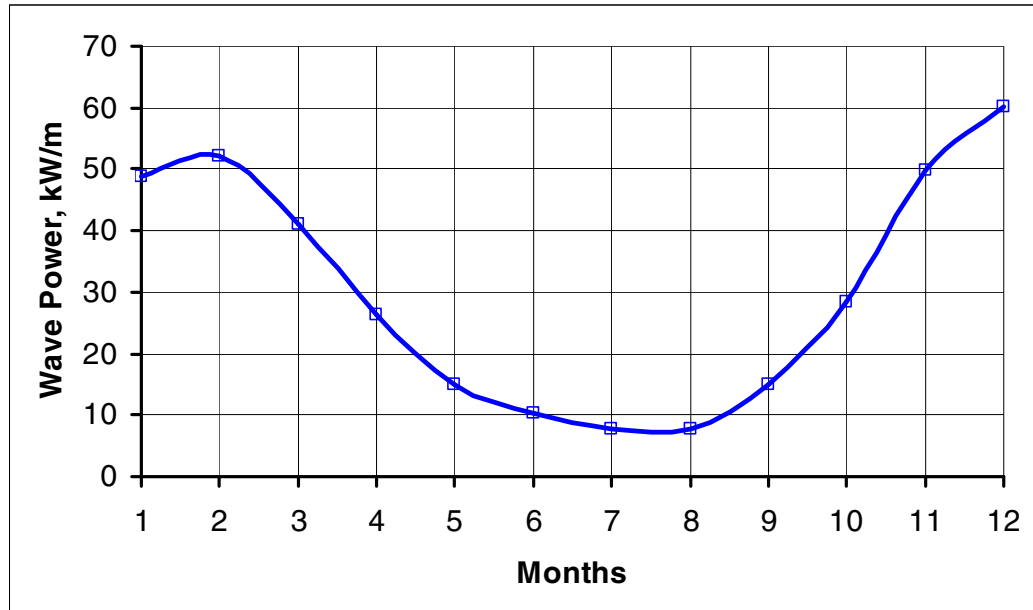


Figure 2.10 – Seasonal Variation in Wave Power.

If we take a look at the global distribution of the ocean wave energy resource we see that polar regions generally have greater wave energy potential than equatorial regions primarily due to their more extreme weather conditions. Figure 2.11 shows this global wave power distribution in units of kW per meter crest length.

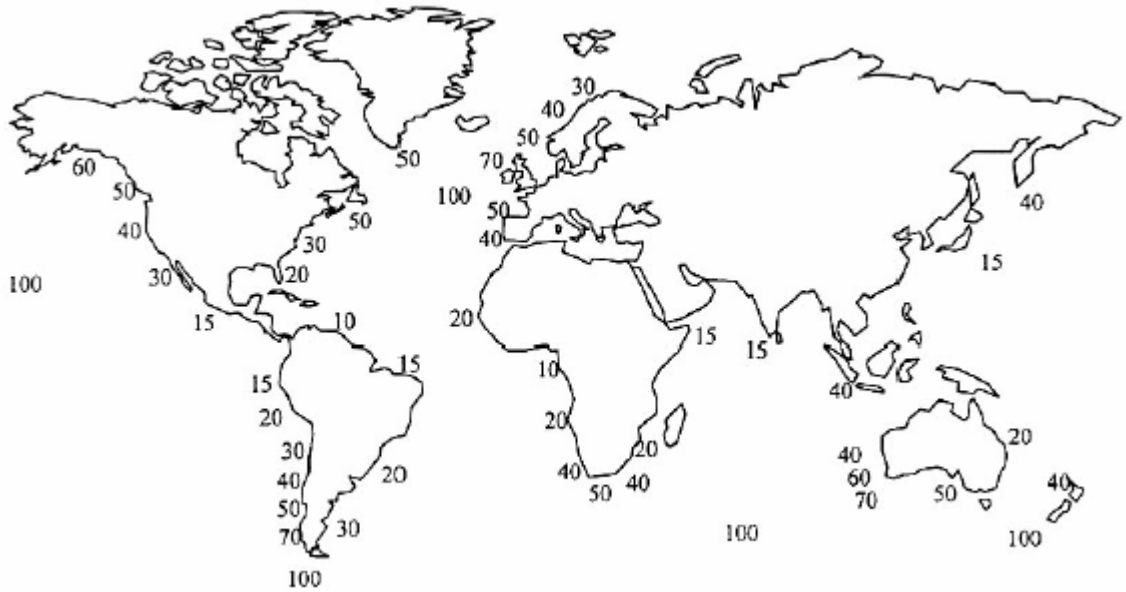


Figure 2.11 – Global Available Wave Power in kW/m.- T.W. Thorpe, ETSU, 1999 [27].

## 2.5 Pulsed Power

Looking back at the two forms of energy that are present in an ocean wave, we see how various wave energy converters attempt to capture the energy from each of these sources. It is the intended design of a symmetrical point-absorber buoy to primarily capture the potential energy of the wave. As the water level rises in a given location it undergoes a time-rate of change in the potential energy. It is this time-rate of change that gives us the output power. By capturing the potential energy we expect that the output power from the WEC will pulsate with a frequency twice that of the incident wave. This pulsed power corresponds to the buoy's velocity and is at a maximum when the buoy is rising or falling and is at a minimum when the buoy comes to rest at the crest or trough of the wave. It becomes a design challenge to effectively utilize this pulsed power. To smooth these pulsations you would need an extremely large amount of energy storage.

### 3. OPTIMUM CONTROL THEORY

After gaining a firm understanding of the ocean wave environment, the next challenge is to look at the relationship that a floating body has with the wave surface which it rides on. The first section of this chapter develops the equations of motion for a floating body. This shows us how forces from the wave are exerted on a body in order to drive the heaving motion. Later we will see how being able to accurately control the heaving motion of the buoy will allow us to absorb the maximum power possible.

#### 3.1 Morrison Model

Hydrodynamics, which means literally “water motion,” is the study in fluid dynamics which focuses on the dynamic behavior of liquids. Our focus is on the nature of the ocean’s wave generation and propagation near the waters surface, as well as wave interaction with a floating body.

There are several key concepts that must be developed in order to describe wave behavior. The most fundamental laws of hydrodynamics are known as the conservation laws. The conservation of mass states that mass cannot be created or destroyed. The conservation of momentum states that for every water particle, momentum must be conserved. The conservation of energy states that energy cannot be created nor destroyed but only converted. Additionally near the water’s surface, water can be considered incompressible, leading us to the continuity equation.

$$\frac{\partial u}{\partial t} + \frac{\partial v}{\partial t} + \frac{\partial w}{\partial t} = 0 \quad (3.1)$$

The continuity equation satisfies the nondivergent flow criterion. This means for a unit cube of fluid, if there is a change in flow in a particular direction across the cube, there must be a corresponding flow change in another direction, to ensure that no fluid accumulates in the cube. If a fluid is constrained to laminar flow, without turbulence, it is considered irrotational and we can use the Bernoulli equation.

$$-\frac{\partial \phi}{\partial t} + \frac{1}{2}(u^2 + v^2) + \frac{p}{\rho} + gz = C(t) \quad (3.2)$$



The Bernoulli equation is an extension of Euler's equations and represents the conservation of energy for a fluid in motion.

There have been many attempts at extending the Bernoulli equation and the conservation laws to a floating object on the free surface of a wave. Perhaps one of the most widely accepted linearization of this is the Morrison model. A derivation of the Morrison model is presented by Patel in his book Dynamics of Offshore Structures [5]. In this book the concept of the wave excitation force is displayed. The excitation force is dependent on the incident wave and the hydrodynamic characteristics of the floating object:

$$F_e = m_B \ddot{z}_W + c_B \dot{z}_W + k_B z_W \quad (3.3)$$

where  $z_W$  is the vertical position of the water surface,  $m$  is the mass,  $c$  is the linear damping coefficient,  $k$  is the stiffness, and  $F_e$  is the excitation force. Here the damping force is taken to be linear and the stiffness term  $k$  is given by the Froude-Krylov force for the buoy geometry, where the draft is small compared to the incident wave lengths.

The second governing equation is the dynamic response of the buoy from the excitation force and any applied generator force.

$$F_e + F_{Gen} = (m + A)_B \ddot{z}_B + c_B \dot{z}_B + k_B z_B \quad (3.4)$$

where  $z_B$  is the vertical position of the buoy and  $A$  is the added mass. The added mass is a term used to describe the viscous behavior that water has on a surface that is moving through it. In order to accelerate a surface through water you must also accelerate some water that is in contact with the surface.

It is typical to use this two stage approach when describing the motion response of a floating body. Having this approach from wave elevation to force and from force to motion allows access to the important excitation force term. It is possible to combine these equations into a single transfer function, with the loss of excitation force which is crucial for the optimum control of a WEC. Such a combined equation looks like:

$$m_B \ddot{z}_B + F_{Gen} = A_B (\ddot{z}_W - \ddot{z}_B) + c_B (\dot{z}_W - \dot{z}_B) + k_B (z_W - z_B) \quad (3.5)$$

Before we could accurately model the 1kW WEC we still have to determine the values of the coefficients  $m$ ,  $A$ ,  $c$ , and  $k$ . In order to find  $m$  we simply need to sum the

mass of all of the components that are enclosed in the float portion of the WEC. The added mass term can be a complex term to determine. In order to simplify this task we use the fact that our buoy is cylindrical in shape and that we are only concerned with motions in the vertical direction. This streamlines the calculations to [5]:

$$A_B = \rho C_m V \quad (3.6)$$

where  $C_m$  is the added mass coefficient equal to 0.5, and  $V$  is the volume of the buoy. The last variable  $k$ , is the water plane stiffness which can be calculated by the buoyant force due to the buoy's geometry.

### 3.2 Energy Absorbtion

Ocean waves with long fetch lengths tend to develop in a periodic nature. This periodic wave train once created will progress long distances across the ocean without significant energy loss. For the initial discussion on optimum control theory it is assumed that the ocean is composed of a single frequency monochromatic wave train that propagates across its surface. It would then be the design goal to create a WEC that can completely absorb this wave train. If this were possible no wave would be transmitted past the wave generator and no wave would be reflected from it.

Anytime a body oscillates in water it will produce a wave. Generally it can be said that a good wave absorber must be a good wave maker. Therefore in order to absorb wave energy you must create a wave that can completely cancel the incident wave. Absorbing wave energy for conversion means that energy has to be removed from the incident waves. Hence there must be a cancellation or reduction of the waves which are passing the wave energy converter. Such a reduction can be achieved by a heaving buoy, if it generates waves which interfere destructively with the incident waves. This explains what was meant by Falnes when he said "To destroy a wave means to create a wave." [1].

Falnes also shows that it is theoretical possible to absorb 100% of a wave's energy. The example he uses involves an infinitely elongated buoy that runs perpendicular to the incident wave. Complete absorption of the incident wave is shown to be possible provided the body oscillates both vertically and horizontally in a precise manner. It can be shown also that the theoretical maximum of only 50 % absorption is

possible when a symmetrical WEC is limited to only the vertical heaving motion. Likewise, if only the horizontal motion is allowed, then also no more than 50 % absorption would be possible. Falnes also suggested that a sufficiently non-symmetric buoy allowed to oscillate in only one direction, may have the ability to absorb almost all of the incident wave energy.

Figure 3.1 shows how the incident and generated wave profiles created from this infinitely elongated buoy are able to completely absorb the energy from the incident wave.

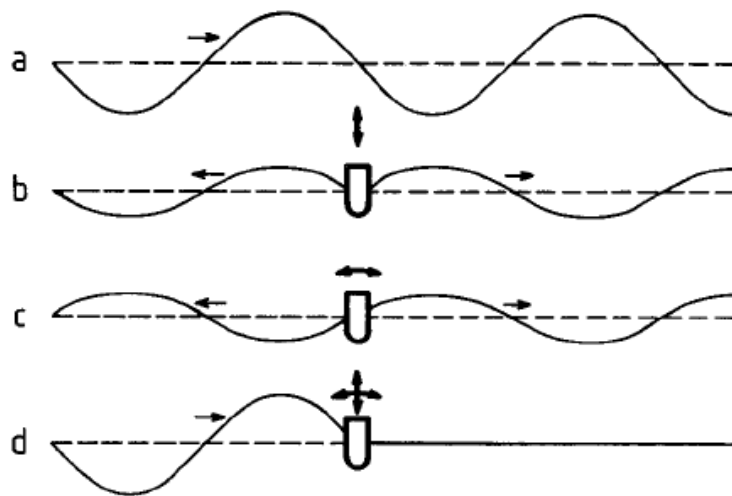


Figure 3.1 - Curve *a* represents the incident wave. Curve *b* illustrates symmetric wave generated by the heaving body. Curve *c* illustrates antisymmetric wave generated by motion in the horizontal direction. Curve *d* represents the superposition of the above three waves, illustrating complete absorption of the incident wave energy [1].

This argument can be extended to a heaving point absorber, which by definition is very small compared to the wavelength. For a point absorber the motion must be controlled so that we create a circular wave that radiates properly in order to interfere destructively with the incident wave. A point absorber can however capture more power than that of the incident wave power of width equal to that of the point absorber. The maximum power that can be absorbed by a heaving symmetric buoy equals the incident wave power of width equal to the wavelength divided by  $2\pi$ . This width is often referred to as the “absorption width” [7]. Early experimenters, not being aware of this

relationship, were surprised by measuring absorption rates larger than the physical width of their test buoy.

### 3.3 Maximum Power Capture.

In order to obtain maximum power from the waves it is necessary to control the correct oscillation of the wave energy converter. Assuming a sinusoidal incident wave there will be an optimum phase shift and amplitude in order to achieve maximum energy capture. Looking back at Fig 3.1 we see that the amplitudes of the radiated waves; curves *b* and *c*, have to be exactly half of the amplitude of the incident wave; curve *a*. This means that the amplitudes of the vertical and horizontal oscillations of the WEC have to be accurately controlled. The two waves radiated towards right, generated from the WEC must have the same phase as one another and opposite that of the incident wave. To illustrate this we see that the crests of the waves *b* and *c* radiated towards right must coincide with the trough of the incident wave *a*. Additionally the two waves that are radiated towards the left must also cancel one another.

For a point absorber buoy we are limited to one mode of oscillation in the vertical heaving direction. This limits us to generating waves that are represented by curve *b*. The resulting superposition of the waves *a* and *b* should have the same amplitude and phase as in the two-mode oscillating case. The wave radiated towards the left and the resulting waves transmitted towards the right both have amplitudes equal to half of the amplitude of the incident wave. Because wave energy is proportional to the square of the wave amplitude this means that 25 % of the incident wave energy is reflected towards left, and 25% of it is transmitted towards right. The remaining 50 % is absorbed by the WEC, and this is the theoretical maximum previously mentioned. This only occurs when the buoy is at resonance with the incident wave. It also coincides with the buoy's velocity being in phase with the wave's exciting force acting on the system [1],[2].

The most effective way to achieve the precision motion of the buoy to obtain maximum power capture is through resonance. If a buoy is designed to be at resonance with the incident wave frequency it will become locked in phase with the incident wave. The only control that is needed in resonance is to modulate the amplitude of the

oscillations. This optimum phase condition can be approximately fulfilled for wave frequencies close to resonance. This relative tolerance is known as the resonance bandwidth of the system. WECs of very large physical dimensions have broad bandwidths. In order to be cost effective it is often desirable to utilize a WEC system of smaller physical size. The drawback of this is that the resonance bandwidth becomes rather narrow. Then for small-sized WECs it is very important to apply some form of phase control, in order to obtain the optimum phase condition.

In practice the optimum oscillation amplitude is somewhat smaller than the theoretical amplitude. This smaller amplitude required to maximize the converted useful energy is the result of unavoidable lost energy due to friction, viscosity, heating etc. Often times, with the exception of small or moderate wave heights, this desirable amplitude may be limited by the design amplitude of the WEC [1]. Even for the case when the oscillation amplitude is limited by design, the absorbed energy, as well as the converted useful energy, is maximized when the heave velocity is in phase with the exciting force due to the incident wave.

In practice, the maximum rating of the WEC is also limited. For economic reasons the WEC ought to be designed in such a way that it works close to its design limit a rather large portion of the time. As a consequence much of the wave energy remains in the ocean, except during time periods of rather moderate wave activity.

In order to obtain the optimum oscillatory motion for maximizing the absorbed energy it may be necessary to return some energy back into the sea during some fractions of each oscillation cycle and profit from this during the remaining portion of the cycle. For this reason “optimum control” of WECs can be called “reactive control”. To achieve this in practice it is required to utilize reversible electromechanical machinery with very high efficiencies.

In order to achieve the optimum control over the WEC a complex controller must be used. Such a controller will take input from various sensors and measurements. A closer look at this controller will be discussed in Chapter 4 on Novel Control.

### 3.4 Phase control by latching.

If the WECs electromechanical machinery is not reversible or if there is not sufficient energy storage to back drive the WEC such as in reactive control there is still one alternative for increasing the energy capture of the system. Optimum phase can be roughly approximated by “latching phase control” if the wave periods are longer than the WEC’s natural period. Such a control scheme generates a WEC motion profile like the one indicated by curve *c* of Fig 3.2. In order to employ a latching control scheme a mechanical clamp must be employed to stop the motion of the WEC when it reaches its extrema. This position coincides with the point at which the velocity becomes zero. The clamp is then released a predetermined time before the next extreme in the wave excitation force. This time can be approximated by about one quarter of the natural period of the WEC. The result of this clamping technique is that the buoy’s velocity profile is roughly in phase with the wave’s excitation force.

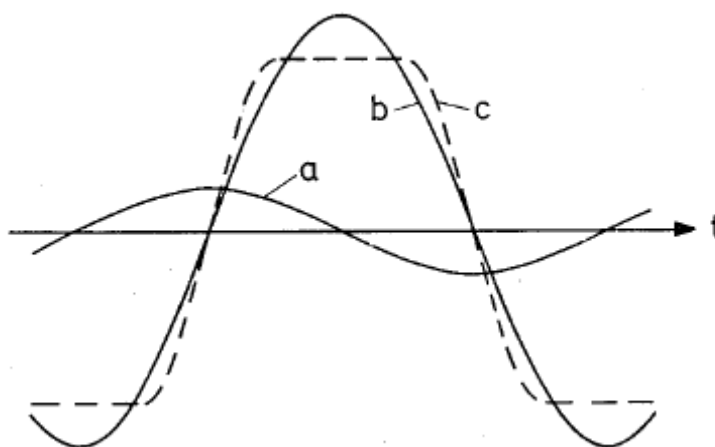


Figure 3.2 - Vertical displacement of a heaving body. Curve *a* is the wave profile or the excitation force on the buoy. Curve *b* is the vertical displacement of a buoy with reactive control. Curve *c* is the vertical displacement of a buoy with latching control [1].


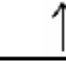

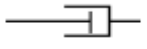




While a fairly close approach to the optimum phase can be attained by latching phase control, the amplitude may be less than optimal. By holding the buoy at the extrema before releasing it, the driving force is allowed to increase which drives the buoy to greater displacements than it would without latching control.

### 3.5 Electrical Analogy

An electrical circuit analogy was developed to explain and calculate the effects that generator damping control has on a WEC system this analogy is also supported in literature [4]. This analog uses the well know concept of the resistor, inductor, and capacitor (RLC) circuit to explain the behavior of a floating buoy in the water. For this analogy the buoys hydrodynamic damping terms will be represented as the hydrodynamic source impedance ( $Z_{HD}$ ) and the generator damping terms will be the generator impedance ( $Z_{Gen}$ ). It is important to keep in mind that  $Z_{HD}$  and  $Z_{Gen}$  are mechanical damping impedances used only for the circuit analogy and are in no way related to the electrical impedances of the generator or the load. For this analog we replace all of the circuit elements with their corresponding mechanical elements.

The excitation force is represented as an independent voltage source whose magnitude and frequency are equal to the force exerted on the buoy by the incident wave. The source impedance  $Z_{HD}$  and the load impedance  $Z_{Gen}$  will have both real and reactive parts. This allows for the alteration of both the real and reactive generator damping terms to see how the system will respond. Table 3.1 shows the mechanical to circuit analogies and their corresponding impedances and representative equations.

Table 3.1 – Mechanical and Circuit Equivalency Table.

Circuit Elements			Mechanical Elements		
Element	Impedance [Z]	Voltage [V]	Element	Mechanical "Z"	Force [N]
 $V_S$		$V$			$Fe$
	$R$	$IR$		$C$	$Cv$
	$\frac{1}{sC}$	$\frac{1}{C} \int Idt$		$\frac{k}{S}$	$k \int vdt$
	$sL$	$L \frac{dI}{dt}$		$sM$	$m \frac{dv}{dt}$

The final piece of the analogy is the buoy velocity which is represented by the current that would flow in the circuit analogy. It can be shown that by varying the  $Z_{Gen}$  we can directly affect the buoys velocity.  $F_{Net}$ , shown in the schematic of the circuit analogy in Fig 3.3 is the net force available to accelerate the buoy against the generator loading force and the excitation force.

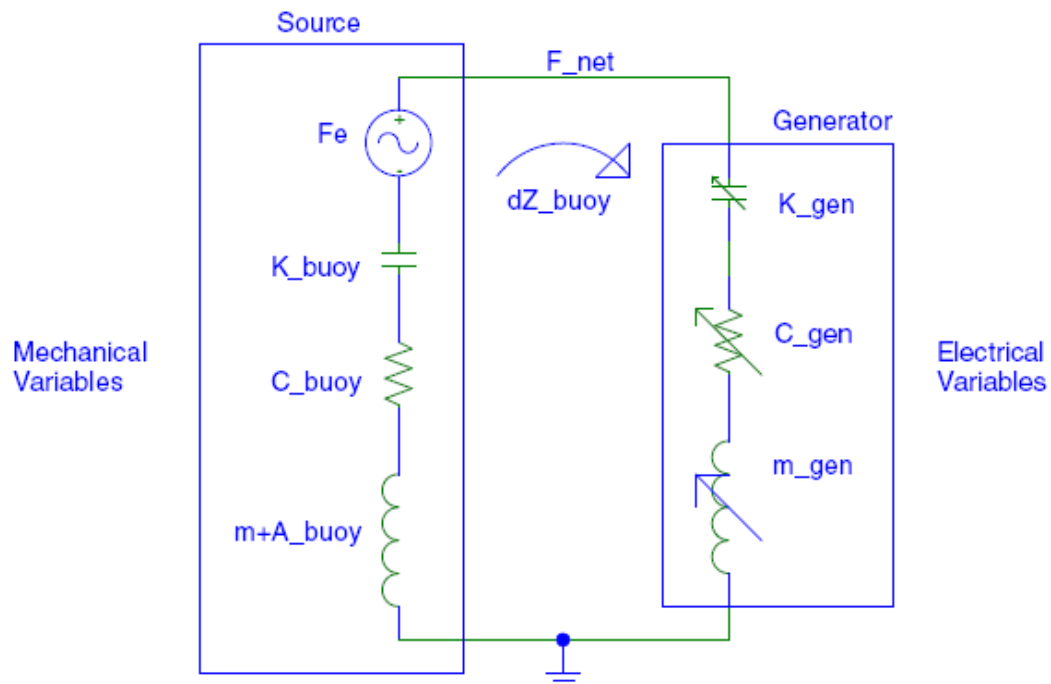


Fig. 3.3 - Electrical Circuit Analogy to Wave Energy Converter.



In order to find the resonant frequency we can use the well known RLC series circuit equation:

$$\omega_0 = \frac{1}{\sqrt{LC}} \quad (3.7)$$

It is also interesting to note that the optimum control conditions of the WEC can be equated to the maximum power transfer conditions of the circuit analogy. To achieve maximum power transfer in a circuit we want the load impedance to be the complex conjugate of the source impedance which results in the current being in phase with the voltage source. For the WEC we would want the generator's spring, damping, and mass terms,  $Z_{Gen}$ , to be the complex conjugate of the hydrodynamic terms from the Morrison equation,  $Z_{HD}$ . This results in the velocity being in phase with the excitation force. By employing this analogy we have opened the doors to many of the powerful circuit analysis tools and techniques, to study the behavior of the system and to aid in the development of a control system.

## 4. NOVEL CONTROL

Under ideal circumstances optimum control techniques would be favored in order to maximize energy harvest. Unfortunately we rarely encounter an ideal situation and are often challenged with designing a system that is constrained by real-world criteria. Our 1kW WEC is no exception; there are a variety of limitations that we must consider in the design of an effective control scheme for this and any WEC system.

### 4.1 Limitations

To help explain the effects of the various limitations have on the optimum control conditions I will continue to use the electrical circuit analogy developed in the previous chapter. The difference for the novel control design is that instead of targeting the optimum control conditions we have to make exceptions for real-world constraints that will change the loading behavior of the generator.

#### 4.1.1 Velocity and Stroke Limit

Normally high velocities are desired in a WEC system in order to increase the generator voltages. We have however, designed the permanent magnet linear generator to have large diameter coils and a large number of turns in order to increase the voltages at the terminals. With the generator velocity being directly proportional to the voltage we have to be careful not to exceed the voltage ratings of the windings and the power electronics. Limiting the generator velocity also helps to keep the overall stroke within its limits. In an effort to keep costs and dimensions of our generator within reason we designed the 1kW WEC with a maximum of one meter of stroke. This presents a very real limitation to the control behavior of the system. Under optimum control we would expect to see buoy strokes as large as 4 times that of the incident wave. Then for a 1.5 meter wave we could expect the buoy to travel as far as 6 meters!

The challenge then becomes, identifying a way to limit the velocity and stroke of the buoy so that it does not travel beyond our limits. By controlling the net available driving force on the buoy we can control its acceleration and in turn its velocity and

stroke. The excitation force is only dependent on the incident wave and the hydrodynamics of the buoy; it is therefore not possible to reduce this excitation force. The only way to reduce the net driving force is to cancel out the excitation force with generator loading. Recalling the three generator damping control variables; mass, spring and damping, we see that we can reduce the net driving force of the system by any one of the following adjustments; increasing mass, reducing spring, or increasing damping.

The circuit analogy to this is to increase  $Z_{HD}$  or  $Z_{Gen}$  or in order to reduce the overall current in the circuit.  $Z_{HD}$  has three mechanical control variable and  $Z_{Gen}$  has three generator damping control variable resulting in six total control variables. We would like to retain the same physical size and weight of the WEC so mechanical mass and spring are to be considered set variables. Adding mechanical damping is a considerable loss and should only be considered under extreme circumstances. This leaves us with only generator damping control to act on the motion of the buoy.

#### 4.1.2 Energy Storage Limit

The remaining control variables left to affect control of the velocity and stroke are the elements contained in  $Z_{Gen}$ , which are the generator mass, spring, and damping. Because generator damping control effectively simulates the presence of a mass or spring force that does not exist, we need the ability to store and release large amounts of energy at the wave's frequency. Various energy storage methods have been considered for a single generator system. Capacitor banks, flywheels, and buoyant storage may all be capable of meeting the energy storage needs but come with added cost, size, and complexity. This large amount of energy storage is considered unpractical and will not be employed in the single WEC system.

The circuit analogy equivalents to this mass and spring energy storage are the inductor and capacitor in  $Z_{Gen}$ . These elements store energy in the circuit just as mass and spring do in the WEC. To eliminate the electrical mass and spring components will be to remove the inductor and the capacitor from the circuit analogy. We expect that we will no longer be able to achieve max power transfer without these reactive elements, so

the question becomes what is the best we can do? To find out we represent the equivalent circuit with a purely resistive generator damping and calculate the resistance that gives us the greatest power output. We know:

$$P_{Out} = \dot{z}_B(t)^2 C_{Gen} \quad (4.1)$$

where,

$$\dot{z}_B(s) = \frac{F_e}{Z_{Total}} \quad (4.2)$$

and,

$$Z_{Total} = \frac{k_B}{s} + C_B + (m + A)_B s + C_{Gen} \quad (4.3)$$

Then we find the value for  $C_{Gen}$  where  $P_{Out}$  is maximized. To do this we set the  $C_{Gen}$  derivative of  $P_{Out}$  to zero and solve for  $C_{Gen}$ .

$$\frac{dP_{Out}}{dC_{Gen}} = \frac{d}{dC_{Gen}} (\dot{z}_B^2 (\frac{k_B}{s} + c_B + (m + A)_B s + C_{Gen})) = 0 \quad (4.4)$$

Interestingly it turns out that the best performance you can achieve from a purely real generator damping occurs when the load damping has the same magnitude as the source impedance. Now we have an electrical damping coefficient for the ideal loading condition when energy storage is not feasible. We will call this  $C_{Gen}^*$ .

If the WEC system was part of an array of generators with a sufficiently stiff DC buss, we could use energy from other generators to meet the back-driving needs of our WEC then return energy back into the array during periods of generation. This array wide energy storage works very well with each generator being placed at different positions and in different phases of the generation cycle.

Another reason to avoid energy storage is to avoid large generator ratings. With the additional power flowing into and out of the energy storage device the generator must be able to handle the total output capacity plus this additional energy storage capacity. Building a generator that can handle such extra capacity would ultimately become more costly.

### 4.1.3 Current Limit

One very important constraint to consider is the maximum current that can be handled by the machine. The maximum current limit is a function of the generator's ability to handle thermal dissipation. This occurs when the generator can no longer cool itself sufficiently to operate at a safe temperature. This large current can be due to insufficient load impedance or by applying too much force on the generator. The force and current are directly proportional and the current limit can also be thought of as a force limit.

### 4.1.4 Maximum Power Limit

When we talk about maximum power there are two things to consider; the instantaneous power and the average power. The instantaneous maximum power occurs at the current limit for the conductors at their maximum voltage rating. In a wave energy converter the pulsed power makes it more important to consider the instantaneous power than the average power. Due to the pulsed nature of the wave energy converter the average power is only  $\frac{2}{\pi}$  times the peak power.

## 4.2 Control Design

The proper design of an effective controller should accomplish two main goals. The first and most important is to protect the generator from any damage that is the result of operating outside of its area of safety. In order to design a controller that will protect the WEC from all of the possible limitations we need to identify what control actions can be taken to avoid each of these limits. The first limit that we have encountered was the availability of energy storage. Since it is not practical to use a reactive control scheme for the single generator case we have developed a control scheme that is only dependent on generator damping and does not utilize energy storage.

The limits that can be most destructive to the WEC are the velocity and stroke limits. When the generator is in violation of the velocity limit or is on a trajectory to violate the stroke limit we need to increase the generator damping to effectively slow the

buoy. The result is that the generator voltage will be reduced while the current being drawn from the generator will increase. If the generator's current becomes too high we can perform this same control in reverse.

This brings us to the consideration of maximum power, what if the WEC becomes in violation of the voltage limit and the current limit at the same time? This is a very serious condition that would likely be the result of an unusually large incident wave. Under these conditions the controller will have the ability to open a set of circuit breakers located at the terminals of the generator and isolate it from the load. By unloading the generator we are allowing it to heave freely and expect that it will exceed its over travel limits. This operation will likely cause the buoy to "pop-off" the spar and should only be considered under unusually extreme circumstances.

The second major goal of an effective control scheme is that it produces the highest and most reliable power that it can. The best way to accomplish this is to operate the generator at an optimized  $C_{Gen}^*$ . This only works well in moderate sea conditions, but when the wave height grows we run the risk of exceeding our stroke limits. Then in order to protect the generator we need to damp the motion by increasing the value of  $C_{Gen}$  beyond  $C_{Gen}^*$ .

A series of simulations performed on a statistical average summer wave climate, with  $H_{1/3} = 1.5$  meters and  $T = 6$  seconds, allowed for the creation of a plot of the average generator force, buoy velocity and output power versus the generator's velocity proportional damping constant. See Fig. 4.1. It is interesting to note that the curve for  $F_{Gen}$  flattens out as  $C_{Gen}$  increases. This reduction can be accounted for by the significant decrease in the buoy velocity under increased damping. The advantage of this is that it makes it unlikely that we will exceed the current rating of the generator for a velocity proportional damping control. The disadvantage however is that we may not be able to provide sufficient generator force to keep the buoy within its stroke limits.

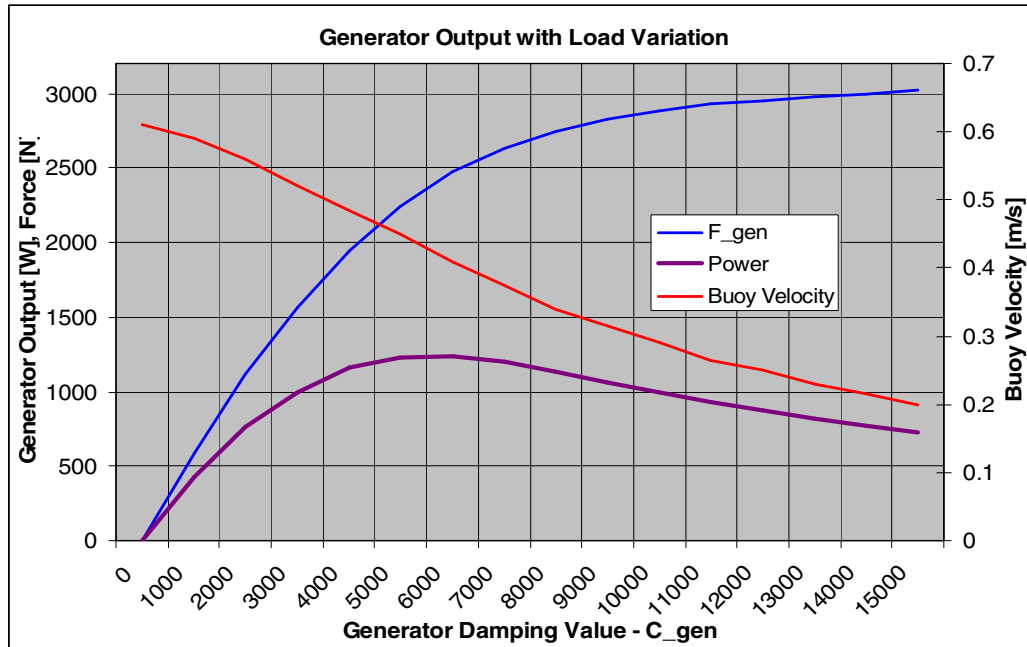


Figure 4.1 – Generator Output Variation with Generator Damping.

#### 4.2.1 Conditional Damping Control

The design goal is to determine a control method that responds well to a moderate wave climate but also has the ability to protect the system from an extreme wave condition. There are two major components to a protective controller. The first is the trigger, this defines the condition or set of conditions that have to be satisfied in order to initiate a control response. These conditions can be any number of inputs from wave height, buoy position, buoy velocity, generator current or even generator temperature. For our controller we are most interested in the buoy's velocity and position and all of our triggering conditions will be based on these two variables.

The second major component is the augmented damping control law. This is the function that defines how the generator damping  $C_{Gen}$ , is augmented as it satisfies the trigger conditions. There are a variety of methods to do this, the challenge becomes selecting the method that best meets our design needs. Figure 4.2 shows how the trigger and augmentation law can affect the generator damping. Here  $C_{Gen}$  is dependent on  $\dot{z}_B$ .

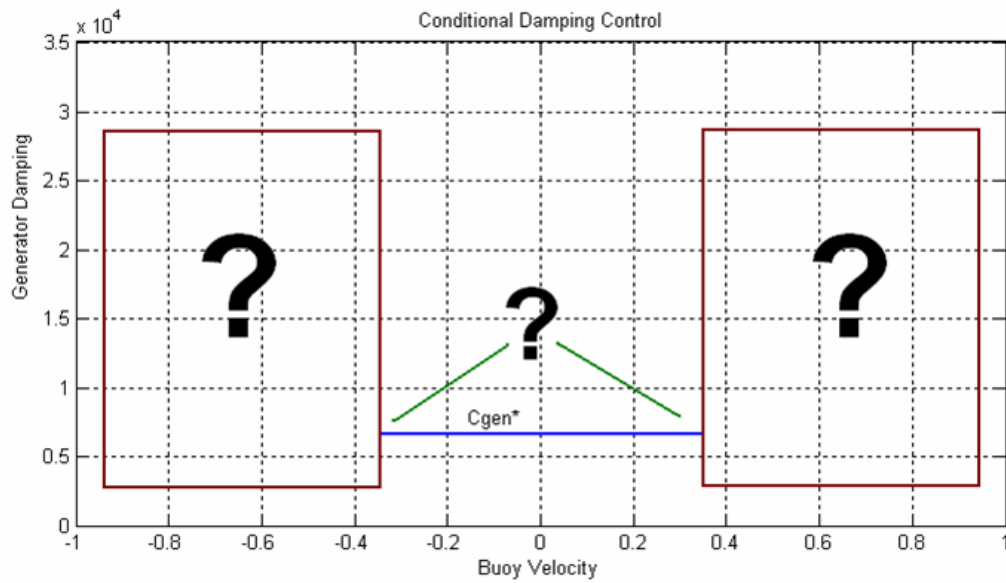


Figure 4.2 – Conditional Damping Control.

The first logical approach is to use a limit based approach where limits are defined and  $C_{Gen}$  is discretely increased as it exceeds the limit conditions. For this I used two limits for each, one that modified  $C_{Gen}$  slightly and a second that modified it more drastically. The idea was that if it exceeded the first limit, preventative control would be taken to correct the impending violation and if the second limit was exceeded a more forceful approach would be taken. Figure 4.3 shows a block diagram of what this control would look like.



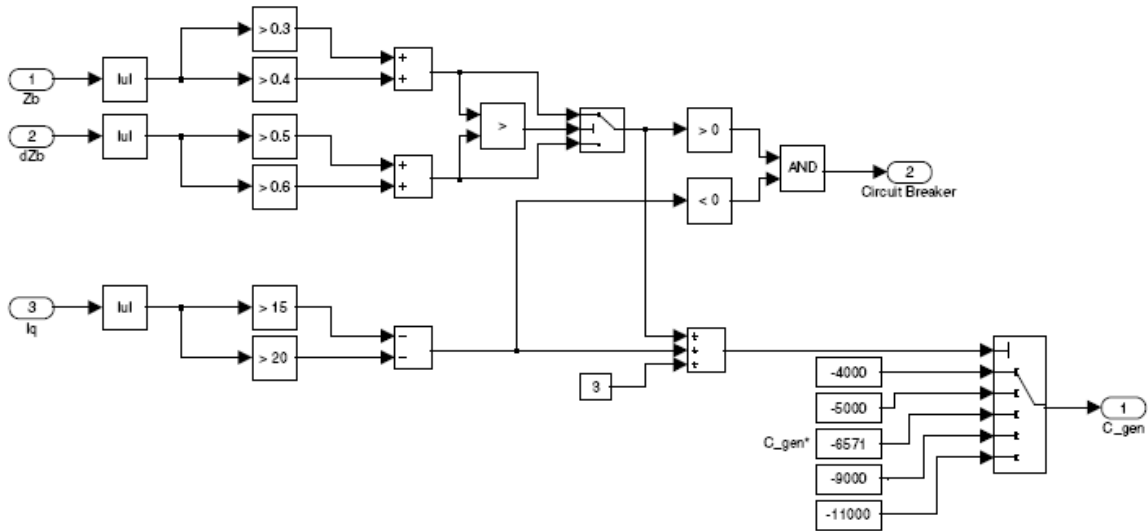


Figure 4.3 – Limit Based Generator Force Controller.

This design has many unfortunate drawbacks. This type of control causes discontinuous force that can have damaging affects throughout the system. Also by tuning the limits and damping constants for a given wave profile it would not respond adequately to different wave climates.

A controller was needed that would operate as independently as possible to the wave while providing continuous control over the full range of operating conditions. The idea of exponential control is an extension of the limit based control but eliminates the step change increases in  $C_{Gen}$ . Exponential control can be based on a single input variable or a combination of variables known as multivariable control. This means  $C_{Gen}$  could be defined as:

$$C_{Gen} = f(\dot{z}_B) \text{ or } C_{Gen} = f(z_B, \dot{z}_B, \ddot{z}_B, I_{Gen}, \dots) \quad (4.5)$$

By using generator damping coefficients that are exponential quantities of the control variables, limit violations can be prevented by delivering a gradual yet forceful increase in the generator force. As the velocity grows the control force will grow with the exponent to prevent the violation from occurring. It has been shown that larger values of the exponent are more independent of the wave profile and perform well in a wide variety

of sea conditions. These large exponents exaggerate the control response and act to restrain the buoy velocity.

Conditional damping control creates a hybrid approach between ideal loading and exponential augmentation control. This type of hybrid can provide the best of both worlds. Operation with  $C_{Gen}^*$  would occur during moderate sea conditions. When the wave climate increased the controller would be driven into the augmented protective control region. Figure 4.4 illustrates what this conditional damping control would look like implementing exponential control augmentation. Here the augmented  $C_{Gen}$  is proportional to  $\dot{z}_B^2$ .

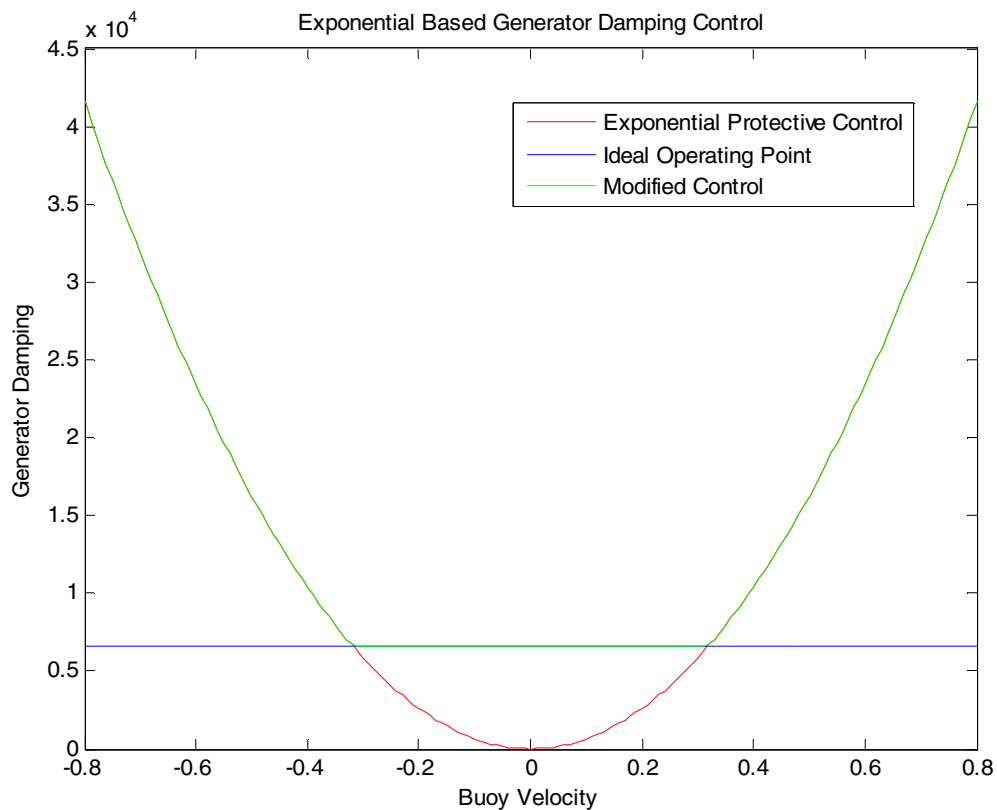


Figure 4.4 – Plot of Hybrid Generator Damping Control.

Figure 4.5 shows a schematic of what a conditional damping control will look like. Notice that the  $\dot{z}_B$  input is cubed in order to develop the generator force used. The maximum power condition is also being checked to protect the generator from damage caused by overloading.

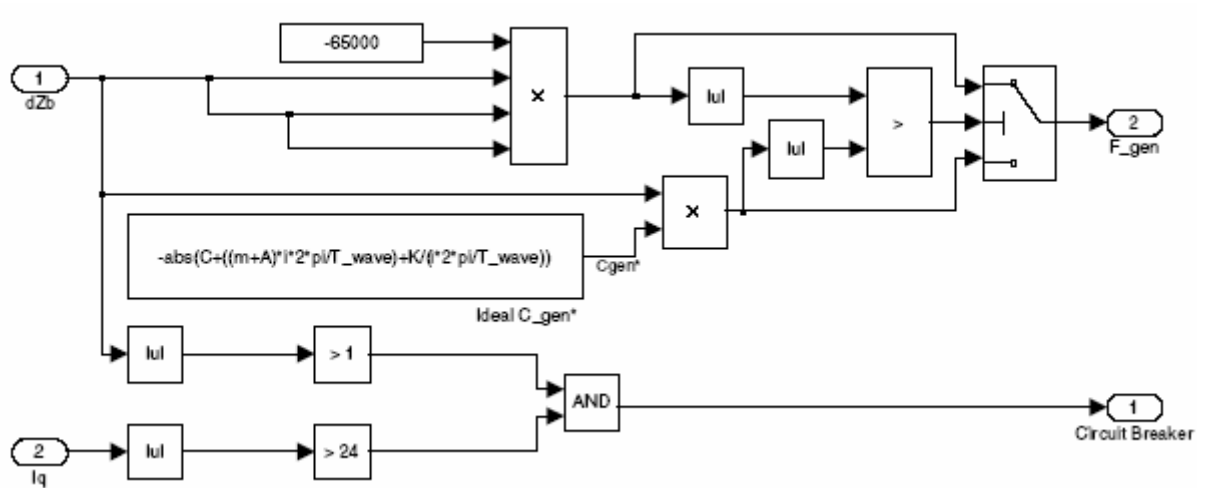


Figure 4.5 – Schematic of Generator Hybrid Control.

Figure 4.6 shows a plot of the 1kW response to the conditional damping control. Notice that the buoy velocity is nearly in phase with the excitation force, this is a very important condition that leads to high energy absorption from the waves [1],[2]. Notice that the buoy velocity is rarely low which ensures the generator is being well utilized.

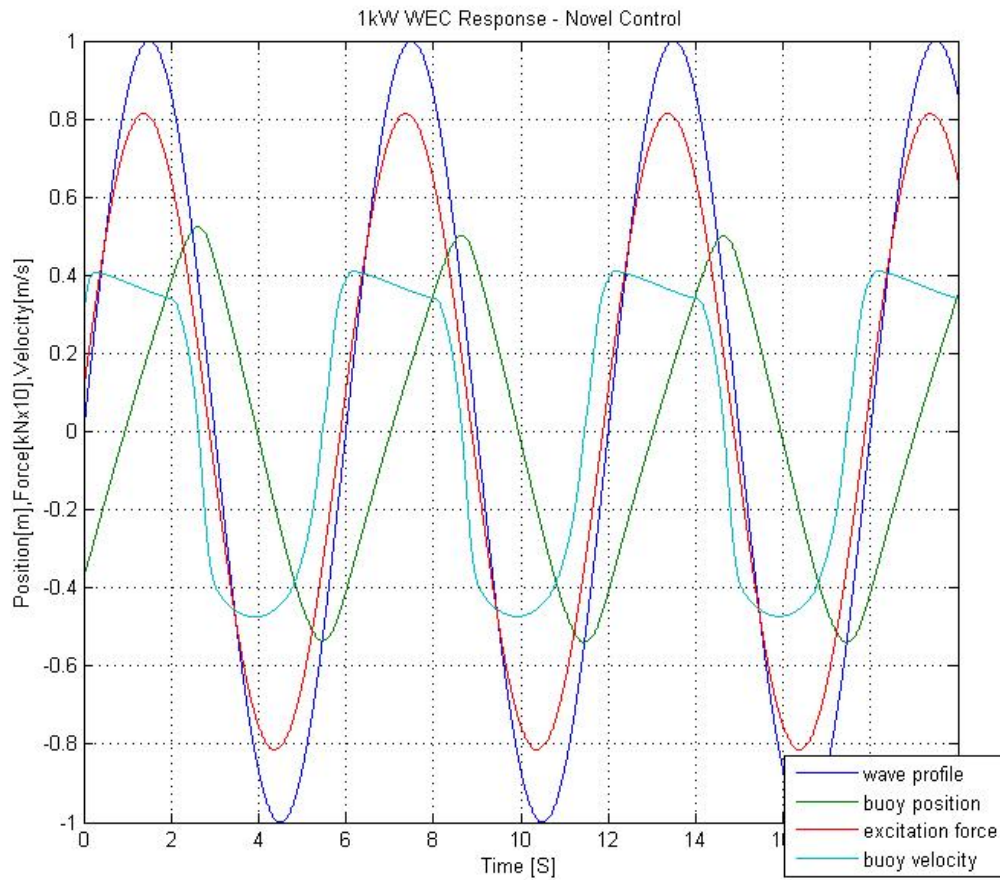


Figure 4.6 – Plot of the 1kW WEC Response to Conditional Control.

The most important parameter to be concerned with in the case of the 1kW WEC is the stroke limit. For this reason we should consider using the buoy's position as an input variable to our conditional trigger as well as our augmented damping law. There are however a few items to be aware of when we are using a position based controller. It is important to keep in mind that the generator force will always be proportional to the velocity due to:  $F_{Gen} = C_{Gen} * \dot{z}_B$  which means you will not be able to exert significant force on the buoy when the velocity approaches zero. Also without having reactive control it is necessary to make all of our control actions in phase with the buoy velocity. This means we must keep the value of  $C_{Gen}$  negative at all times. If we were to command generator damping in the same direction as the velocity, i.e. in phase with the position, it

would require external power to back-drive the generator. For the sake of visualization, all plots of  $C_{Gen}$  will be shown as positive.

Now that we have the means of controlling the motion of the WEC we need to identify the optimal trigger to initiate the control response. To illustrate how the combination of position and velocity can be used as triggers for our control action, Figure 4.7 demonstrates an elliptical control area. Here we have added a position axis to Figure 4.4 which now illustrates the ellipse shown by Equation 4.6, making it a multivariable control condition.

$$\left( \frac{|z_B|}{z_{B\_Limit}} \right)^2 + \left( \frac{|\dot{z}_B|}{\dot{z}_{B\_Limit}} \right)^2 = 1 \quad (4.6)$$

If the operating point of the WEC is within this ellipse the controller acts only as  $C_{Gen}^*$ , but if it is operating outside of the ellipse it invokes the control action, in this case the controller again augments  $C_{Gen}$  to be proportional to  $\dot{z}_B^2$ .

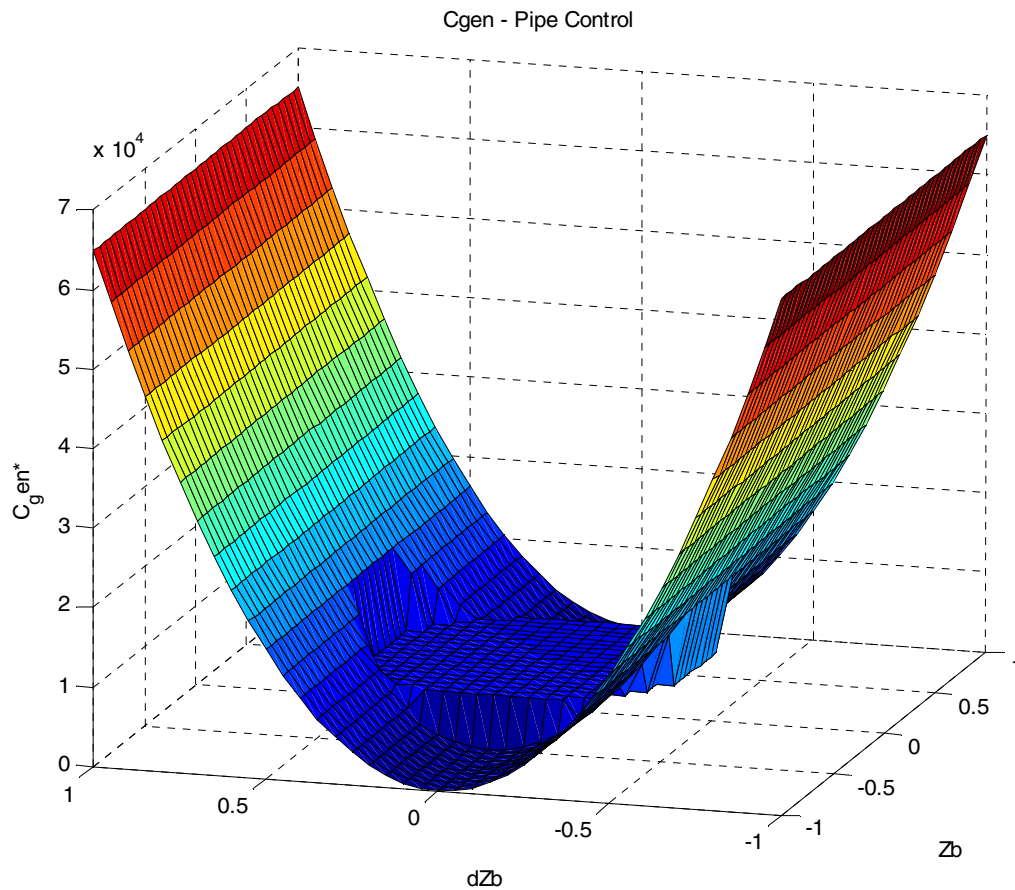


Figure 4.7 – Plot of Exponential Control Surface.

It also may become desirable to include the position in the controls augmentation law. This can significantly deter the motion of the WEC away from its stroke limits. It is very important to keep in mind that we cannot apply  $C_{Gen}$  to be proportional to the buoy position, doing this you would cause  $C_{Gen}$  to be negative during half of the wave cycle. Figure 4.8 shows what a control surface might look like if:  $C_{Gen} \propto z_B$ . Notice the negative values of  $C_{Gen}$  that would correspond to a back-driving situation.

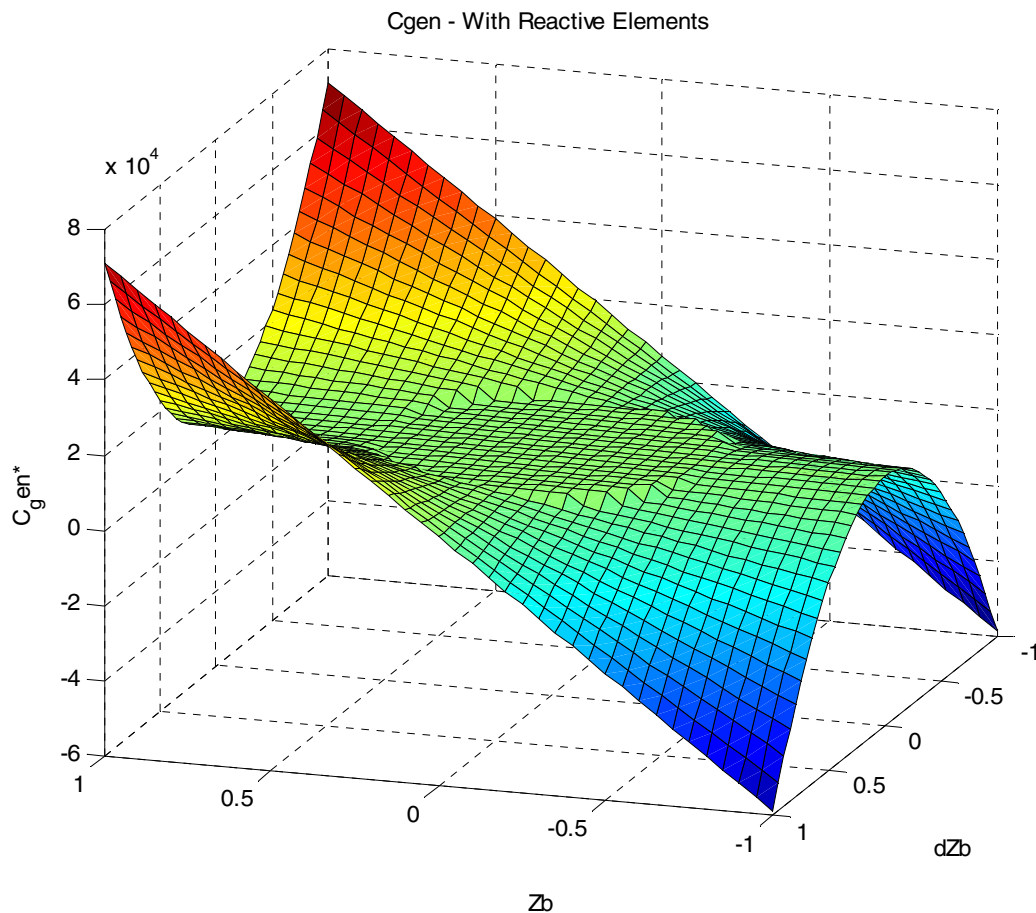


Figure 4.8 – Plot of  $C_{Gen}$  with Position Proportional Dependency.

In order to use the position input in the augmentation control law and to avoid back-driving the WEC we must use either the absolute value of  $z_B$  or an even exponent of  $z_B$  in the augmentation control law. An example of using the position without requiring energy storage is to take  $C_{Gen}$  to be:  $C_{Gen} = C_2 * \dot{z}_B^2 * z_B^2$ . This type of control responds well to increases in either the position or the velocity. Notice in Fig. 4.9, the level area in the middle is exactly equal to the value of  $C_{Gen}^*$  giving us optimum control when both the position and velocity are low.

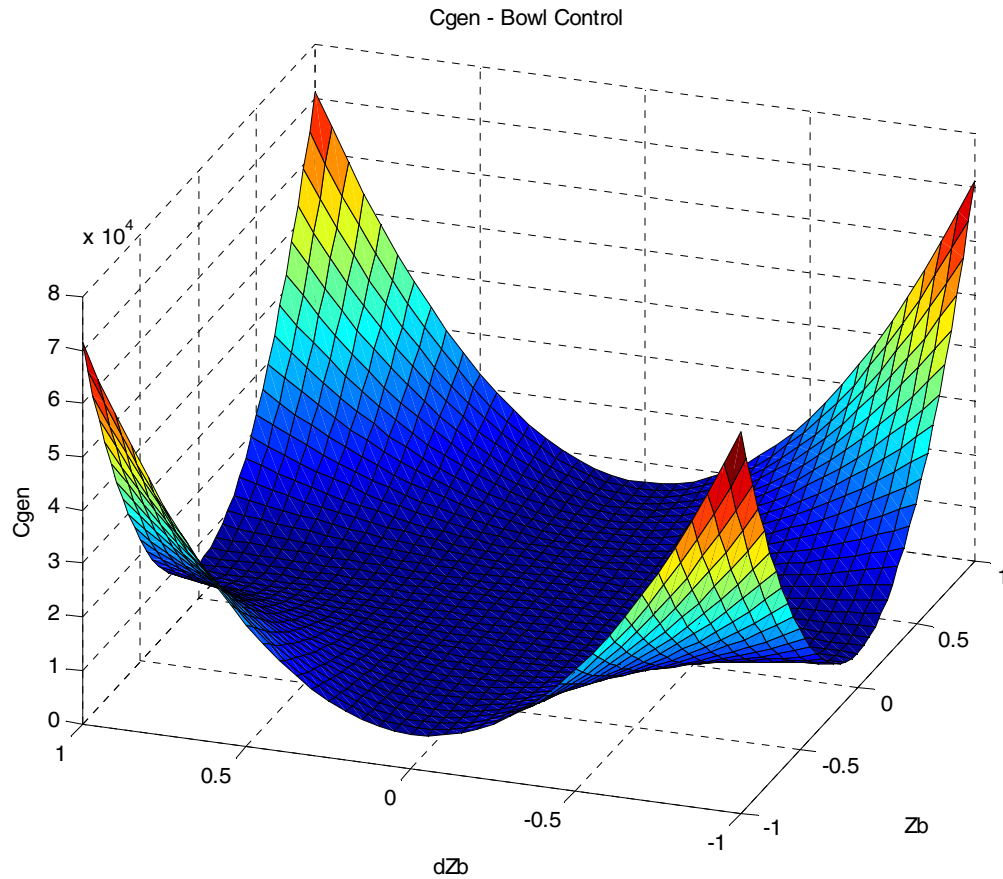


Figure 4.9 – Plot of Multivariable Control Surface.

Exponential augmented control has proven to have many benefits over many other augmentation laws. It provides great generator protection by limiting the velocity and stroke of the buoy. In a set of simulations to compare the efficiencies of using exponential augmentation versus control based on  $C_{Gen}^*$ , there was only a 3% decrease in the output power for a nominal wave.

We can extend the conditional damping control design to account for the current limit. We know that the generator current is proportional to the generator force, then the current limit corresponds to a maximum generator force. Because,  $F_{Gen} = C_{Gen} * \dot{z}_B$ , we can represent force in Fig. 4.10 as the area enclosed by  $C_{Gen}$  and  $\dot{z}_B$  shown in blue.



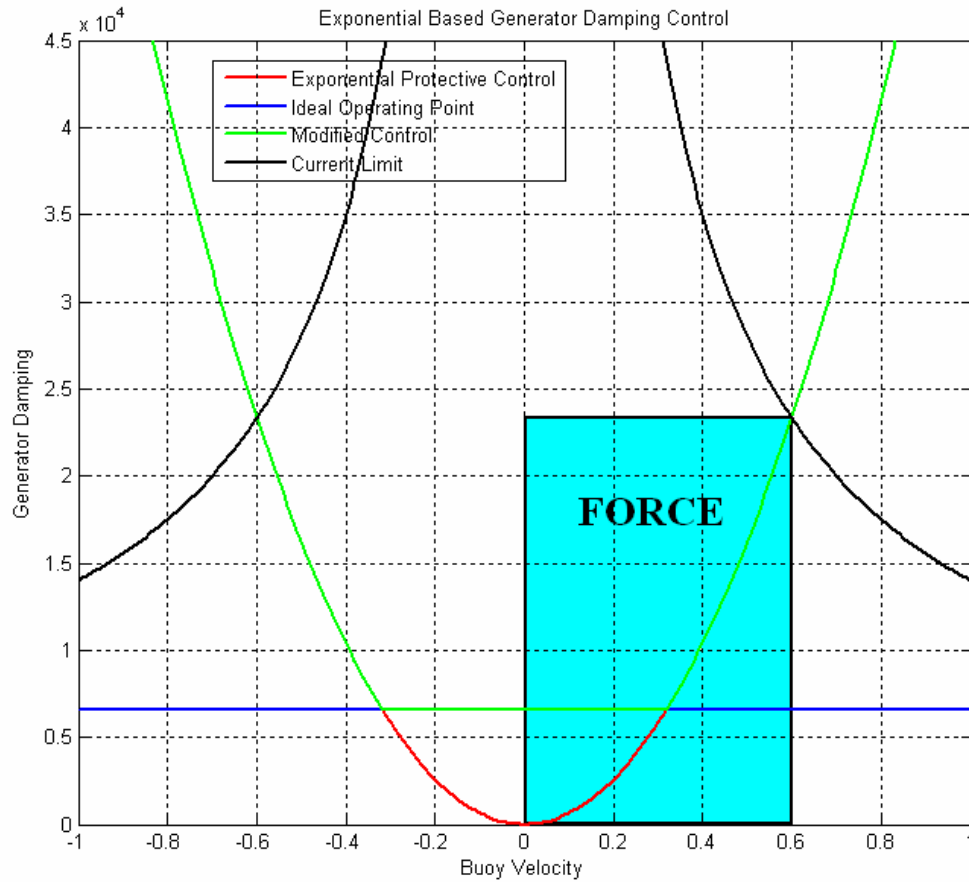


Figure 4.10 – Plot Representing Control Curve and Maximum Power Point.

The real advantage of exponential control is the buoy's ability to handle a variety of input wave climates while producing high generator outputs. Simulations and discussion using this control method on random sea states will follow in Chapter 5.

## 5. MODELS and SIMULATIONS

For every event and process that we observe in nature, mathematical equations can be used to describe their behavior. The ocean wave environment and electromechanical machines are no exception to this rule. In order to design an ocean energy converter, understanding the nature of the forces involved and developing equations to quantify their behavior is required. Models can be seen as an arrangement of interrelated equations that describe these events or processes. The accuracy of these models is dependent on the accuracy and precision of the equations that are used to build them. It is often convenient to make approximations or linearizations to equations for the ease of modeling. Often times such approximations have little effect on the overall accuracy of the model, but it is very important to verify these approximations with hardware testing or other proven models to ensure their relative accuracy.

For my work in ocean wave energy I developed models using the Simulink tool for Matlab. Simulink is a graphical interface to the very powerful Matlab workspace. This utility allowed me to implement all of the equations into a single workspace, whether they were hydrodynamic equations or solid state switching signals. Matlab also allows for convenient import and export of data to and from simulations. This allows for easy organization and presentation of relevant results.

Figure 5.1 shows a high level look at the organization of the entire wave energy system and is the basis for the following discussion on modeling.

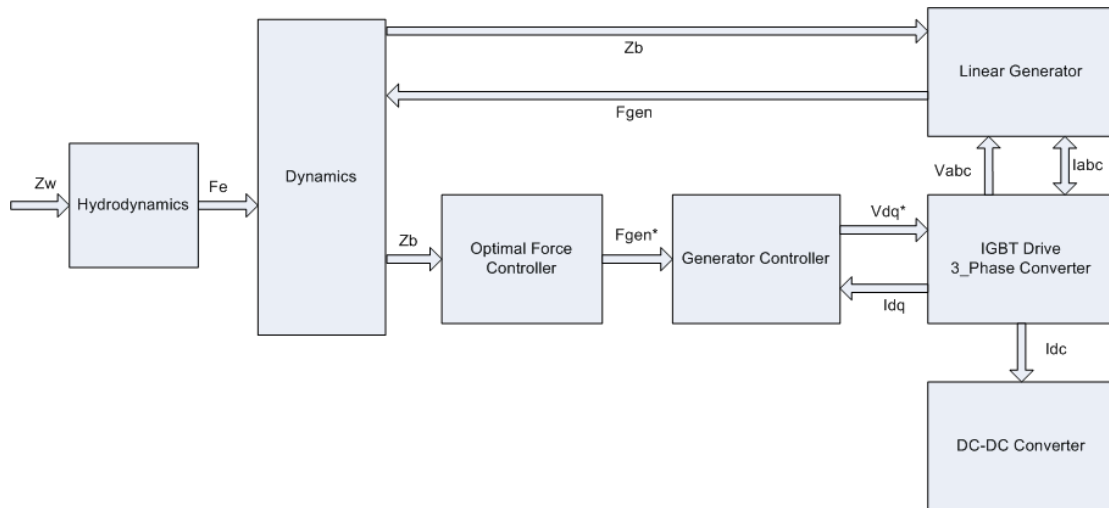


Figure 5.1- Schematic of WEC Controller.

## 5.1 Hydrodynamics

The first piece of the simulation puzzle is the hydrodynamics. In section 3.1 we showed how the Morrison Model was able to describe the behavior of a floating body on the surface of the ocean. With this we are now able to assemble a complete hydrodynamic model that is representative of the 1kW WEC. Since the two part hydrodynamic approach is desirable for control applications we have divided the hydrodynamics into its two sub-systems. The first part generates the excitation force from the wave profile while the second part gives the dynamic response of the buoy and can accommodate the generator forcing term. For now we will leave the generator forcing term out in order to characterize the undamped buoy response.

Zw - Water Surface Position  
 Zb - Buoy Position  
 dZb - Buoy Velocity  
 ddZb - Buoy Acceleration  
 Fe - Buoy/Excitation Force  
 Fgen - Generator Force

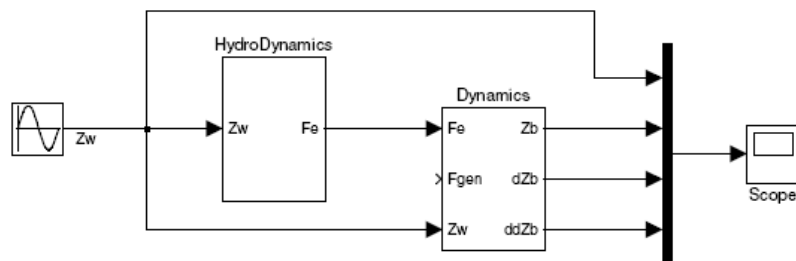


Figure 5.2 – Schematic of Hydrodynamic Model.

Figure 5.3 looks into the hydrodynamics block which is based on Equation 3.3. The wave profile is differentiated once for the wave velocity, and again to find the wave acceleration. Normally a standard differentiation block would be used to perform this task, but instead I chose an integrator and gain feedback loop that can be set with initial conditions in order to converge on a steady-state response in a more timely matter. Once the excitation force has been calculated from the wave profile it leaves the hydrodynamics block and is fed into the dynamics block.

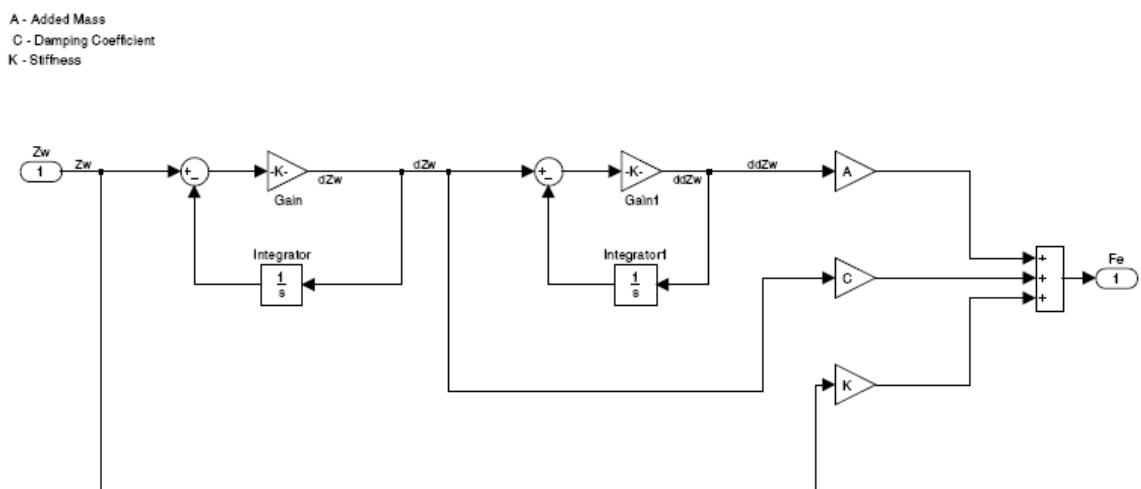


Figure 5.3 – Schematic Developing the Wave Excitation Force.

Figure 5.3 shows the dynamics block. This block can be seen as the summation block of all the forces acting on the buoy. The excitation force, the generator force, the buoyant force, and the viscous damping force all add together into a net force that is responsible for the acceleration of the buoy. From this acceleration we can then determine the velocity and position through integration.

In early dynamic models based on Equation 3.4 alone, we noticed an over amplitude condition that was the result of larger than expected buoyant forces. This is explained by the lack of vertical dimensions representing the 1 kW buoy, i.e. the buoy was defined as having an infinite height. Including the finite dimensions of the buoy in our model we see a non-linear response to the incident wave. The buoy's position is

measured from the mean water level to the mean water line of the buoy. When the water line minus the buoy's position is greater than the freeboard of the buoy it is fully submerged and a maximum buoyant force is achieved. This submergence routine has been temporarily added to the dynamics block to verify its accuracy.

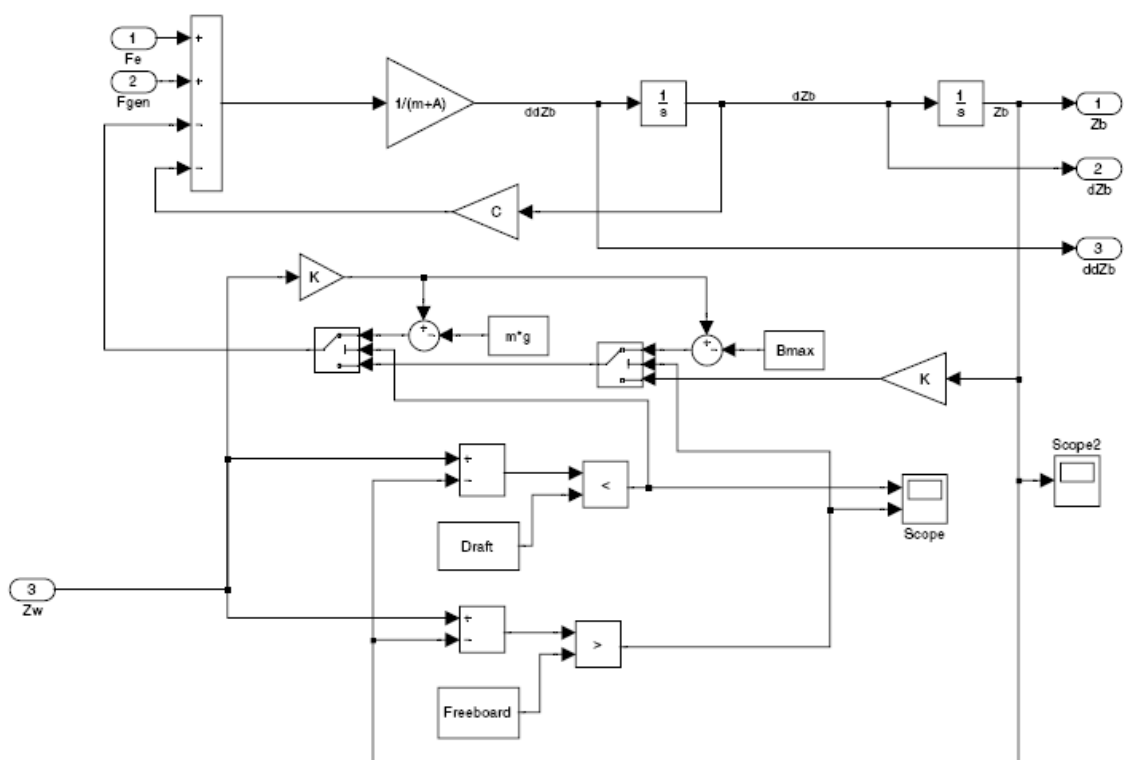


Figure 5.4 – Schematic of the WEC Dynamic Response.

Feeding a monochromatic wave profile that is representative of a summer day off the Oregon coast into the hydrodynamic model, we are now able to see the unrestrained response of the proposed 1kW buoy. The input wave has a magnitude of 1.5 meters and a period of 6 seconds. The buoy response is captured in Fig. 5.5 showing the incident wave profile plotted with the buoy's position, velocity, and acceleration.

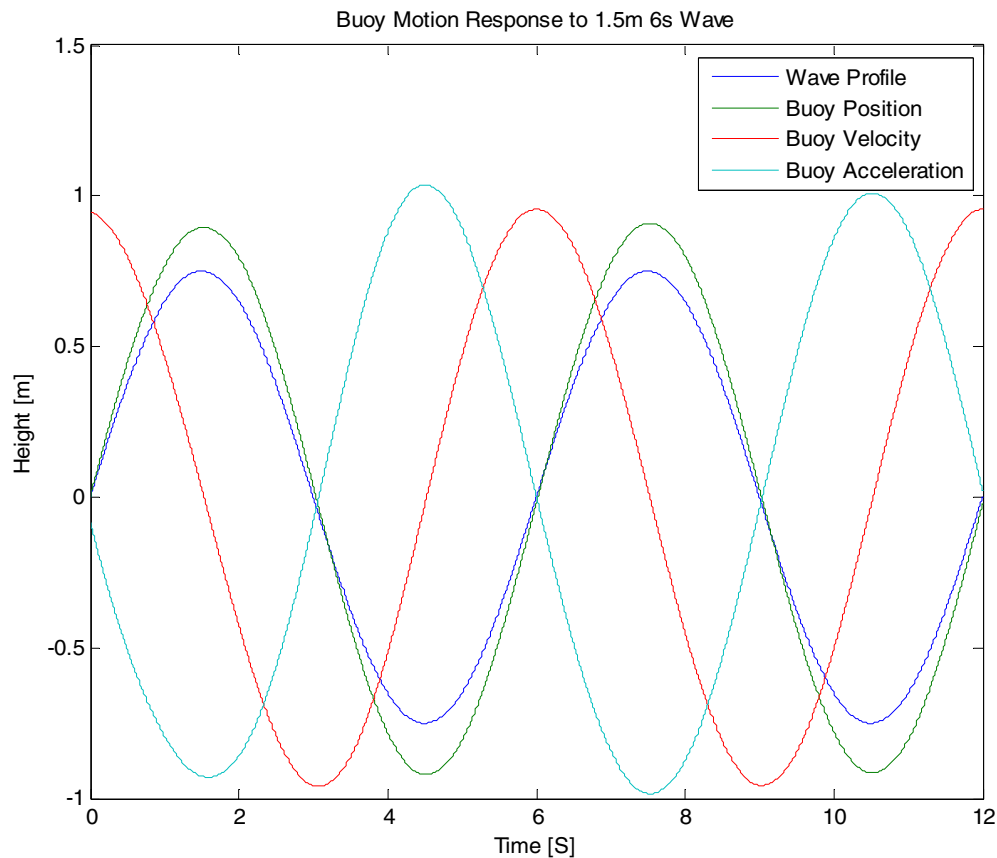


Figure 5.5 – 1kW WEC Response.

The amplitude of the unrestrained buoy is greater than the amplitude of the incident wave profile. This is due to resonance, which can play a large role in a floating body's response to a periodic excitation force. If a floating body is at or near resonance, the heave response of the buoy can become many times larger than the original incident wave. A heavier body has a wider resonant band than a body that is less massive.

Equation 5.7 from Patel, solves for the undamped natural frequency of a heaving body. It is interesting to note that Equation 5.7 takes the same form as Equation 3.1 for the resonant frequency of the circuit analogy.

$$\omega_o = \sqrt{\frac{k_B}{(m + A)_B}} \quad (5.7)$$

Using this equation we can design our system to target a desired natural frequency. Plugging in the hydrodynamic coefficients for the 1kW WEC we can see that the system has a natural frequency of 2.09 rad/s or a natural period of 3 seconds.

To show the effects that resonance has on the system, I have modeled the buoy hydrodynamics with a 1.5 meter, 3 second incident wave. The undamped system under resonance drives the buoy to positions that are an order of magnitude greater than the incident wave height.

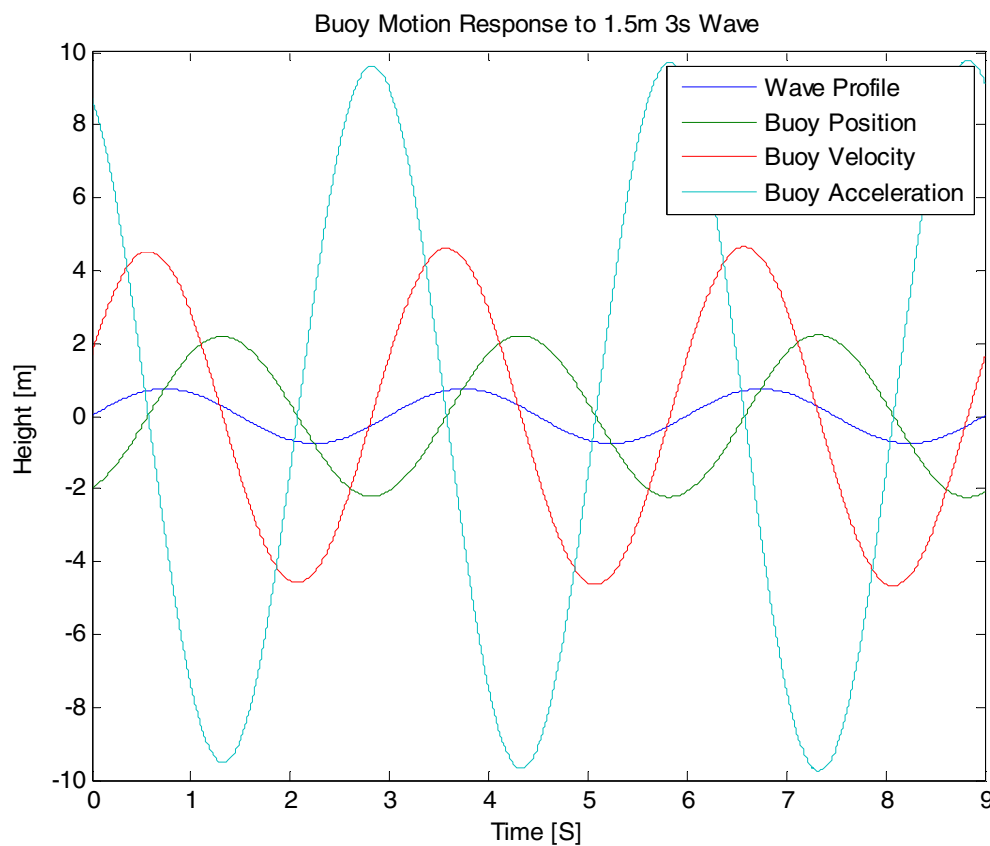


Figure 5.6 – 1kW WEC Response at Resonance.

Figure 5.7 is a Bode plot of the 1kW WEC frequency response characteristics. The natural frequency (2.09 rad/s) is clearly represented in the plot. It is also interesting to note that the response drops off rapidly as you move away from the natural frequency. This is consistent with the concept that small WECs have narrow resonance bands.

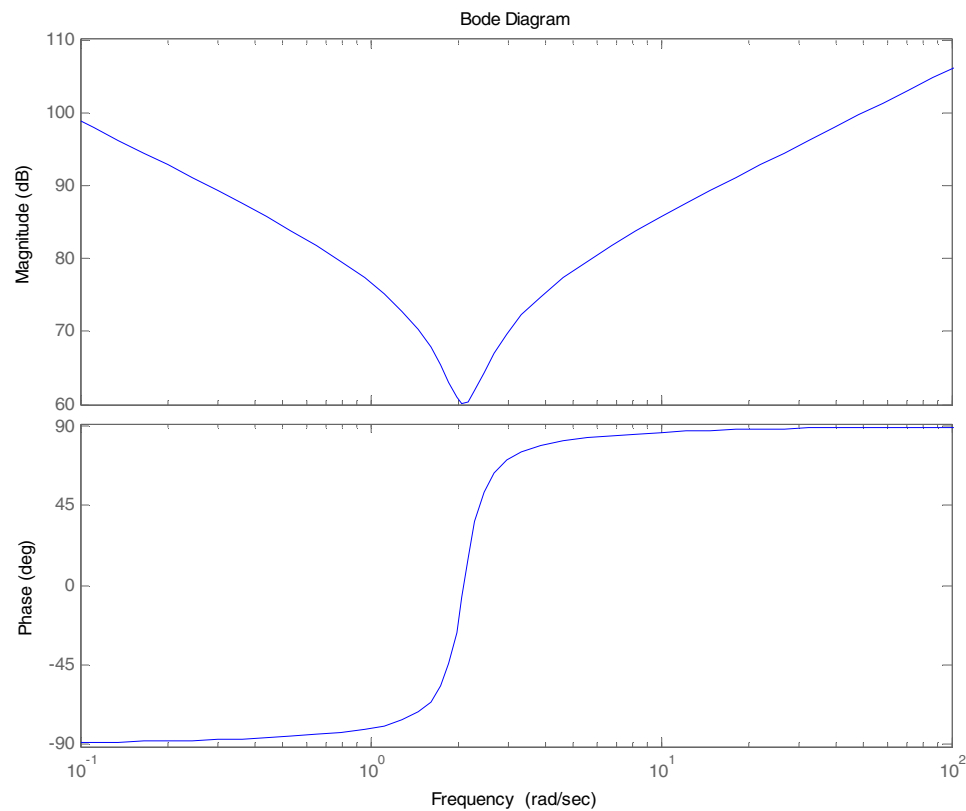


Figure 5.7 – Bode Plot of the WEC Hydrodynamic Response.

It is not always practical to design a WEC that has a resonant frequency at the excitation frequency. Because resonance leads to larger than normal heave responses it is desirable to move away from resonant conditions if the stroke limit is a consideration. Another compelling argument, deduced from Equation 5.7, is that in order to increase the natural period a WEC would either have an increased total mass or reduced stiffness. The stiffness is the primary driving force for energy conversion; therefore it is not reasonable to reduce this significantly. Increasing the mass requires a larger buoyant force and would require a heavier more massive machine in order to achieve resonance. This situation may not be advantageous due to size, weight, and cost constraints. Using generator loading to simulate the presence of additional mass or spring stiffness, as with a reactive controller in the system, can also drive the WEC into a resonant condition.



Then the next component of the hydrodynamic model is the generator forcing term,  $F_{Gen}$ . The generator force is the link between the buoy dynamics and the generator model. This critical force is not only key to controlling the buoy motion; it is also responsible for driving the linear generator to produce electric power.

## 5.2 Generator Models

In order to produce electric power any WEC system needs to include an electromechanical generator of some form. Many WEC designs rely on very efficient, reliable and well proven rotary generators. Rotary generators can take on many forms and have a wide variety of applications. The simplest rotary generators are DC machines; though not widely used they offer many advantages with their ease of controllability and large low speed torque characteristics. Induction generators, although very useful as motors and high speed generators, may lack the ease of implementation in a WEC. Since induction machines must have an excitation voltage that is near their rotational frequency they have many operating limits. If an induction machine is directly connected to the grid then the generator must rotate at a speed that is nearly constant and slightly faster than synchronous, at all times. For WEC systems this requires the addition of some form of energy storage. The other option is to use a bidirectional converter that generates an excitation voltage that is at the same frequency as the motion of the generator. This would allow the generator to follow the velocity profile of the incident wave.

A better machine alternative is the synchronous machine which can achieve the same low speed torque as a DC machine and it will produce power without a synchronous excitation voltage. Synchronous machines are the preferred choice for many generator applications, including use in ocean wave energy applications. Field excited synchronous machines can even control the amount of real and reactive power that is generated. The disadvantage to field excited machines is that they require a separate field excitation source and controller. A simpler method is to use a permanent magnet synchronous generator. Then the magnetic flux field is provided by the permanent magnets and all that needs to be controlled is the terminal voltages.

The alternative to rotary generators is the utilization of a linear generator. Machines of every design can be realized in a linear form. Linear machines are often described as taking a rotary machine and slicing it open then rolling it out flat. For this reason the same equations that govern rotary machines can be used to describe linear machines as well. The only difference is the development of the electromagnetic force from the torque equations.

The 1kW WEC employs a custom built transverse flux permanent magnet linear generator. This generator can more accurately be described as a tubular generator since it is constructed as a pair of concentric tubes that contain the permanent magnet field array and the stator windings. As the permanent magnet field array translates over the stator, an electric current is induced in exactly the same way that it is in a rotary machine.

Reference frame transformations are often used to describe the behavior of electromechanical machines. It is often advantageous to use a transformation to decouple variables, to simplify difficult time variant equations, or to refer to all variables in a common reference frame. By being able to remove the time dependencies from equations without any loss of information, we can significantly reduce the complexity of the system model. Some of the more widely recognized transformations are the Clarke transform and the Park transform [9]. The Clarke transform is used to transform a stationary three phase machine into an equivalent two phase machine. This new equivalent machine with its  $\alpha\beta$  reference frame makes controlling a machine more straightforward. A still more useful transformation is the Park's transform. Here a stationary three phase reference frame is transformed into a rotating two axis reference frame. In this new  $dq$  reference frame the controlling equations are as simple as those of a basic DC machine. Mohan uses a version of the Park transform in which he adds a power invariance term [6]. Power invariance means that the calculated power in the machine is the same whether in the three phase reference frame or in the  $dq$  reference frame. By putting a  $dq$  model in place control calculations can be made quickly and control can be accomplished in real-time with significantly less processing power.

To model the linear generator I used permanent magnet synchronous machine equations from Mohan. The first step in implementing a  $dq$  model is the use of the  $dq$

transformation. I selected the Mohan  $dq$  transformation in order to maintain power invariance.

$$\begin{bmatrix} V_{sd}(t) \\ V_{sq}(t) \end{bmatrix} = \sqrt{\frac{2}{3}} \begin{bmatrix} \cos(\theta_{da}) & \cos(\theta_{da} - \frac{2\pi}{3}) & \cos(\theta_{da} + \frac{2\pi}{3}) \\ -\sin(\theta_{da}) & -\sin(\theta_{da} - \frac{2\pi}{3}) & -\sin(\theta_{da} + \frac{2\pi}{3}) \end{bmatrix} \begin{bmatrix} V_a(t) \\ V_b(t) \\ V_c(t) \end{bmatrix} \quad (5.8)$$

where  $[T_S]_{abc \rightarrow dq}$  is the transformation matrix.  $[T_S]_{abc \rightarrow dq}$  can be used to transform stator currents, voltages, or flux linkages into corresponding  $dq$  axis terms. I will be using  $[T_S]_{abc \rightarrow dq}$  to find in the terminal voltages,  $V_{dq}$ . A graphical representation of this transformation is shown in Fig 5.8.

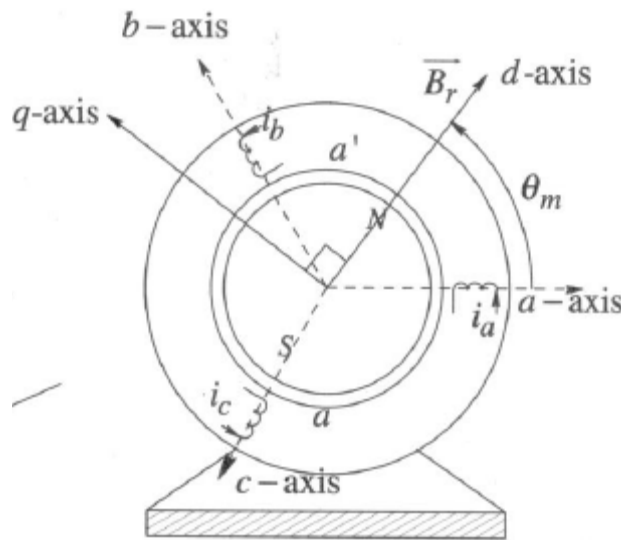


Figure 5.8 – DQ Reference Frame [6].

Implementing in Simulink looks like:

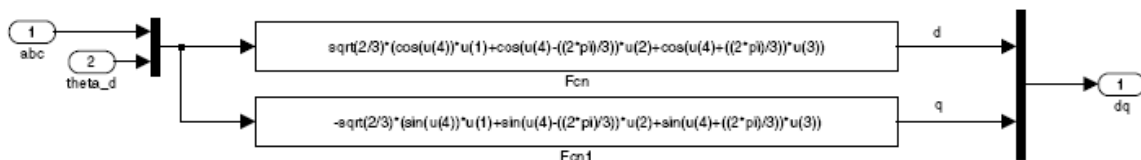


Figure 5.9 – Schematic of  $dq$  Transformation.

The next part of the  $dq$  model is to develop the machine equations. The stator  $dq$  winding flux linkages are:

$$\lambda_{sd} = L_s i_{sd} + \lambda_{fd} \quad (5.9)$$

$$\lambda_{sq} = L_s i_{sq} \quad (5.10)$$

where,  $L_s = L_{ls} + L_m$  (5.11)

and,  $\lambda_{fd}$  is the flux linkage of the stator  $d$ -winding due to the flux produced by the rotor magnets. Looking at the  $dq$  winding voltages gives:

$$V_{sd} = R_s i_{sd} + \frac{d}{dt} \lambda_{sd} - \omega_m \lambda_{sq} \quad (5.12)$$

$$V_{sq} = R_s i_{sq} + \frac{d}{dt} \lambda_{sq} + \omega_m \lambda_{sd} \quad (5.13)$$

where  $\omega_m$  [electrical rad/s] is the electrical speed of the equivalent  $dq$  windings in order to keep the  $d$ -axis aligned with the rotor magnetic axis. The actual mechanical rotor speed is related by:

$$\omega_{mech} = \frac{2\omega_m}{p} \quad (5.14)$$

where  $p$  is the number of pole pairs. Putting this all together gives an idea of how current draw corresponds to the terminal voltages and the electrical speed. Figure 5.10 shows how this is implemented in Simulink.

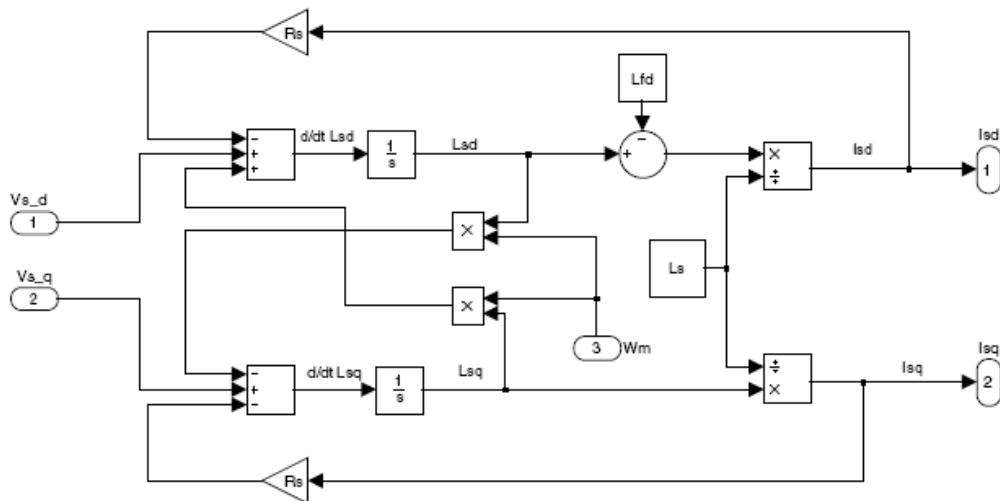


Figure 5.10 – Flux Linkages of Permanent Magnet Motor Model.

The next step is to calculate force produced by the machine. For a non-salient permanent magnet machine we have:

$$F_{em} = \frac{P}{2} \frac{\pi}{\tau} \lambda_{fd} i_{sq} \quad (5.15)$$

where  $\tau$  is the magnetic pole pitch. The final step is to calculate the electrodynamics of the machine. The acceleration is determined by the difference between the electromechanical force and all other forces acting on the mass of the system.

$$\frac{d}{dt} \omega_{mech} = \frac{F_{em} - F_{Load}}{m} \quad (5.16)$$

With the linear generator being mechanically coupled to the floating buoy, the resulting acceleration will be computed in the dynamics block within the hydrodynamics model. The velocity of the buoy is directly related to the velocity of the rotor by:

$$\dot{z}_B = \omega_{mech} \quad (5.17)$$

Putting all of this together gives us a representation of the relationship between the terminal voltages, the buoy velocity, and the electromechanical generator force. This relationship is essential for asserting accurate control over the motion profile of the buoy. Figure 5.11 is a high level look at the generator model.

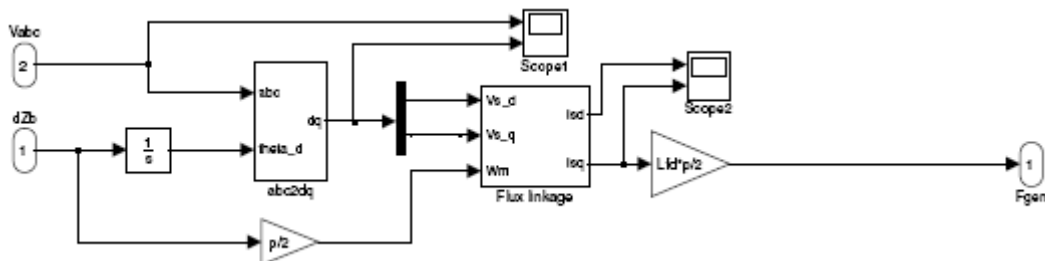


Figure 5.11 – Entire Permanent Magnet Model.

Figures 5.12 and 5.13 show how the  $dq$  transformation can simplify the three phase voltages to the transformed  $dq$  voltages. This is for the case of steady state fixed voltage and frequency excitation; as if it were grid connected.

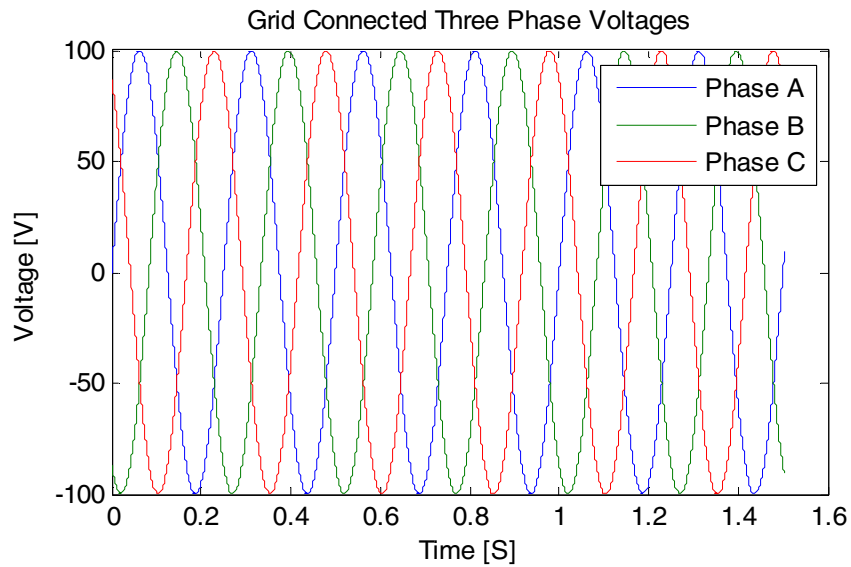


Figure 5.12 – Fixed Three Phase Voltage Waveforms.

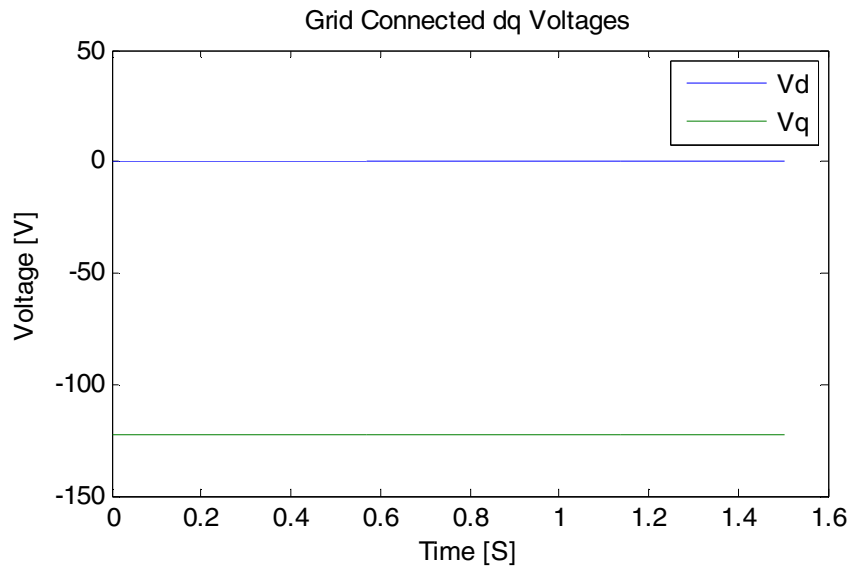


Figure 5.13 – DQ Voltage Waveforms.

Figures 5.14 and 5.15 show how the  $dq$  transformation simplifies the three phase voltage for a voltage profile that is representative of that from a wave energy converter. It is important to identify the variable voltage and variable frequency nature of the terminal voltages. It is this pulsed power that makes controlling the WEC a unique challenge.

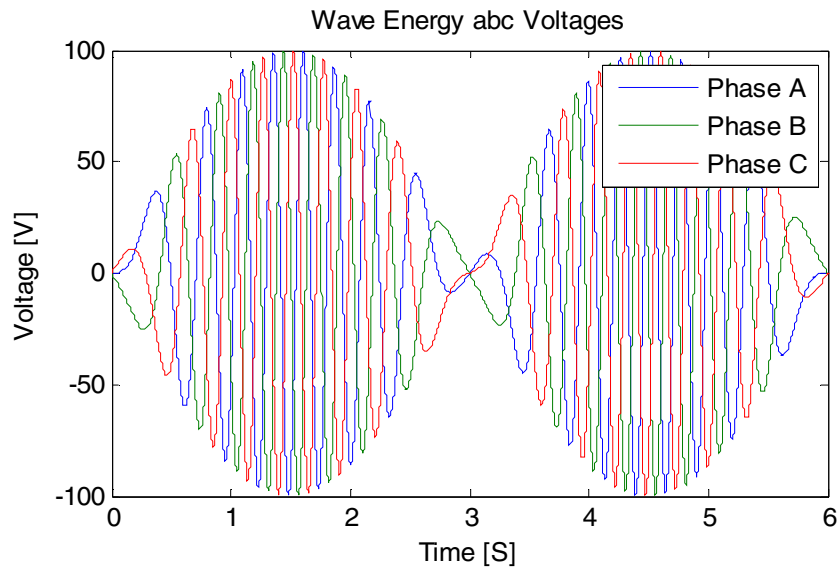


Figure 5.14 – Variable Three Phase Voltage Waveforms.

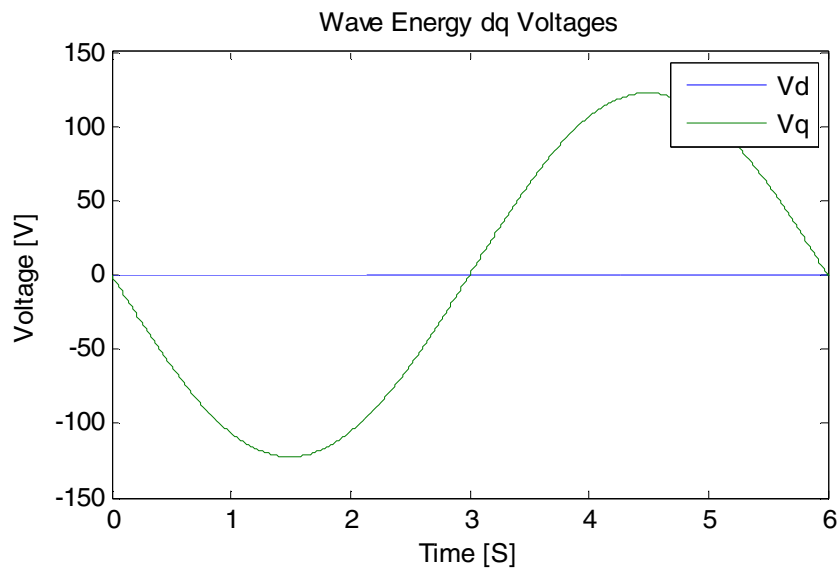


Figure 5.15 - Variable DQ Voltage Waveforms.

It becomes interesting to note that the transformed quadrature axis voltage waveform holds a strong correlation to that of the incident wave velocity. This waveform is a good demonstration of the pulsed power nature of the WEC and shows the need for some form of filtering in order to achieve a constant power output. The direct axis

voltage, on the other hand, will always be zero since there is no need for field excitation in a permanent magnet machine.

It is an interesting exercise, and one worth noting to see how the space vector representation of the quadrature axis voltage varies with time in an ocean wave environment. The following simulation generates a plot of the  $V_q$  vector in time:

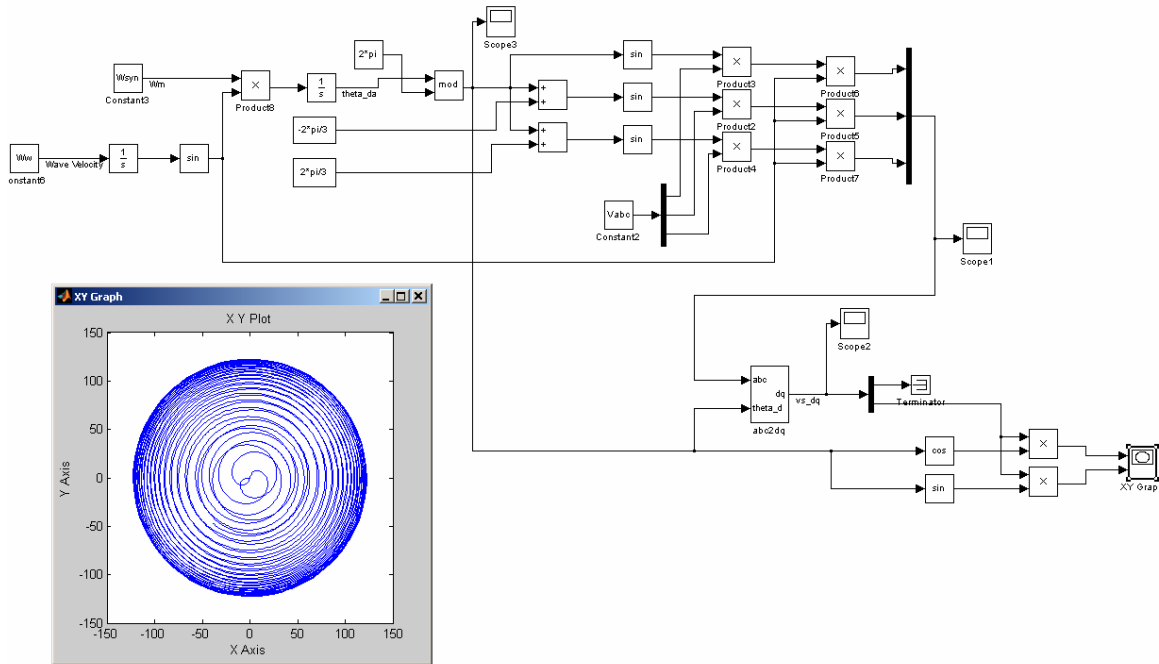


Figure 5.16 – Space Vector Representation of WEC Voltages.

Here we see the quadrature voltage vector rotating about the origin where it grows in magnitude corresponding to an increased velocity and decreases in magnitude as the velocity slows. This type of analysis can be used in a control design and may be able to eliminate the need for an external position sensor.



### 5.3 Power Take-Off Models

The last piece of the modeling puzzle is the power take-off. This is the essential portion of the project that recovers the electric power and affects control over the WEC system. Without a power take-off there would be no way of electrically controlling the behavior of the buoy. The role of the power take-off is to prescribe precise voltages to the terminals of the generator in real-time, to achieve the desired generator output currents. The most convenient method to do this is to use a bidirectional IGBT full-bridge inverter. This gate array allows us to implement PWM or vector control techniques to generate the exact terminal voltages we are looking for. In addition to the full-bridge converter we have also added a buck converter onto the DC bus. This buck converter allows for the regulation of the DC bus voltage in order to keep it within an allowable range to be used by the full-bridge converter. The last item of the power take-off system is the load. For our system the load will be a resistive load bank that will burn off the generated electrical power. In a full scale system this load could be anything from the power grid to a remote power station at sea or possibly even a water desalinization facility.

A well designed power take-off will operate in two modes. The controlled mode will offer the best power production for a given wave climate and will utilize the full functionality of the full-bridge and buck converters. There will also be a default mode that acts as a backup in case the WEC controller fails. This default mode will still be able to generate electric power, but would not have control over the buoys motion. In this case the full-bridge inverter would function as a diode rectifier and the buck converter would have no effect. During this default mode the output voltages and currents would be unregulated so great care must be taken to protect the generator and the load from over-voltage or over-current conditions. The generator and the load will be equipped with over-current protection to avoid any damage caused by operation in this passive generation mode. Figure 5.17 shows a schematic of the complete power take-off for the 1kW WEC. Here the capacitor only acts to stabilize the DC bus and does not allow for energy storage.

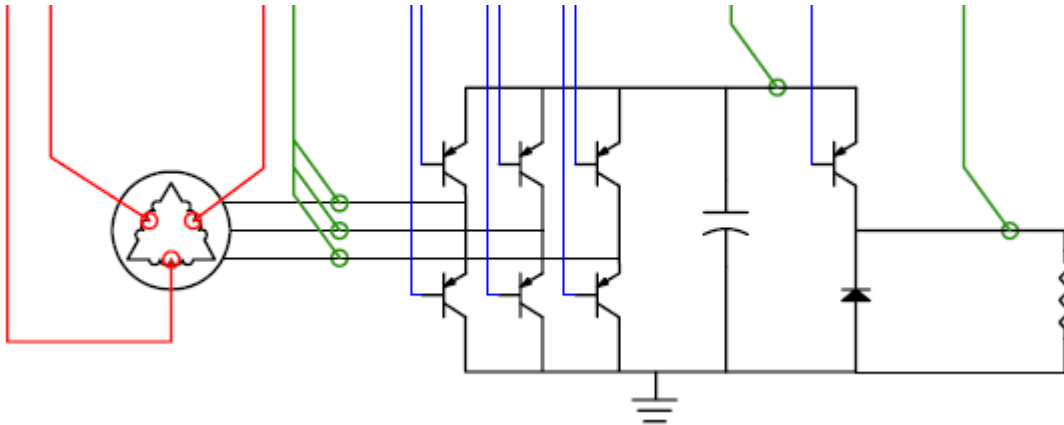


Figure 5.17 – WEC Power Take-Off.

Figure 5.18 is a schematic of the generator and generator PI controller. It is the job of the generator controller to determine and prescribe the terminal voltages to the machine in order to achieve the desired value of  $F_{Gen}$ .

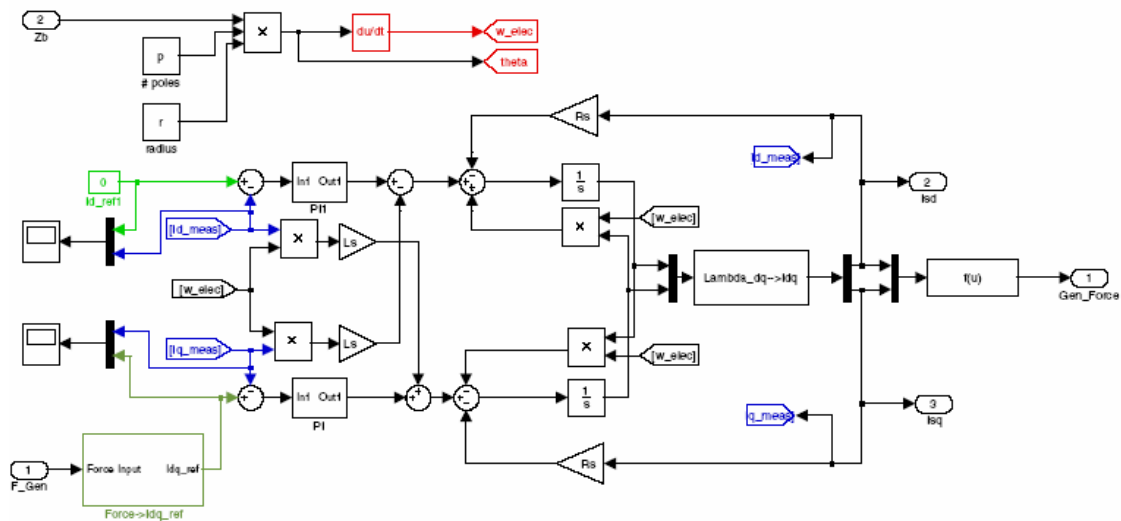


Figure 5.18 – Model of Power Take-Off. [Vandamage]

## 5.4 Simulations

With all of the essential models developed describing the behavior of the various pieces in our system I am able to assemble simulations on the entire system. Developing these simulations is very useful to help understand the way the whole WEC system



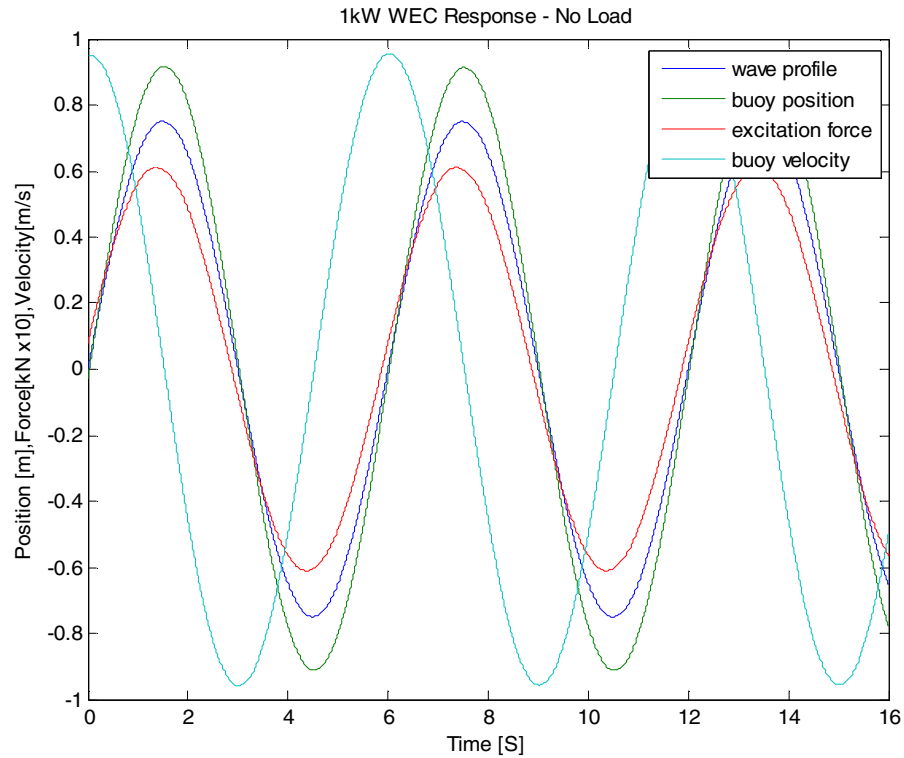


Figure 5.20 – 1kW WEC Response with No Load.

### 5.4.2 Optimum Reactive Control

The first and most obvious generator loading simulation is to run the WEC under optimum reactive control. To do this we take a look back at our circuit analogy and see that in order to maximize the output power we will make the generator damping terms,  $Z_{Gen}$  equal to the complex conjugate of the source impedance,  $Z_{HD}$ . Because the source impedance varies with the excitation frequency, we chose a frequency that is the statistical average for summer waves. For the 1kW WEC this becomes:

$$k_B = 8802 \quad [\text{N/m}],$$

$$C_B = 1000 \quad [\text{N/m/s}],$$

and  $(m + A)_B = 2005 \quad [\text{N/m/s}^2].$

The mass and spring terms are the reactive elements of the system and it will be these terms that adopt the sign change. Then:

$$k_{Gen} = -8802 \quad [\text{N/m}],$$

$$C_{Gen} = 1000 \quad [\text{N/m/s}],$$

and  $m_{Gen} = -2005 \quad [\text{N/m/s}^2].$

Figure 5.21 gives a look at the heave response to the 1kW system under optimum control. Notice that the buoy undergoes a significantly greater response amplitude than in the no load condition. It is this large amplitude response which helps this control scheme to achieve such a large power output. The vertical line drawn in Fig. 5.21 shows that the buoy velocity is exactly in phase with the excitation force. This agrees completely with the reactive wave control theory proposed by Falnes [1],[8].

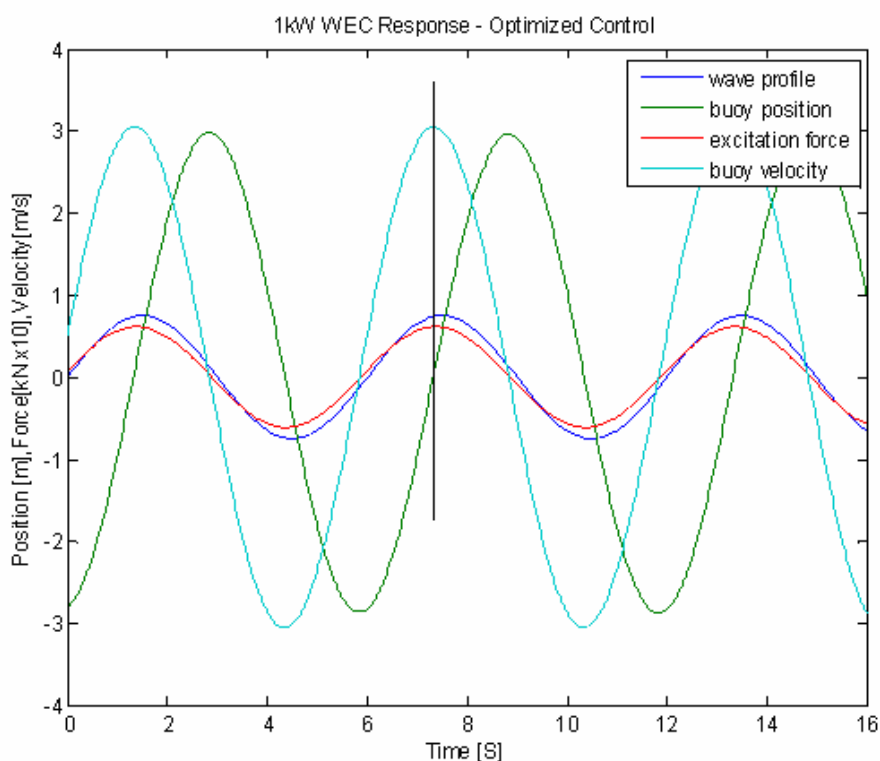


Figure 5.21 – 1kW WEC Response with Reactive Control.

A remarkable feature about using the optimum control approach is revealed when you look at the power flow plot. Figure 5.22 shows the overall output power from this simulation. Here negative values of output power represent power that is being generated

by the WEC while positive values, represent power that must be delivered to the WEC. These extreme variations in positive output power shows that a significant amount of external energy storage is required to back-drive the WEC during these periods. Remembering back to the discussion in Chapter 5 on practical limitations, we saw that such a large capacity of energy storage is not practical and optimum control is no longer feasible for the 1kW WEC. Figure 5.22 illustrates that the net power output from the WEC is negative and is generating nearly 4.5kW!

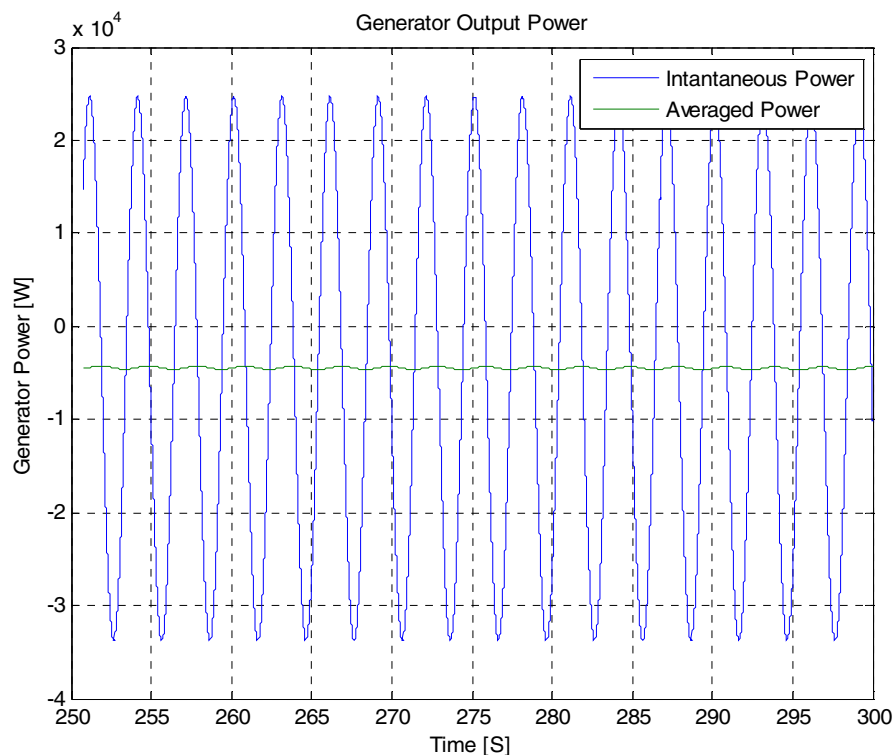


Figure 5.22 – 1kW Generator Output with Reactive Control.

With the energy storage constraints limiting us to using velocity proportional damping control we look back at Chapter 5 to see how best to accomplish this. As you recall the ideal loading procedure for a purely resistive circuit is to make the damping term equal to the magnitude of the source impedance or  $C_{Gen}^* = |Z_{HD}|$ . With the source impedance varying as a function of the incident frequency, we need to determine how  $C_{Gen}^*$  will change with frequency. Figure 5.7 showed us a Bode plot which gives an idea

of how this magnitude varies with frequency. Another interesting simulation details how the output power varies with the generator damping and the incident frequency. Figure 5.23 shows that there is a maximum output power for each frequency corresponding to the ideal value for  $C_{Gen}$  for that frequency;  $C_{Gen}^*$ . It also displays that the maximum output power occurs at the WEC's resonant period of 3 seconds or around 2 radians per second.

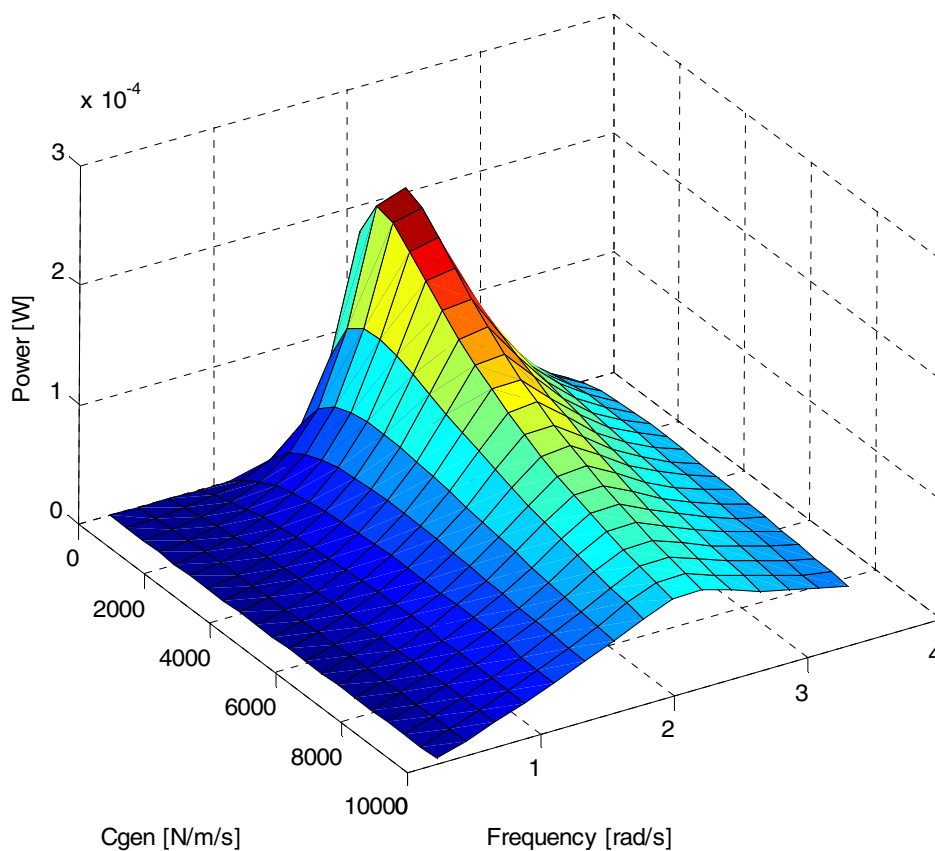


Figure 5.23 – 1kW Generator Output versus Frequency and Damping.

This illustration is a strong indication that a WEC might be best designed to have a resonant period at the dominant incident wave period. We would also expect to achieve greater heave responses at this period so increasing the available stroke length should be considered.

### 5.4.3 Optimum Damping Control

The next set of simulations was run using  $C_{Gen}^*$  as the generator damping constant. With our statistical fundamental summer wave period of 6 seconds we calculate that  $C_{Gen}^*$  should be equal to 6571 [N/m/s]. Below is the WEC response with a generator damping coefficient set to  $C_{Gen}^*$ . With only a real component for the generator damping we see that the buoy velocity is no longer in phase with the excitation force, and is significantly reduced when compared to the optimum control response.

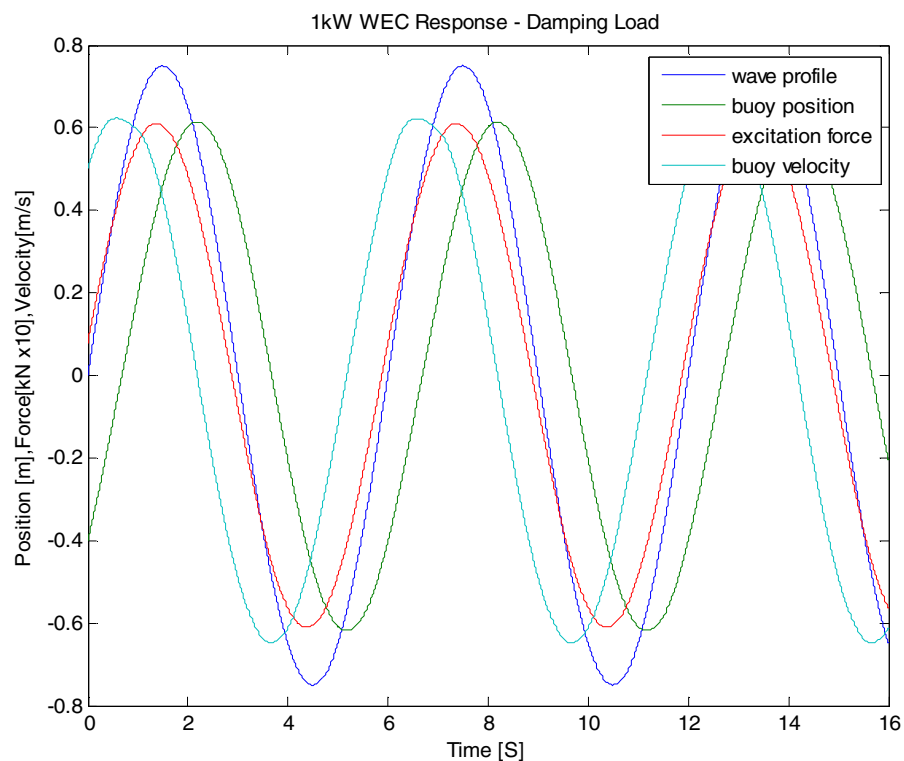


Figure 5.24 – 1kW WEC Response with Optimum Damping.

By eliminating the reactive terms in the generator damping force we have eliminated the need for energy storage. Now when we look at the power output graph, Fig. 5.25 we see that the generator is always producing power and never needs to be



supplied with external power. Even with this deviation from optimum control we are still able to produce an average of 1.2kW!

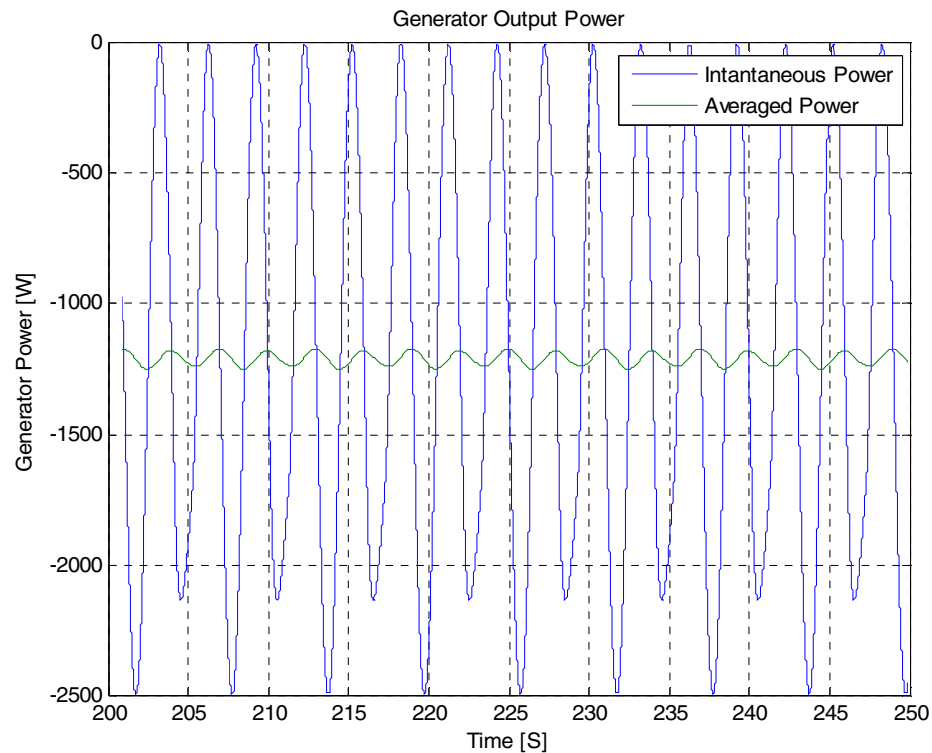


Figure 5.25 – 1kW Generator Output with Optimum Damping.

#### 5.4.4 Increased Damping Control

The problem with the optimum damping controller is noticed when we look back at Fig. 5.24. Here see that the buoy's total stroke is about 1.2 meters. This exceeds the stroke limit that was a constraint of the WEC design. In order to reduce this stroke we need to increase the amount of generator damping. By doing this we are moving away from the ideal operating point so we expect the output power will be reduced. Figure 5.26 shows the buoy WEC response to an increased generator damping coefficient of 9000. We can see now that the buoy stroke is well within the generator limits.

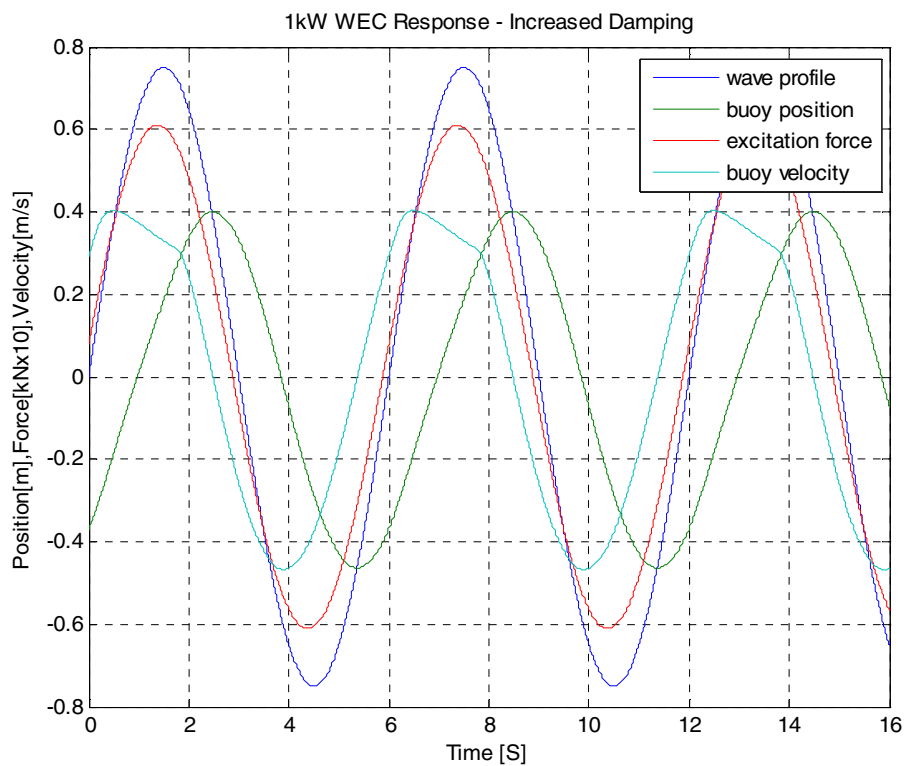


Figure 5.26 – 1kW WEC Response with Increased Damping.

Figure 5.26 shows the non-linear effects to the buoy's response that occur when the buoy becomes submerged. The buoy velocity displays this non-linearity as excitation force reaches a maximum when it becomes submerged.

Figure 5.27 for the increased damping condition confirms that there has been a slight reduction in power output, but ultimately we are still able to produce an average of 1kW of generation.

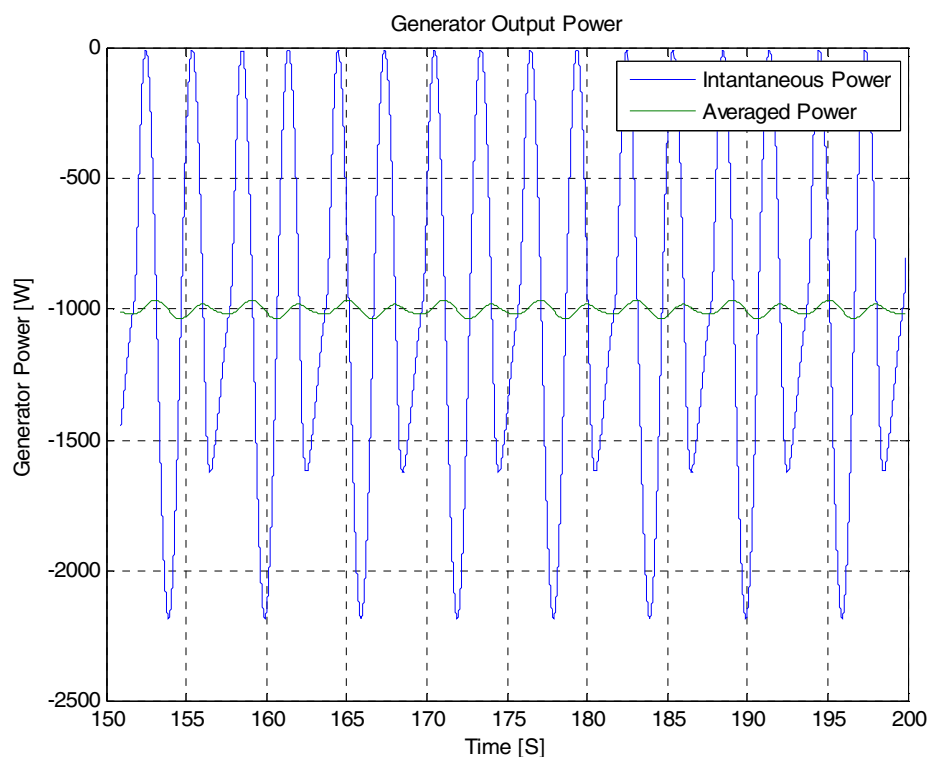


Figure 5.27 – 1kW Generator Output with Increased Damping.

It was briefly considered that static values of generator damping could accurately control the motions of the buoy while protecting the generator limits. For a well-behaved wave profile this can very easily be accomplished by varying the value of  $C_{Gen}$  to restrain the buoy.

While increasing the generator damping works very well for a given sea state, a problem arises when you enter a variable sea state. If  $C_{Gen}$  is set too low it will not protect the generator in large waves and if it's too high it will not operate efficiently. Using limits to increase the generator damping as discussed in Novel Control, has shown to be non-ideal due to large torque ripples and inability to adapt to various wave climates. Below is the buoy response using limit control techniques that have been tuned to the given input wave.

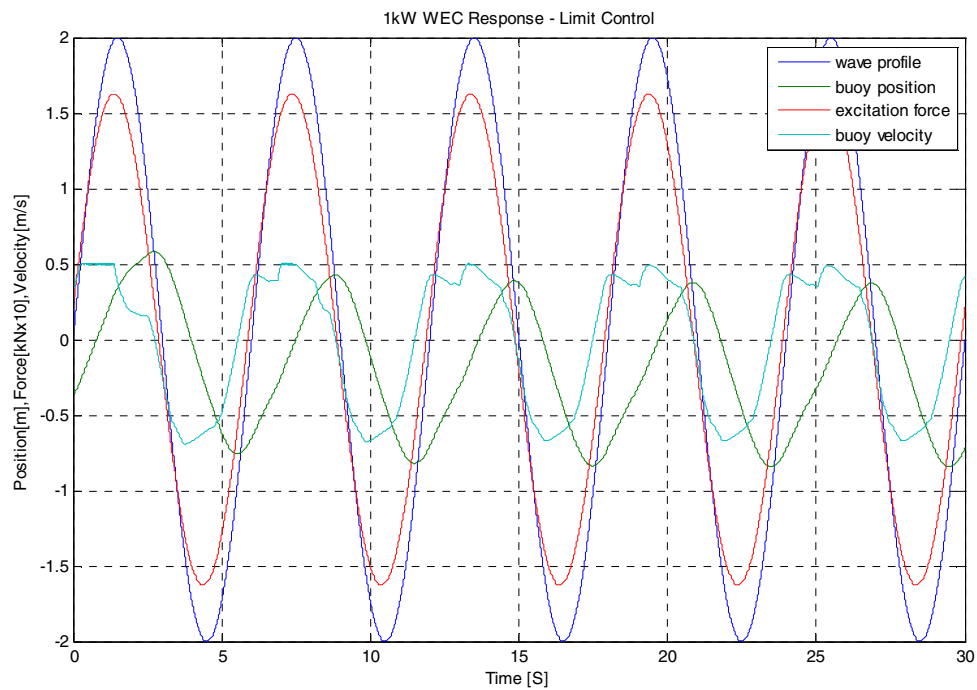


Figure 5.28 – 1kW WEC Response with Limit Control.

#### 5.4.5 Conditional Damping Control

The shortcomings of limit based control lead to the development of conditional damping control with exponential augmentation laws. Simulations show that this proves most effective at protecting the generator in a wide variety of wave climates while efficiently absorbing wave energy. With exponential control we are able to limit the generator velocity without introducing large torque ripples into the system. Exponential control has also proven to be as efficient, and in some cases more efficient, than proportional control. Figure 5.29 shows the 1kW response to conditional damping control.

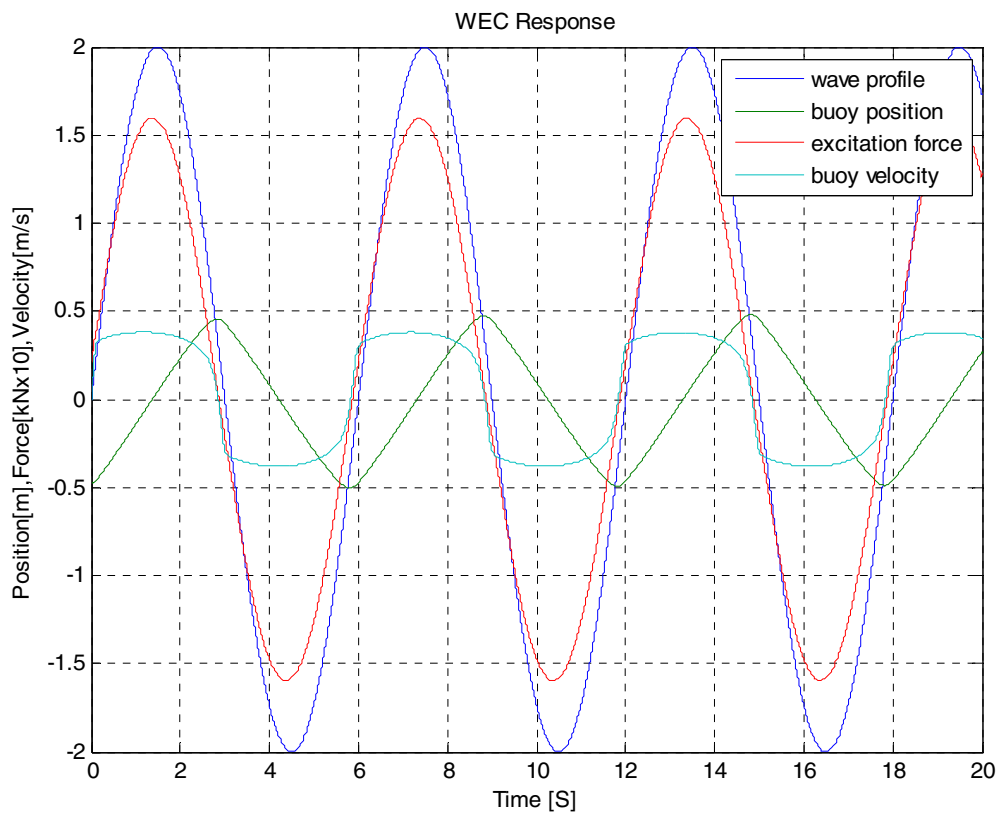


Figure 5.29 – 1kW WEC Response with Conditional Damping Control.

Figure 5.30 shows the curve of  $C_{Gen}$  plotted versus buoy velocity from the actual simulation. Comparing this with Figure 4.3 we see that that  $C_{Gen}$  never drops below  $C_{Gen}^*$  and follows the exponential augmentation law when the velocity exceeds the conditional limits.

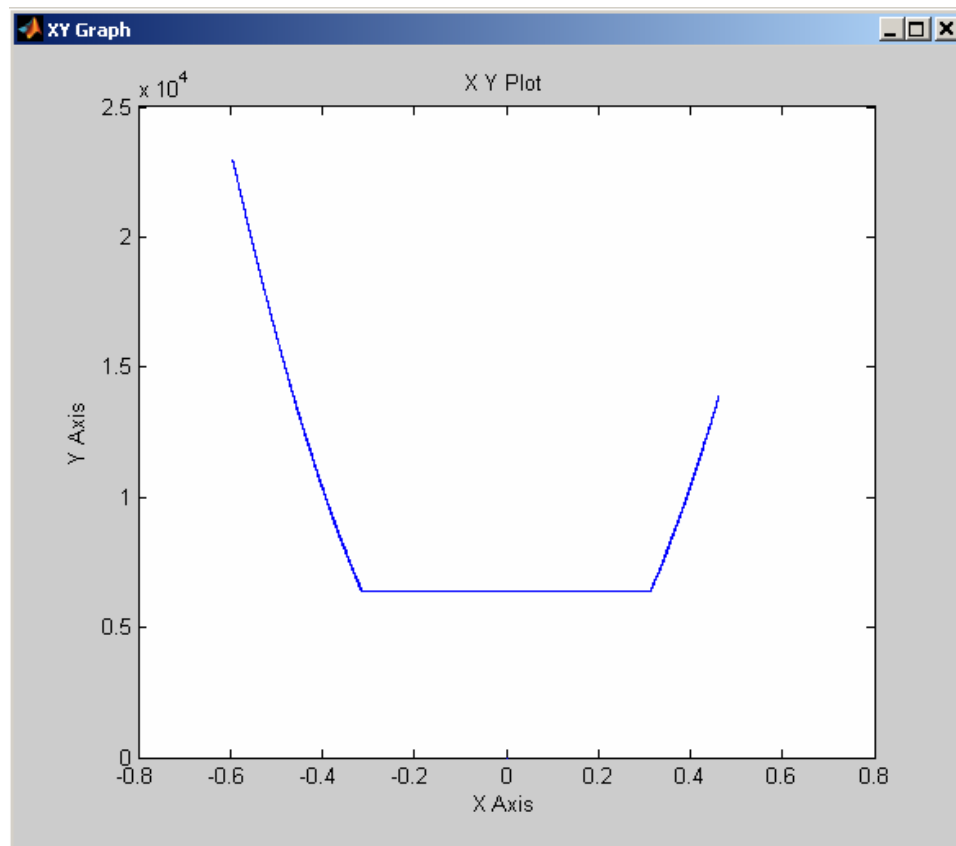


Figure 5.30 –  $C_{Gen}$  versus  $z_B$  from Simulation.

## 5.5 Random Seas

In order to prove the effectiveness of any control design we need to generate a realistic wave profile which is representative of actual ocean waves. Much more can be learned from a completely stochastic sea than from any number of individual tests with a monochromatic wave profile. To do this we need to include incident wave frequencies from the entire ocean wave spectra. The first step is to obtain wave spectral density data. This can either be acquired from ocean monitoring like the NOAA NDBC or by generating it from one of several wave spectrum calculations. Pierson-Moskowitz (1964) may be one of the best known and is my choice for determining the wave spectrum.

Pierson-Moskowitz calculated the wave spectra for various wind speeds, and found that the spectra were of the form:

$$S(\omega) = \frac{\alpha g^2}{\omega^5} \exp\left[-\beta\left(\frac{\omega_0}{\omega}\right)^4\right] \quad (5.18)$$

where  $\omega = 2\pi f$ ,  $f$  is the wave frequency in Hertz,  $\alpha = 8.1\text{E-}3$ ,  $\beta = 0.74$ ,  $\omega_0 = g/U_{19.5}$  and  $U_{19.5}$  is the wind speed at a height of 19.5 m above the sea surface, the height of the anemometers on the weather ships used by Pierson and Moskowitz in 1964. We can also use Equation 5.19 to calculate the spectra from a known wave height.

$$H_{1/3} = 0.21 \frac{(U_{19.5})^2}{g} \quad (5.19)$$

Generating the wave spectra gives us the amplitudes and frequencies for all of the component waves in the ocean. Below is an ocean wave spectra generated from Pierson-Moskowitz calculation using an input  $H_{1/3}$  of 1.5 meters, representing summer conditions.

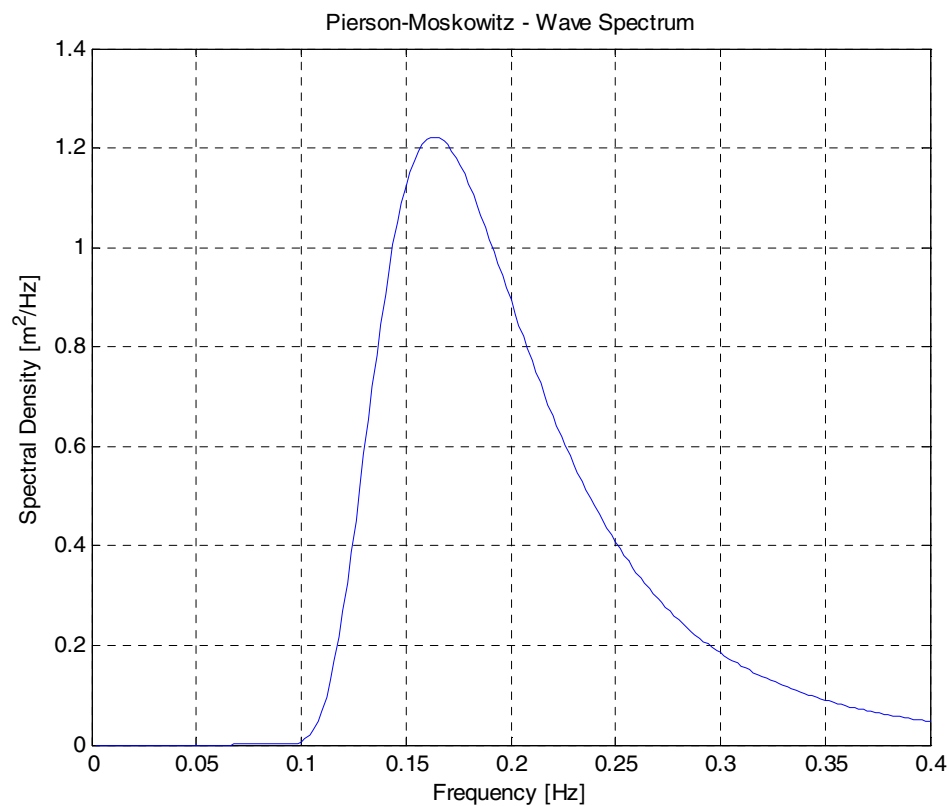


Figure 5.31 – Pierson Moskowitz Wave Spectral Density.

Once we have the wave spectra we can determine the relative wave amplitudes for each wave frequency. To do this we take an interval length of the frequency spectrum and integrate over it. This gives us the variance over that interval. The variance  $\langle \zeta^2 \rangle$  is related to the wave height by Equation 5.20:

$$H_{1/3} = 4\sqrt{\langle \zeta^2 \rangle} \quad (5.20)$$

Now that we have the wave height information we can generate a wave surface profile by adding all of the component frequencies at their relative magnitudes together in superposition. Using a random phase for each frequency component we can represent a truly random sea state that behaves just like that of an actual wave climate. To do this I used a Matlab script file which is attached as Appendix A. Below Figure 5.32 shows a sample wave profile with  $H_{1/3}=1.5$ .

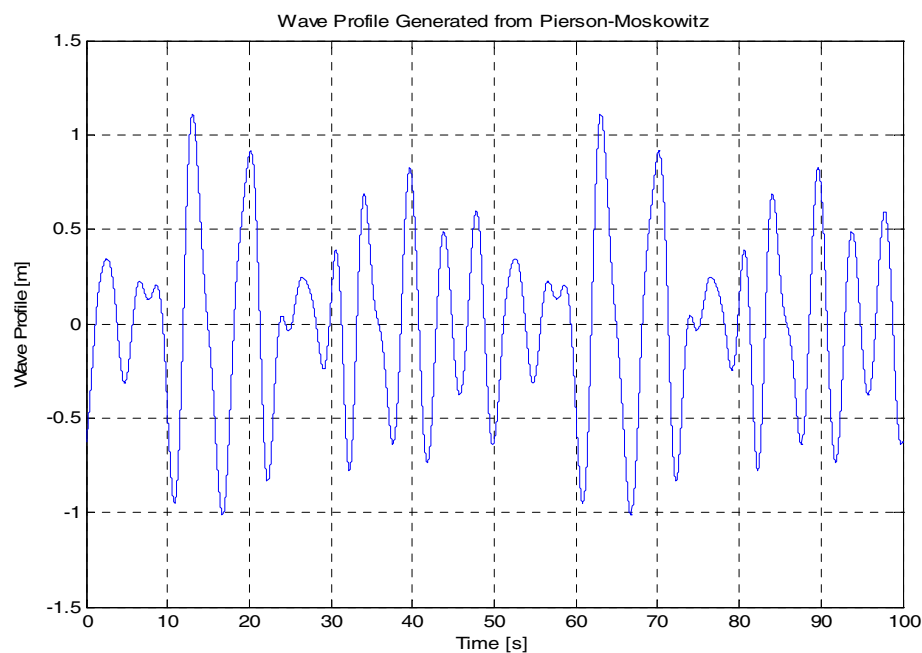


Figure 5.32 – Randomly Generated Wave Profile with  $H_{1/3}=1.5$ .



In order to sufficiently stress the controller we want to use a wave profile that is larger than what we would expect to see during our ocean tests. Figure 5.33 shows the sample wave profile that we will use with  $H_{1/3}=2$ .

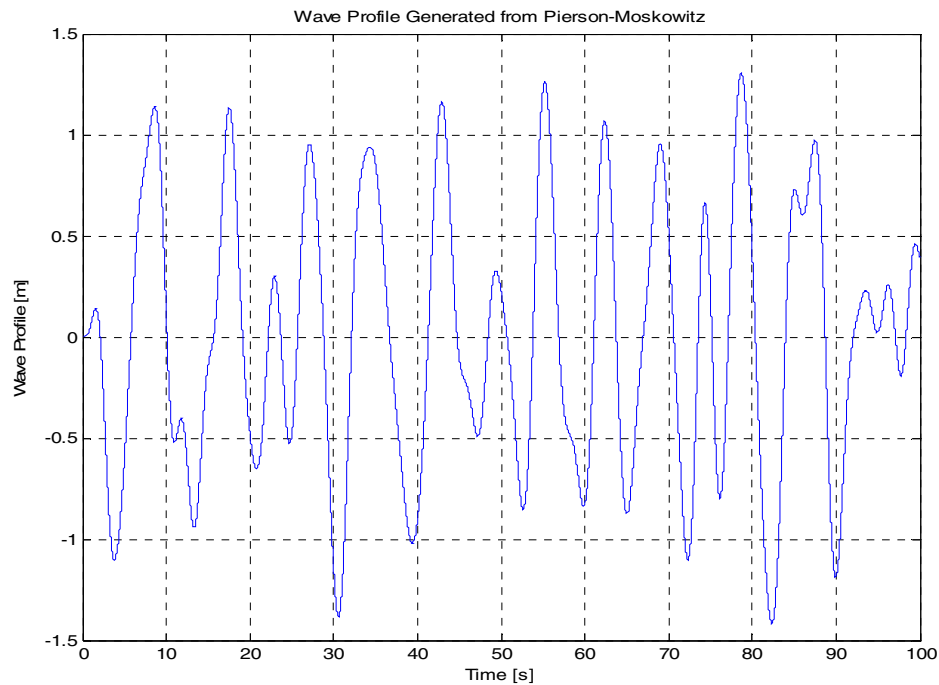


Figure 5.33 – Randomly Generated Wave Profile with  $H_{1/3}=2$ .

To see how this compares to the well behaved wave profile Figure 5.34, shows both the well-behaved wave profile with  $H=1.5$  and the random wave profile with  $H_{1/3}=2$ . We can see from the large deviations, that the random sea profile should provide the sufficient stress in order to adequately test the controller.

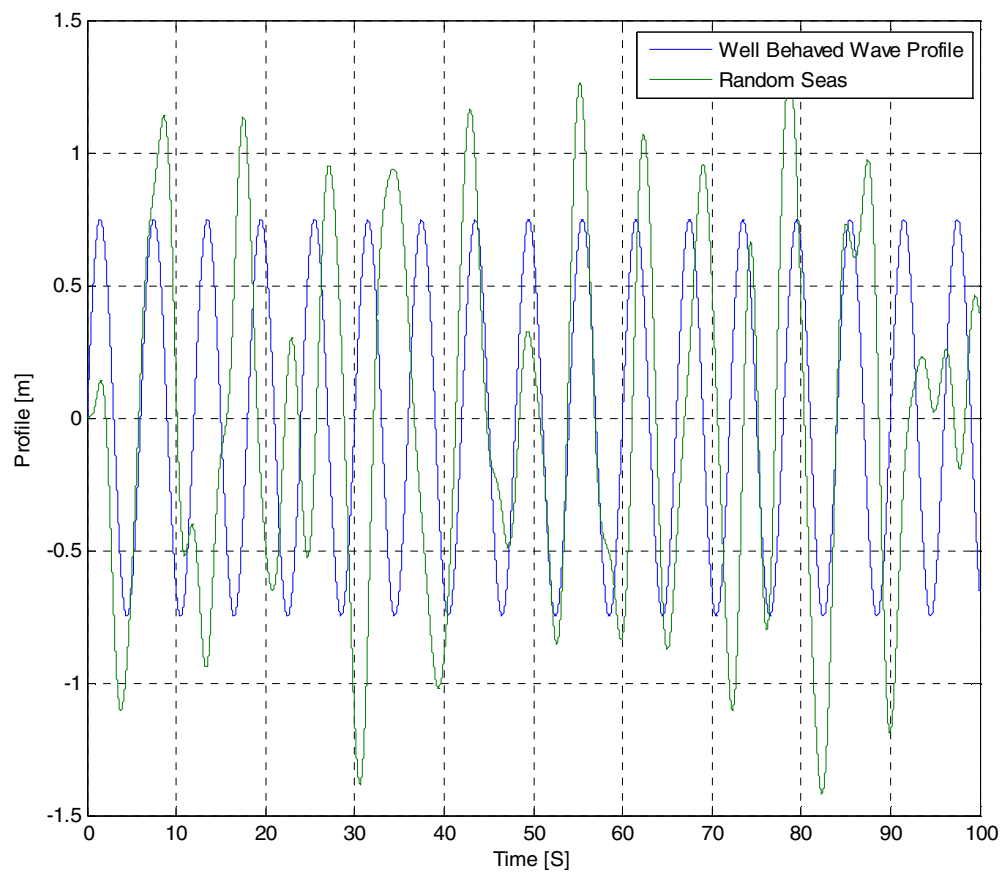


Figure 5.34 – Comparison of Two Incident Wave Profiles.

Feeding this random wave profile into our control simulations we can see how well the WEC will respond to this stochastic wave environment. Figures 5.35-5.38 shows the 1kW WEC response using conditional damping control with exponential augmentation.

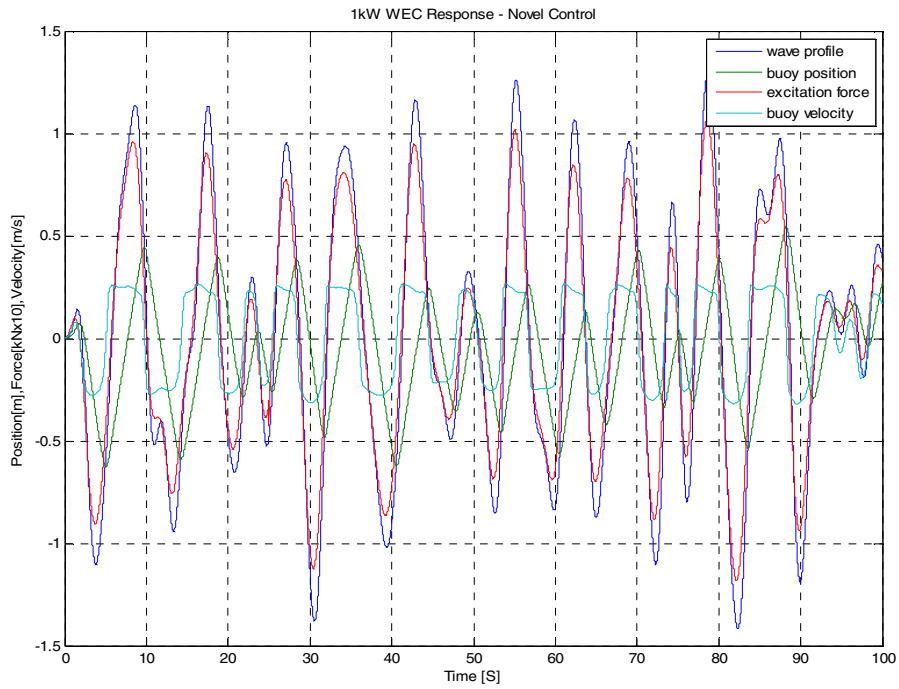


Figure 5.35 – 1kW WEC Response to Random Wave Profile with  $H_{1/3}=2$ .

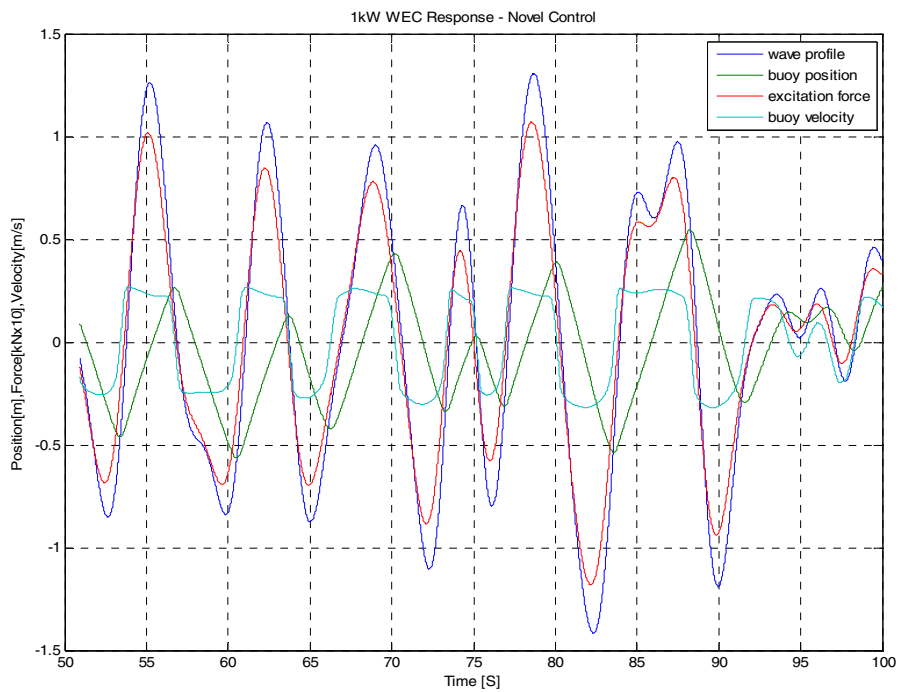


Figure 5.36 – Close-up of WEC Response to Random Wave Profile with  $H_{1/3}=2$ .

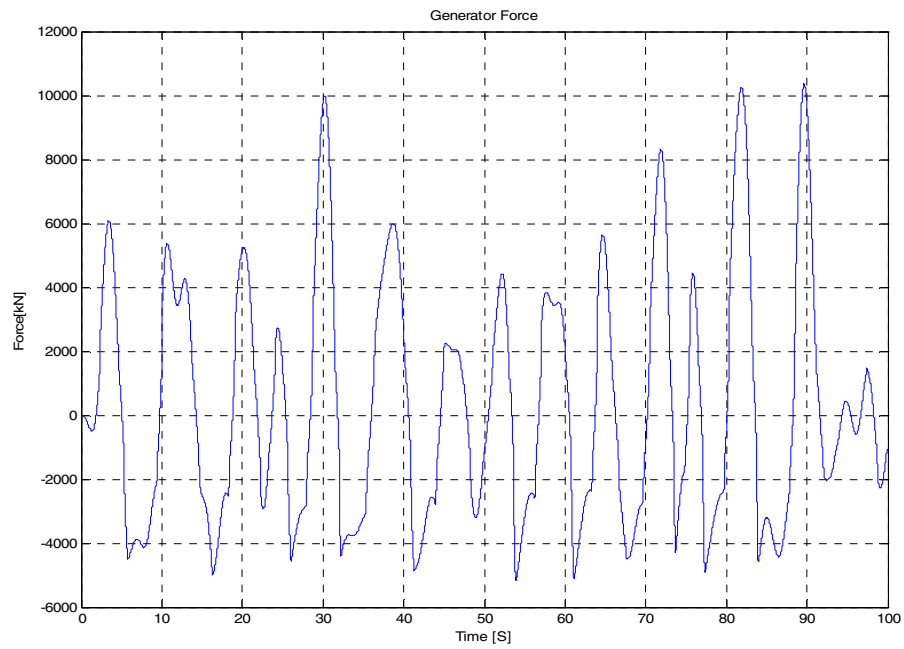


Figure 5.37 – Generator Force from Random Wave Profile with  $H_{1/3}=2$ .

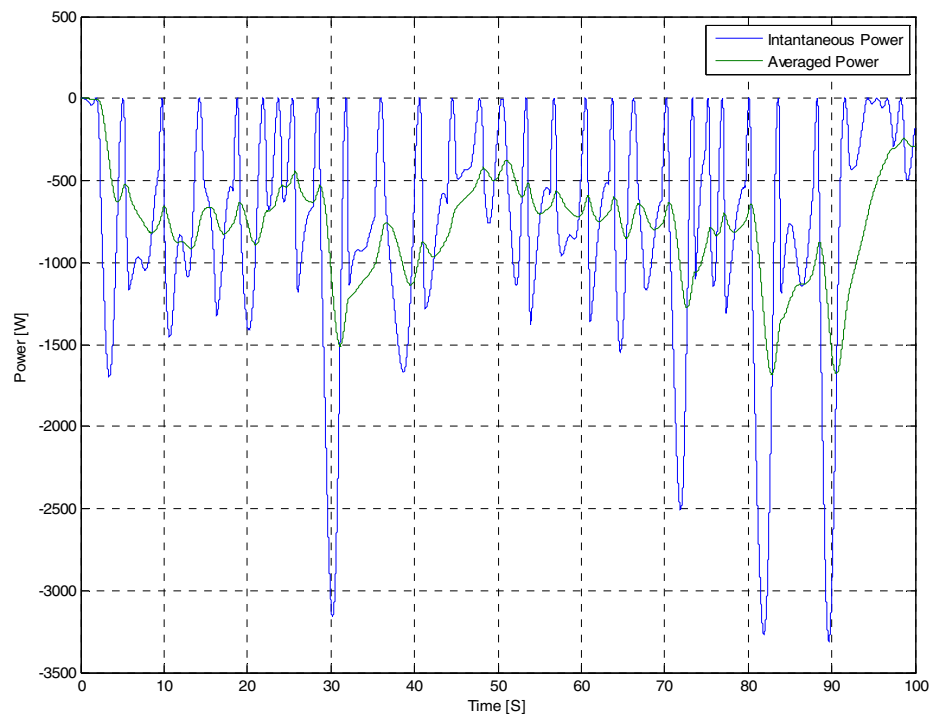


Figure 5.38 – Generator Output Power from Random Wave Profile with  $H_{1/3}=2$ .

This simulation shows that conditional control with exponential augmentation performs very well even with waves with larger amplitudes than those expected during ocean testing. The buoy stroke is constrained to be within our stroke limit accomplishing the first major design goal of the controller. The generator force never exceeds the limit set by the machine design. In fact the highest generator force that was experienced during the test was 10,000 N, this is 40% less than the maximum allowable.

The output power from the WEC during this random sea test proves to be chaotic in nature. It is very difficult to determine what the average power generated during this simulation would be. It appears to be generating something slightly less than 1kW.

## **6. HARDWARE**

### **6.1 The WEC**

The wave energy converter being built is based on a 1kW design. The WEC is composed of several main parts. The buoy and spar make up the hydrodynamic portion of the WEC which are designed to provide the relative motion that is needed to drive the linear generator. The spar is the stationary piece which the float rides on. In order to remain stationary we are employing a tension mooring system which allows for additional buoyant force on the spar to pull a mooring line tight. With the mooring line tensioned the spar is no longer allowed to move in the vertical heaving direction. The buoy or float is designed with the opposite goal; the job of the buoy is to maximize the heaving motion. By designing a float that has a large buoyant force we are able capture a large amount of mechanical power.

The ocean environment is a harsh, corrosive, and all around destructive environment. Everything that we include on the WEC needs to be resistant to moisture and corrosion. The float and the spar have been chosen to be a fiberglass composite material that is very durable and will not corrode. All other major components will be made of either aluminum or stainless steel.

### **6.2 Generator**

The generator that we are employing in the 1kW WEC is a tubular transverse flux permanent magnet linear generator. The field is a permanent magnet array that is located on the float. This magnetic array creates the flux field that penetrates the air gap and induces the current in the windings. The windings are located in the stationary spar and are wound like bobbins into the stator laminations. Both the permanent magnet field and the stator are made from iron laminations. These laminations help guide the flux path while reducing eddy currents to increase the overall efficiency. Once the field and stator laminations are assembled they are then dipped into an epoxy resin to ensure that the coils do not move and to protect the iron from corrosion.

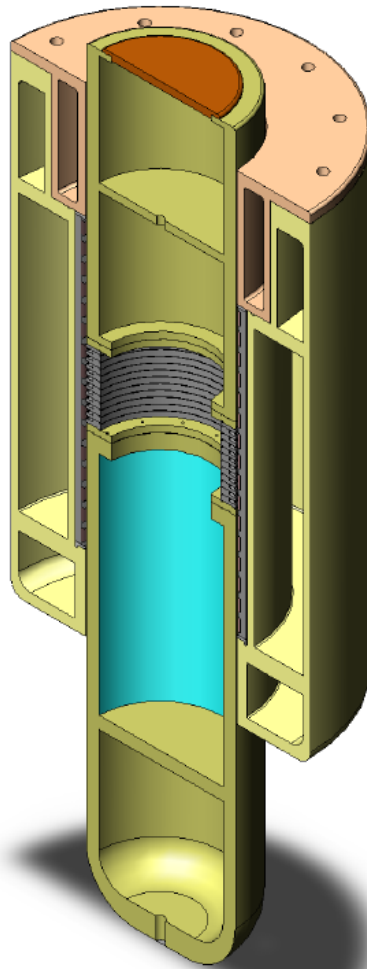


Figure 6.1 – Physical Diagram of the 1kW WEC.

### 6.3 Power Take-Off

The power take-off is a term used to describe all of the components on the WEC that are electrically downstream from the generator terminals. The power take-off includes the IGBT full-bridge converter, the DC bus and filter, and the DC/DC converter. The power take-off is responsible for controlling the generators terminal voltage while converting the electrical power.

We have chosen two PowerEX POW-R-PAK 3-phase IGBT modules for our full-bridge converter and for the DC/DC converter. With help of Manfred Dittrich we were able to assemble a single module that could handle both of the converter needs. The modules are fitted with three phase LEM current sensing modules that will be used by the CompactRIO to make control decisions. The modules are also fitted with DC bus capacitance; these are not large enough to be used as energy storage but will be helpful to filter switching harmonics between the full-bridge and the DC/DC converter.

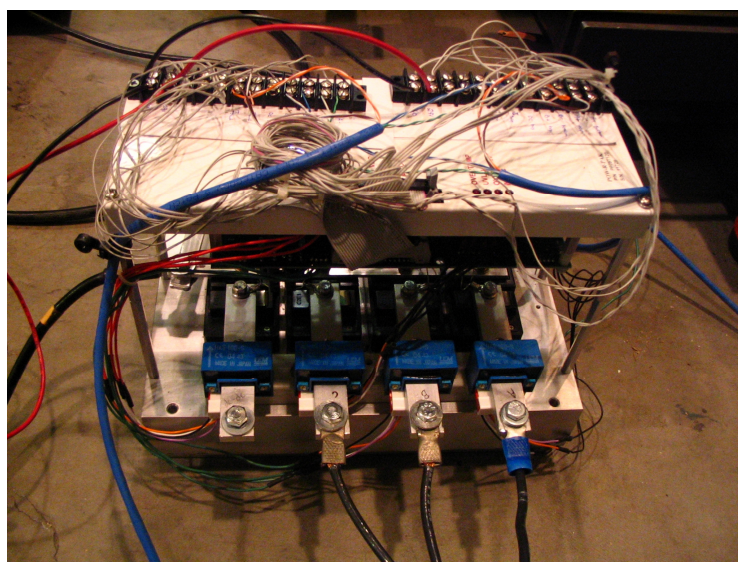


Figure 6.2 – PowerEx PowerPack Module.

#### 6.4 Compact RIO

It became evident early on that the 1kW WEC would be the most actively monitored and controlled WEC prototype built by OSU to date. In order to achieve this level of control and data acquisition we knew that we needed to use a powerful controller. There were many data acquisition and control needs that would need to be accomplished in order to effectively control the 1kW WEC. Figure 6.3 shows how all of the data acquisition and controls signals will be routed through the controller.



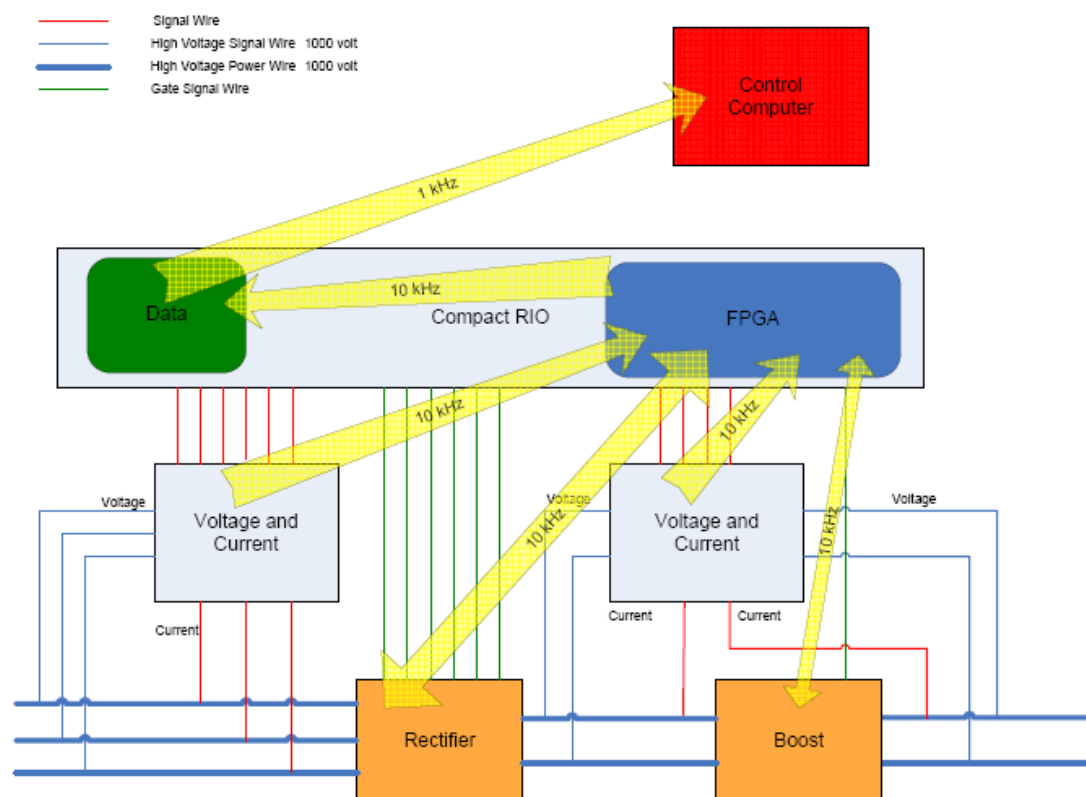


Figure 6.3 – Control Hardware Schematic.

We compared products from several of the leading rapid prototyping manufacturers and determined that the CompactRIO from National Instruments would be the best fit for our unique needs. We had some very selective constraints and the cRIO had the performance to deliver them. We needed a device that was high speed, portable, durable, flexible, remotely controllable, and cost effective. The CompactRIO is a small and rugged embedded control and data acquisition system that features extreme industrial certifications and ratings including -40 to 70 °C operating temperature, up to 2,300 Vrms isolation, and a 50 g shock rating. The cRIO features an embedded real-time processor for reliable stand alone operation. In addition to that it has an embedded FPGA chip that provides the flexibility, performance, reliability, and speed that we were looking for. The cRIO is powered by National Instruments LabVIEW graphical programming tools which are available at no cost to university based projects.

The CompactRIO is comprised of the real-time processor, the reconfigurable FPGA chassis, and a variety of the I/O modules. This combination of hardware and software allows for maximum speed and flexibility. Figure 6.4.

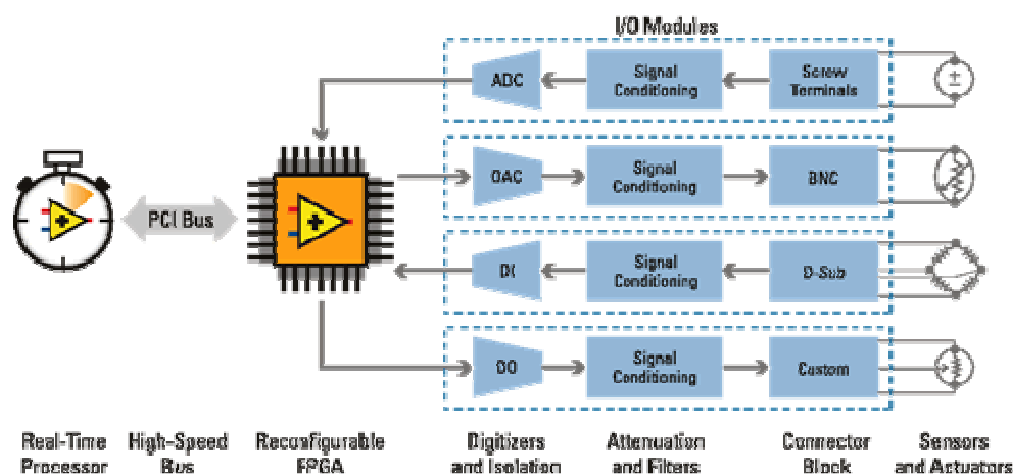


Figure 6.4 – Interface layout of the NI Compact RIO [28].

We selected the NI cRIO-9012 real-time controller because of its full speed USB port for connection to USB flash and memory devices. This will allow us to store extremely large amounts of data locally on the WEC. The NI cRIO-9012 also has the fastest real-time controller available featuring a 400 MHz processor and 64 MB DRAM memory. It is equipped with an RS232 serial port and 10/100BaseT Ethernet port that has an embedded web and file servers with remote panel user interface. It is equipped with dual 9 to 35 VDC supply inputs which make it excellent for remote applications.



Figure 6.5 – cRIO Real-Time Controller [28].

The CompactRIO reconfigurable FPGA chassis that we selected was the NI cRIO-9102. This is an 8-slot reconfigurable FPGA chassis that accepts any CompactRIO I/O modules. It features a 1 million gate reconfigurable I/O FPGA core that allows you to automatically synthesize custom control and signal processing circuitry using LabVIEW.



Figure 6.6 – cRIO FPGA Chassis [28].

C series I/O modules are used to perform various tasks in our controller. The NI-9205 is a very adaptable analog input module that features 32 single-ended or 16 differential analog inputs. It has 16-bit resolution and a 250 kS/s aggregate sampling rate. Input ranges are software selectable and can be set at  $\pm 200$  mV,  $\pm 1$ ,  $\pm 5$ , and  $\pm 10$  V. The NI-9211 is a thermocouple module with 4 thermocouple or  $\pm 80$  mV analog inputs. It has 24-bit resolution and features 50/60 Hz noise rejection. The NI-9474 is an 8-channel, 1  $\mu$ s high-speed digital output. It has sourcing digital output ranges from 5 to 30 V.



Figure 6.7 – cRIO I/O Modules [28].

The I/O modules are all hot-swappable and have built-in signal conditioning for direct connection to a variety of sensors and actuators. They feature extreme industrial certifications and can operate at temperature ranging from  $-40$  to  $70$  °C.

All of the CompactRIO system is programmed using the LabVIEW graphical programming environment. LabVIEW allows us to take in data from all of the remote sensors, run control operations, and effect control with output signals.

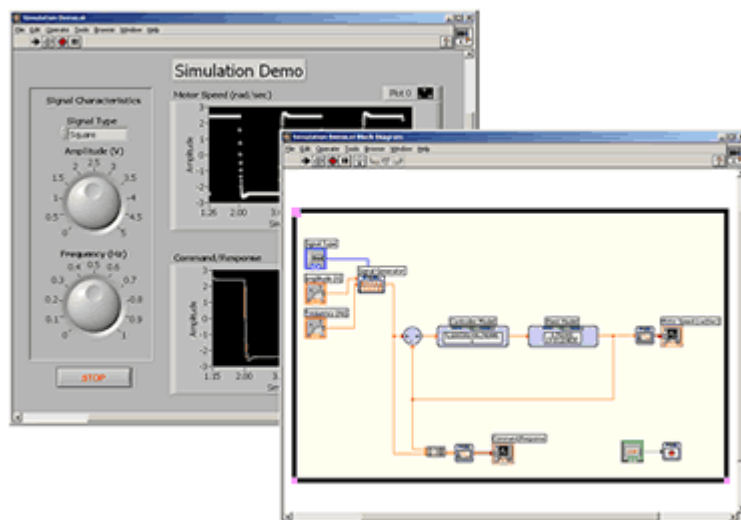


Figure 6.8 – LabView Programming Environment [28].

#### 6.4.1 Data Acquisition

The first step in creating a controller is to identify the input variable that will need to be collected. For the 1kW WEC we will collect data for control calculations and also for various machine and environment monitoring. All of the data will be stored locally as well as transmitted to a remote user interface where it can be observed and adjustments can be made.

The data acquisition includes the generator terminal voltages, generator currents, DC buss voltage and current, load voltage and current, 12 generator temperature measurements, linear position measurement, and leak detection. Below is a wiring schematic showing the various I/O to the cRIO. Additional electrical wiring diagrams can be found in Appendix (C).

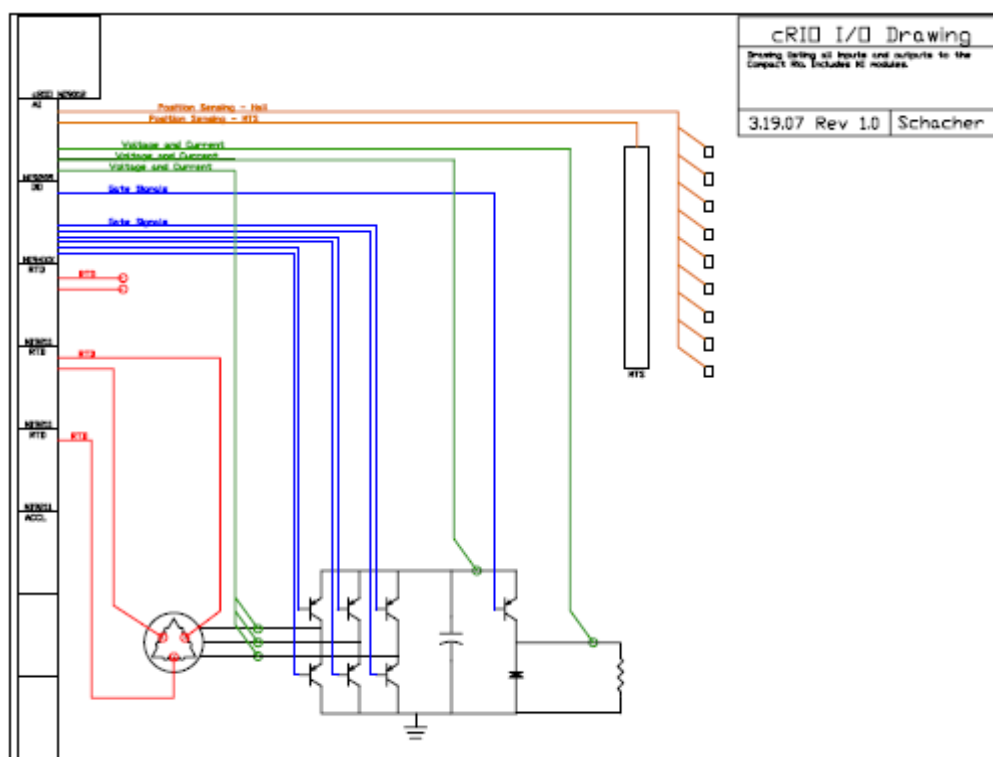


Figure 6.9 – Wiring schematic for the cRIO.

The various sensors were acquired from a variety of sources. Some of which were borrowed from industrial control applications. The three phase current sensors came as part of the PowerEx power pack. The DC bus currents and voltages, as well as the three phase voltages are acquired using a sense resistors and voltage dividers designed and built by our senior design group. This group also developed a leak detection sensor to be placed in the buoy that will send an output signal when it comes into contact with salt water. The most unique sensor is the linear position sensor from MTS. This linear-position sensors use a time-based magnetostrictive position sensing principle. The sensor sends an electromagnetic pulse into a long waveguide. This pulse is interrupted by a magnetic field attached to the equipment whose position is being determined; in our case the buoy. The position of this magnet is determined with high precision and speed by accurately measuring the elapsed time between the application of the pulse and the arrival of the reflected pulse. This provides us with a non-contact means of sensing the position

of the buoy from within the spar. Figure 6.10 illustrates how this magnetostrictive principle operates.

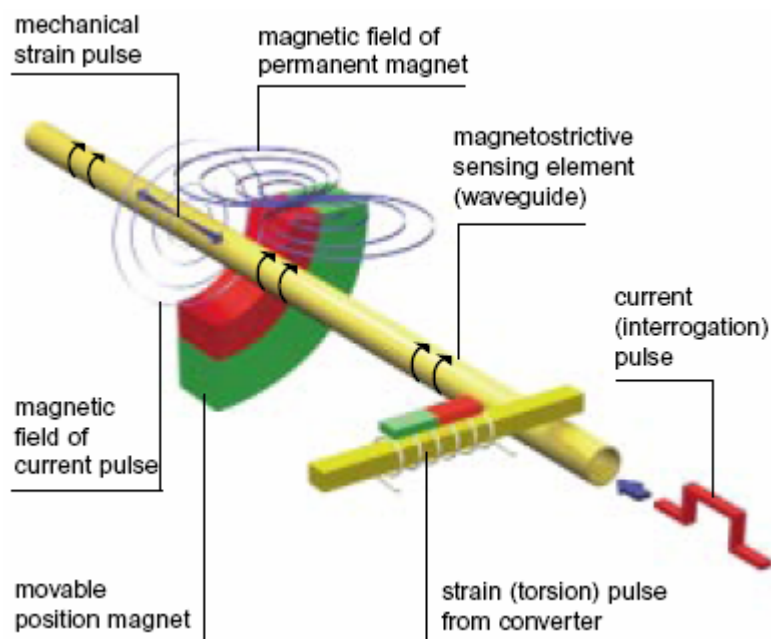


Figure 6.10 – Magnetostrictive Principle [17].



Figure 6.11 – MTS Linear Position Sensor [17].

#### 6.4.2 Controls

The control hardware consists of all of the equipment that is able to affect the behavior of the system. This includes the full-bridge converter, the DC buck converter and the terminal circuit breakers. All of the gating signals to drive this equipment are

generated by the cRIO using the NI-9474 digital output module. These signals give us the ability to control the terminal voltages of the generator, which in turn controls the generator currents and thus the generator force.

### 6.4.3 Communications

Using the 10/100BaseT Ethernet port on the NI cRIO-9012 we are able to connect to it using a direct computer link or via a network connection. The CompactRIO also has an embedded web server which allows any computer on the network to login and monitor the status of the current VI. Computers on the network can even be granted permissions and can take control of the CompactRIO and make online changes to the control program as necessary.

With the addition of a set of Ethernet radios we are able to make this connection to the CompactRIO wirelessly. We chose the FreeWave Technologies HT radio for its high speed, long range, and ability to operate in harsh environments. The FreeWave radio allows transparent bridging of all Ethernet protocols; this means that once the radios are plugged into the Ethernet ports it behaves just like a solid Ethernet cable. This wireless operation is essential for any long term ocean testing where data and controls must be routed to a land based station. For the ocean testing of the 1kW WEC we will setup our controls computer in the research vessel and monitor and control the WEC wirelessly from there. Figure 6.12 show the topology of this connection while Fig 6.13 shows the FreeWave Technologies HT radio.

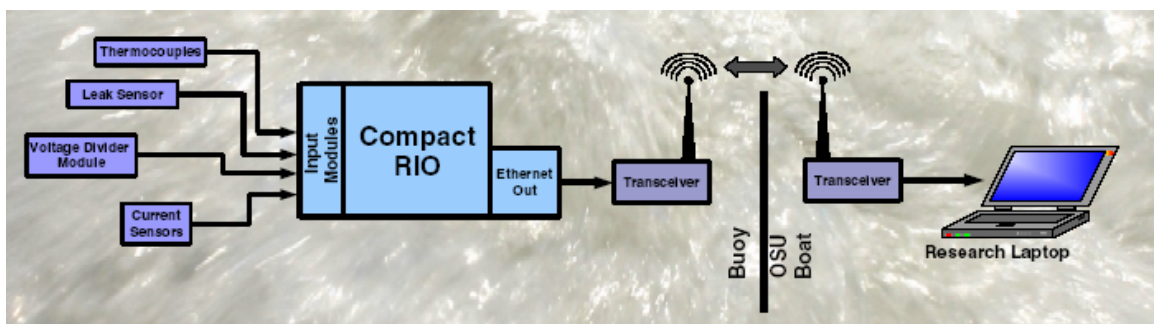


Figure 6.12 – Wireless Communications for cRIO.





Figure 6.13 – FreeWave Ethernet Radios [15].

## **7. RESULTS and CONCLUSIONS**

### **7.1 Results**

The goal of this project was to set out and identify a control method that would be effective at controlling and maximizing energy for the 1kW WEC prototype. This experience led me through many breakthroughs and revelations about the nature of ocean wave energy. I was able to identify many valuable control methods from literature reviews and also from model simulations. The challenge became identifying ways to overcome real-world limitations while attempting to implement a control that was as near to optimum as possible. The result of this investigation was the development of the conditional damping control with exponential augmentations methods. This control method proved to control the WEC in a manner that accomplished our design needs.

As my understanding of the control requirement grew so did my ability to visualize how an ideal WEC should be designed. This being Oregon State's first prototype WEC developed with a control system in place, it is no surprise that there are a few things about the design that I will change in future prototypes.

### **7.2 Conclusions**

I will conclude with a variety of observations that should be considered in the design of future WEC systems. Figure 5.23 illustrates a strong indication that a WEC might be best designed mechanically to have a resonant period at the fundamental incident wave period. By designing for mechanical resonance we can achieve optimum control without the need for energy storage. A resonant WEC would achieve larger heave responses therefore increasing the available stroke length will also need to be considered.

The WEC should have vertical dimensions large enough that it will not become fully submerged during nominal sea conditions. When the buoy becomes submerged the available buoyant force reaches a plateau and generation is sacrificed. Additionally submergence results in non-linear WEC response that can disrupt the heaving motion of the WEC. The vertical dimensions of the buoy should correspond to the maximum allowable generator force in order to maximize the machine's performance.

## 8. FUTURE WORK

Future work includes physical hardware testing in the lab as well as ocean testing to be held in the summer 2007. The energy systems lab at Oregon State University is home to a 120kVA programmable source that is able to output variable frequency and variable amplitude sinusoidal voltages that will be used to verify the control hardware functionality. In addition to this OSU is in the construction phase of a 10kW linear test bed to be used solely for the verification of linear wave energy converters. After testing on the linear test bed is complete, wave flume testing will be carried out at the O.H. Hinsdale Wave Research Lab also at OSU. The final ocean test will be carried out about 1 mile offshore of Newport, OR.

With ocean energy being in its infancy there are nearly limitless directions that future work could seek to explore. Any of these possible directions would lead to increased knowledge about this field that everyone could benefit from. Some areas of research will fit different research groups better than others. For example work focused on buoy interactions with ocean waves would be well suited for researchers with a vast knowledge of fluid behavior and 3D fluid modeling. This work would include investigating the ideal design of the buoy and spar system. Alternatively work in such fields as power take-off or optimum generator control would be well suited for researchers in Energy or Control Systems. Such work might include investigation of ideal buoy control in a widely stochastic wave climate.

The concept of using a wave monitoring buoy or possibly a sea floor mounted sonar profiler could provide us with near real-time information about the harmonic content of the existing wave conditions. This information could be used to modify the control behavior in order to maximize power production. Remember however that every wave frequency travels at different speeds in the ocean and all waves approach at different angles; therefore we cannot predict the actual wave profile at any great distance from the monitoring site.

Work developing the physical layout of the linear generating device should be considered. The organization of the permanent magnets, copper, and iron has not yet fully

been explored. Investigation into the most efficient organization in terms of cost, efficiency, materials and weight could lead to more viable linear generators.

The idea of using damper plates to effectively increase the added mass in order to increase the natural period could provide a very cost effective way of achieving mechanical resonance with the incident wave period.

I am also interested in identifying a new transform that would be able to take the  $dq$  values from an ocean wave generator and create a new DC like set of static values with no loss of information about the system. It would appear that such a transform may be possible in a monochromatic wave environment, the challenge however would be to identify a way to extend this into a stochastic sea state.

## 9. BIBLIOGRAPHY

- [1] Falnes, J., "Principles for Capture of Energy from Ocean Waves. Phase Control and Optimum oscillation." Department of Physics, NTNU, N-7034 Trondheim, Norway
- [2] Umesh A. Korde, "Control System Applications In Wave Energy Conversion", Mechanical Engineering Department, Indiana Institute of Technology
- [3] J. Xiang, P.R.M. Brookings & M.A. Mueller, "Control Requirements of Direct Drive Wave Energy Converters" School of Engineering, University of Durham, United Kingdom.
- [4] Jonathan K.H. Shek, D. Ewen Macpherson, Markus A. Mueller, "Control of Linear Generators for Direct Drive Wave Energy Conversion" *Institute for Energy Systems, Joint Research Institute in Energy, School of Engineering and Electronics, The University of Edinburgh, UK* June 2006.
- [5] Minoos H. Patel, "Application to Floating Bodies," in Dynamics of Offshore Structures, Butterworth & Co. Ltd., pp. 283-286, 1980.
- [6] Ned Mohan, "Advanced Electric Machines – Analysis, Control and Modeling using Simulink" MNPERE, Minneapolis 2001
- [7] E.B. Agamloh, A.K. Wallace, A. von Jouanne, "A novel wave energy extraction device with contactless force transmission system," 44th AIAA Aerospace Sciences Meeting, Reno, Nevada, Jan 2006.
- [8] Falnes, Johannes, "Optimum Control of Oscillation of Wave-Energy Converters", *Department of Physics, Norwegian University of Science and Technology, Norway*, The International Society of Offshore and Polar Engineers, June 2002
- [9] Chee-Mun Ong, "Dynamic Simulation of Electric Machinery" 1998 Prentice Hall, Inc
- [10] K. Budal, "Theory for absorption of wave power by a system of interacting bodies," *Journal of Ship Research*, vol. 21, pp. 248-253, 1977.
- [11] K. Budal, J. Falnes, "A resonant point-absorber of ocean wave power," *Nature*, vol. 256, pp. 478-479, 1975.
- [12] Robert G. Dean, Robert A. Dalrymple, "Water Wave Mechanics For Engineers and Scientists" World Scientific Publishing Co. Pte. Ltd., 1991

**BIBLIOGRAPHY (Continued)**

- [13] J. Falnes, *Ocean Waves and Oscillating Systems*, Cambridge University Press, 2002.
- [14] Ocean World; [http://oceanworld.tamu.edu/resources/ocng\\_textbook/chapter16](http://oceanworld.tamu.edu/resources/ocng_textbook/chapter16)
- [15] FreeWave Radios Webpage;  
<http://www.freewave.com/products/industrial-radios.html>
- [17] MTS Sensors Webpage;  
<http://www.mtssensors.com/linear.html>
- [18] Schacher, A.C., "Investigation and Comparison of Generators for Dynamic Operation in Ocean Buoys" Thesis for Master of Science, June 2004
- [19] M. A. Mueller, "Electrical generators for direct drive wave energy converters," IEE Proc. Gen. Transm. Distrib., vol. 149, No. 4, pp. 446-456, 2002.
- [20] Schacher, A.A., "Novel Control Design for Point Absorber Wave Energy Converters" Thesis for Master of Science, June 2007
- [21] K. Rhinefrank, E. B. Agamloh, A. von Jouanne, A. K. Wallace, J. Prudell, K. Kimble, J. Ails, E. Schmidt, P. Chan, B. Sweeny, A. Schacher, "Novel ocean permanent magnet linear generator buoy," *Journal Renewable Energy*, Elsevier 2005, in press.
- [22] Metzcus, L. Wooderson, A. Heiberg, S. Benton, "Transverse Flux Generator Technical Manual," June 2006.
- [23] McGraw Hill Higher Education Website; [http://www.mhhe.com/earthsci/geology/mcconnell/earths\\_climate/gac.htm](http://www.mhhe.com/earthsci/geology/mcconnell/earths_climate/gac.htm)
- [25] Surfline Webpage;  
[http://www.surfline.com/surfology/surfology\\_forecast\\_index.cfm](http://www.surfline.com/surfology/surfology_forecast_index.cfm)
- [26] Falnes, J. and Budal, K. (1978). Wave power conversion by point absorbers. *Norwegian Maritime Research*, Vol.6, No.4, pp. 2-11
- [27] J. G. Vining and A. Muetze. Ocean Wave Energy Conversion – A Survey. Power Area and CEME Seminar at UIUC, October 2, 2006
- [28] National Instruments Webpage;  
<http://sine.ni.com/nips/cds/view/p/lang/en/nid/14145>

**10. APPENDIX**

## Appendix (A)

```

5/31/07 8:32 PM Z:\Matlab Files\WEC_v3\WEC_v3_init.m 1 of 3
%*****
% Hydrodynamic Buoy and Generator Model
% Al Schacher
% 2.20.07
% Reference Mohan, Brekken, Patel, Elwood
clc
clear
format compact
if 0
Tmax %sec
h13 %H 1/3rd for 20.6m/s
fmax %*****USE 20-25 frequencies 0.016 or 0.02:.4 is great!!!
df %This is very strange as df increases the sea state is averaged
to zero
F=zeros
Offset=zeros
W=zeros
for n = 1:1:fmax/df %Frequency band
F(n)=n*df
phase=rand*2*pi
Offset(n)=phase
end
mTmax=Tmax
W=2*pi*F
dW=2*pi*df
a %Phillips' constant
b
g %gravity
U19=sqrt((h13*g)/0.21) %wind speed at 19.5m
wo=g/U19 %natural frequency
S=((a*g^2./W.^5).*exp(-b.*((wo./W).^4)))*2*pi %2*pi DKW
H13=4*sqrt(S)
Aw=(H13/2)
plot(F,S)
grid on
xlabel('Frequency [Hz]')
ylabel('Spectral Density [m^2/Hz]')
title(['Pierson-Moskowitz - Wave Spectrum'])
Eta = zeros
for t = 1:1:mTmax %mSec
tempEta
for x = 1:1:fmax/df
5/31/07 8:32 PM Z:\Matlab Files\WEC_v3\WEC_v3_init.m 2 of 3
dEta=Aw(x)*sin(W(x)*1/1000*t+Offset(x))
tempEta=tempEta+dEta*dW
end
if t<25000
Start=t^3/(t^3+5000000000)
else
Start
end
end

```



```

Eta(t,1)=t
Eta(t,2)=tempEta*Start
end
figure
plot(Eta(:,1),Eta(:,2))
grid on
xlabel('Time [s]')
ylabel('Wave Profile [m]')
title(['Wave Profile Generated from Pierson-Moskowitz'])
end
diff_pole_freq = 100*2*pi
dZb_limit =
Zb_limit =
Vabc=[100,100,100] %volts
Draft = %meters
Freeboard = %meters
Bmax %[Newtons] Volume above waterline
g %m/s^2
Pole_pitch %72mm
r
% Assume 1 kW. At 1 m/s, 1 kN force.
% Wave period and frequency.
T_wave = % seconds
f_wave = 1/T_wave
W_wave = 2*pi*f_wave
% Wave height in meters (amplitude).
A_wave = 2
%Buoy (float) mass in kg.
m = %mass
A = 0.5*m % added mass
% Friction and viscosity ( N / (m/s)^2 ).
C
% Buoyancy (N/m)
K =
5/31/07 8:32 PM Z:\Matlab Files\WEC_v3\WEC_v3_init.m 3 of 3
% If C is 1000 N/m, then 1 meter submersion will produce 1 kN force.
dZb_0=A_wave
Zb_0=-.45
simulink
open('WEC_v3.mdl')
disp(['WEC_v3_init.m run succesfully'])

```

# Appendix (B)

Trigger Conditions		C_gen = C_gen*	
<p>It is assumed all combinations will work for moderate wave heights.                      All simulations tested using a 4 meter input wave.</p>			
dZb  > dZb_limit	Control Values		N/A
	Stroke Control	3.6 meters	
	Velocity Control	1.7 m/s	
	Generator Output	9000 W	
Zb  > Zb_limit & Zb*dZb > 0	Max Force	10,700 N	
	Force Ripple	Good	
	Control Values	N/A	
	Stroke Control	3.6 meters	
dZb /dZb_limit +  Zb /Zb_limit > 1	Velocity Control	1.7 m/s	
	Generator Output	9000 W	
	Max Force	10,700 N	
	Force Ripple	Good	
( dZb /dZb_limit)^2 + ( Zb /Zb_limit)^2 > 1	Control Values	N/A	
	Stroke Control	3.6 meters	
	Velocity Control	1.7 m/s	
	Generator Output	9000 W	
dZb /dZb_limit +  Zb /Zb_limit > Limit	Max Force	10,700 N	
	Force Ripple	Good	
	Control Values	N/A	
	Stroke Control	3.6 meters	
( dZb /dZb_limit)^2 + ( Zb /Zb_limit)^2 > Limit	Velocity Control	1.7 m/s	
	Generator Output	9000 W	
	Max Force	10,700 N	
	Force Ripple	Good	
C_gen >= C_gen*	Control Values	N/A	
	Stroke Control	3.6 meters	
	Velocity Control	1.7 m/s	
	Generator Output	9000 W	
	Max Force	10,700 N	
	Force Ripple	Good	
	Control Values	N/A	
	Stroke Control	3.6 meters	
	Velocity Control	1.7 m/s	
	Generator Output	9000 W	
	Max Force	10,700 N	
	Force Ripple	Good	
	Control Values	N/A	
	Stroke Control	3.6 meters	
	Velocity Control	1.7 m/s	
	Generator Output	9000 W	
	Max Force	10,700 N	
	Force Ripple	Good	
	Control Values	N/A	
	Stroke Control	3.6 meters	
	Velocity Control	1.7 m/s	
	Generator Output	9000 W	
	Max Force	10,700 N	
	Force Ripple	Good	

Appendix (B) (Continued)

Augment Laws			
C. gen = C2*dZb*2 dZb = [0.3 0.4], C2=1M	C. gen = C. gen*+C2*dZb*2 dZb = [0.3 0.4], C2=200k	C. gen = C. gen*+C2*dZb*2*Zb*2 dZb = [0.3 0.4], C2=400M	C. gen = C2*dZb*4 dZb = [0.3 0.4], C2=300M
1 meter	1 meter	1 meter	1 meter
0.4 m/s	0.4 m/s	0.5 m/s	0.4 m/s
3500 W	3700 W	3500 W	3400 W
<b>35,000 N</b>	<b>16,000 N</b>	<b>30,000,000 N</b>	<b>3,000,000 N</b>
Very Poor	Bad	Extremely Poor	Extremely Poor
Zb = [0.3 0.4], C2=100M	Zb = [0.3 0.4], C2=100M	Zb = [0.3 0.4], C2=200M	Zb = [0.3 0.4], C2=10B
1 meter	1 meter	1 meter	1 meter
1.35 m/s	1.35 m/s	1.35 m/s	1.3 m/s
3000 W	3000 W	3500 W	3200 W
<b>250,000,000 N</b>	<b>240,000,000 N</b>	<b>80,000,000 N</b>	<b>47,000,000,000 N</b>
Bad	Bad	Bad	Bad
Zb=0.5, dZb=0.5, C2=250k	Zb=0.5, dZb=0.5, C2=180k	Zb=0.5, dZb=0.5, C2=4M	Zb=0.5, dZb=0.5, C2=2.5M
1 meter	1 meter	1 meter	1 meter
0.5 m/s	0.5 m/s	1.1 m/s	0.5 m/s
3600 W	3800 W	4000 W	3500 W
<b>30,000 N</b>	<b>25,000 N</b>	<b>27,000 N</b>	<b>80,000 N</b>
Very Poor	Very Poor	Bad	Very Poor
Zb=0.5, dZb=0.5, C2=350k	Zb=0.5, dZb=0.5, C2=4.5M	Zb=0.5, dZb=0.5, C2=4.5M	Zb=0.5, dZb=0.5, C2=3M
1 meter	1 meter	1 meter	1 meter
0.5 m/s	0.5 m/s	1.1 m/s	0.52 m/s
3200 W	1550 W	3400 W	3800 W
<b>44,000 N</b>	<b>550,000 N</b>	<b>3,000 N</b>	<b>110,000 N</b>
Extremely Poor	Extremely Poor	Very Poor	Extremely Poor
Zb=dZb=0.5, Limit=[0.8-1.1], C2=200k	Zb=dZb=0.5, Limit=[0.8-1.1], C2=180k	Zb=dZb=0.5, Limit=[0.8-1.1], C2=4M	Zb=dZb=0.5, Limit=[0.8-1.1], C2=1.8M
1 meter	1 meter	1 meter	1 meter
0.43 m/s	0.42 m/s	1.33 m/s	0.55 m/s
3900 W	3600 W	4200 W	3600 W
<b>15,700 N</b>	<b>15,600 N</b>	<b>35,000 N</b>	<b>90,000 N</b>
Good	Good	Poor	Poor
Zb=dZb=0.5, Limit=[0.8-1.1], C2=250k	Zb=dZb=0.5, Limit=[0.8-1.1], C2=200k	Zb=dZb=0.5, Limit=[0.8-1.1], C2=4M	Zb=dZb=0.5, Limit=[0.8-1.1], C2=3M
1 meter	1 meter	1 meter	1 meter
0.52 m/s	0.52 m/s	1.3 m/s	0.52 m/s
4000 W	3900 W	4200 W	4000 W
<b>36,000 N</b>	<b>32,000 N</b>	<b>35,000 N</b>	<b>110,000 N</b>
Extremely Poor	Very Poor	Poor	Very Poor
C2=200k	C2=180k	C2=4M	C2=2M
1 meter	1 meter	1 meter	1 meter
0.43 m/s	0.43 m/s	1.1 m/s	0.38 m/s
3800 W	3800 W	4000 W	3500 W
<b>15,600 N</b>	<b>15,600 N</b>	<b>27,000 N</b>	<b>15,850 N</b>
Good	Good	Poor	Good

Appendix (C)

Electrical Drawing	
Wiring Diagram for 1kW test WEC.	
2.28.07 Rev 1.0	Schacher

